NEUROMUSCULAR DEVELOPMENT AND METAMORPHOSIS

IN THE SERPULID POLYCHAETE *HYDROIDES ELEGANS*

A DISSERTATION SUBMITTED TO THE GRADUATE DIVISION OF THE UNIVERSITY OF HAWAI‘I AT MANOĀ IN PARTIAL FULFILLMENT OF THE REQUIREMENTS FOR THE DEGREE OF

DOCTOR OF PHILOSOPHY

IN

ZOOLOGY

DECEMBER 2010

By
Brian T. Nedved

Dissertation committee:
Michael G. Hadfield, Chairperson
Mark Martindale
Robert Richmond
Elaine Seaver
Martin Rayner

Keywords: polychaete, larva, muscle, neurogenesis, metamorphosis,

ABSTRACT

Larvae of the serpulid polychaete *Hydroides elegans* display a complex range of behaviors that culminates in settlement from the water column and the induction of metamorphosis. The central nervous system of the larvae coordinates and controls these processes. Little is known about the morphology and early development of the central nervous system in polychaete larvae. Confocal laser scanning microscopy and antibodies raised against serotonin, FMRF-amide, tyrosine hydroxylase and β-tubulin were used to track neurogenesis and neural development from early in larval development through the attainment of metamorphic competence in *H. elegans.* It was determined that the earliest neuron was posteriorly positioned in the hyposphere and its axons may serve as a scaffolding for the later developing ventral nerve cords. Because competent larvae of *H. elegans* have a well developed serotonergic nervous system that innervates both the cerebral ganglia and larval structures fated to be lost during metamorphosis, seven different compounds involved in both the biosynthesis of 5-HT and those altering 5-HT signaling pathways to were tested determine if release of 5-HT coordinates and controls metamorphosis of *H. elegans.* Metamorphic assays utilizing these compounds demonstrated that serotonin was required for metamorphosis of *H. elegans*. Finally, confocal laser scanning microscopy was used to examine myogenesis in larvae of *H. elegans* and then to track the fate of these muscle groups through metamorphosis. Muscles associated with the larval gut and the trochal bands were the earliest muscles to develop. At competence, main muscle systems consisted of three bands of muscle associated with the trochal bands, an additional band of muscle in the episphere, two pairs of longitudinal muscles, an extensive set of muscles associated with the chaetal sacs, and a complex set of muscles surrounding the gut. The majority of these muscles persist through metamorphosis and only the ring muscles associated with the trochal bands disappear during metamorphosis. The relatively small loss of muscle and the precocious development of adult muscles during larval development and may be an evolutionary advantage that allows for the rapid metamorphosis after brief contact with a metamorphic cue.

TABLE OF CONTENTS

LIST OF TABLES

LIST OF FIGURES

LIST OF ABBREVIATIONS

DGGE	Denaturing Gradient Gel Electrophoresis
FSW	0.22 μm Milipore-filtered seawater
CNS	central nervous system
ASO	apical sensory organ
VNC	ventral nerve cords
5-HT	Serotonin
TH	Tyrosine Hydroxylase
PBS	Phosphate Buffered Saline
5HT-LIR	Serotonin-like Immunoreactivity
TH-LIR	Tyrosine Hydroxlyase-like Immunoreactivity
FMRFa-LIR	FMRFamide- like Immunoreactvity
Pro	Prototroch
AP	Apical Plate
Met	Metatroch
NT	Neurotroch
AV	Anal Vesicle
Ret	Reticulated Cells
CEC	Circumesophageal Connectives
tub-LIR	β-tubulin-like immunoreactivity
hpf	hours post-fertilization
5-HTP	5-Hydroxytryptophan
pCPA	p-Chlorophenylalanine
SSRI	Selective Serotonin Reuptake Inhibitor

MM	Metatroch Muscle
FGM	Food Groove Muscle
PM	Prototroch Muscle
LDM	Longitudinal Dorsal Muscle
LMM	Longitudinal Medial Muscle
LVM	Longitudinal Ventral Muscle
PTM	Pretrochal Muscle
PDM	Posterior Diagonal Muscle
ADM	Anterior Diagonal Muscle
PMOM	Posterior Medial Oblique Muscle
AMOM	Anterior Medial Oblique Muscle
ALDM	Anterior Lateral Diagonal Muscle
bun1	Anterior Chaetal Bundle
bun2	Posterior Chaetal Bundle

PREFACE

Marine invertebrate larvae are not passive particles drifting through their environment. Instead, they display a complex range of behaviors that culminates in settlement from the water column and the induction of metamorphosis. As a larval biologist, I am interested in the processes that coordinate and control both larval behavior and metamorphosis. I have chosen to study these processes in larvae of the serpulid polychaete *Hydroides elegans.* My dissertation had three objectives; (1) to describe neurogenesis during the larval development of the serpulid polychaete *Hydroides elegans,* (2) to determine the role the neurotransmitter serotonin plays in the induction of metamorphosis of *H. elegans;,* and (3) to describe the fate of the musculature during metamorphosis.

Classically, annelids and arthropods were thought to be sister taxa within the Articulata clade and the segmented bodies of both groups of animals were presumed to be a synapomorphy. Segmentation can be easily seen in the rope-ladder like morphology of the ventral nerve cords and the iteration of circular muscles within the body wall of polychaetes. However, recent molecular phylogenies have split the Articulata placing the arthopods within the Ecdysozoa and the annelids within the Lophotrochozoa. This new topology, as well as the placement of the polychaetes as the basal clade within the annelids has spurred researchers to reexamine neuromuscular development in polychaete larvae.

Chapter 1.

HYDROIDES ELEGANS (ANNELIDA: POLYCHAETA): A MODEL FOR BIOFOULING RESEARCH

Introduction

The fouling communities that occur on ships and other man-made structures submerged in the sea are diverse assemblages of organisms (Carlton and Hodder 1995; Gollasch 2002; Godwin 2003). Due to that diversity, the variety of adhesives that fouling organisms utilize to cement themselves to settlement substrata are equally diverse (Naldrett and Kaplan 1997; Brady and Singer 2000; Wiegemann 2005; Smith and Callow 2006), posing a significant challenge for the development of new coatings to combat biofouling processes (Holm et al. 2006). Minimizing fouling on ship hulls is important because of the negative influence fouling has on hull performance (Woods Hole Oceanographic Institution 1952), expenses associated with dry-docking, scraping and re-painting hulls, and the substantial costs from propulsive fuel losses required to overcome the increased drag created by hull fouling (Townsin 2003).

Research to find new coatings to combat biofouling has two major thrusts, one in chemically formulating experimental coatings and another in testing these coatings in both field and laboratory settings. The serpulid polychaete *Hydroides elegans* (Haswell 1883) has proven to be an excellent organism for testing experimental coatings under both field and laboratory conditions.

Hydroides elegans is a common member of fouling communities throughout tropical and subtropical seas (Edmondson 1944; ten Hove 1974; Hadfield et al. 1994; Unabia and Hadfield 1999; Bastida-Zavala and ten Hove 2002; 2003). *H. elegans* is a problematic fouling organism because: (1) it quickly colonizes newly submerged surfaces (Unabia and Hadfield 1999; Holm et al. 2000); (2) it grows as much as 1.5 mm/day (Paul 1937); (3) it reaches sexual maturity in as short a time as 9 days in a tropical harbor (Paul 1937); (4) it has a short larval period (Hadfield et al. 1994; Carpizo-Ituarte and Hadfield 1998); and, (5) aggregations of its calcified tubes can accumulate to several centimeters thick on submerged surfaces in as short a time as 1 to 2 months in Pearl Harbor, Hawaii (Fig. 1.1).

Due to its importance as a fouler of ship hulls, there is a growing body of research concerned with the natural inductive cues for recruitment of *H. elegans* (Hadfield et al. 1994; Hadfield and Strathmann 1996; Walters et al. 1997; Unabia and Hadfield 1999; Hadfield and Paul 2001; Lau and Qian 2001; Harder et al. 2002; Lau et al. 2002; Huang and Hadfield 2003; Lau et al. 2005; Shikuma and Hadfield 2006), as well as the metamorphic cascades that are triggered by this process (Carpizo-Ituarte and Hadfield 1998; Holm et al. 1998; Carpizo-Ituarte and Hadfield 2003). Additionally, it has been employed in studies of neurogenesis (Nedved and Hadfield 1998, and unpublished), muscular development (Nedved and Hadfield 2001), segment development (Seaver and Kaneshige 2006; Seaver et al. 2005), and the heritability of egg size (Miles et al. 2007). *H. elegans* will undoubtedly find use as a research model in many other types of studies due to the ease with which is can be maintained and reared in the laboratory.

Upon submersion in seawater, surfaces undergo a well characterized progression from initial coating of adsorbed organic molecules (Zobell and Allen 1935), to the formation of biofilms (Marshall 1981; Baier 1984) composed of a wide variety of microorganisms that form highly organized communities (Costerton et al. 1999). These complex biofilms provide settlement cues for larvae of many sessile marine invertebrate species (reviewed by Hadfield and Paul 2001). Biofilm bacteria produce the inductive cue for settlement of competent larvae of *H. elegans* (Hadfield et al. 1994; Unabia and Hadfield 1999; Lau and Qian 2001; Lau et al. 2002; Huang and Hadfield 2003; Lau et al. 2005; Shikuma and Hadfield 2006). Laboratory evidence that other biofilm organisms may produce inductive cues for larvae of *H. elegans* (e.g., diatoms: Harder et al. 2002) remain provisionary due given the difficulty of producing absolutely axenic cultures of such organisms for testing.

Larvae of *H. elegans* require a minimum bacterial density for the induction of metamorphosis, and increased larval settlement positively correlates with the density of bacteria in a biofilm (Hadfield et al. 1994; Huang and Hadfield 2003). Settlement by *H. elegans* is greatly reduced or eliminated when multi-species biofilms are treated with a variety of agents that act either as fixatives or antiseptics, demonstrating that the microorganisms within the biofilms must also be alive for induction to occur (Unabia and Hadfield 1999). Recent studies by Lau et al. (2005) and Shikuma and Hadfield (2006)

using denaturing gradient gel electrophoresis (DGGE) have examined the effect that changes in the bacterial assemblages of biofilms have on the induction of metamorphosis of *H. elegans*, both demonstrating a stronger positive correlation between settlement of *H. elegans* and bacterial density than between settlement and differences in natural community composition. However, the effectiveness of a bacterial biofilm as an inducer of metamorphosis of *H. elegans* is not solely due to the sheer number of bacteria residing in it. Huang and Hadfield (2003) demonstrated that single-strain, low-density biofilms of *Pseudoalteromonas luteoviolacea* (GenBank accession number EU072022) induced metamorphosis of *H. elegans* (Fig. 1.2), while mono-specific biofilms of *Flexibacter* sp. and *Cytophaga* sp. were non-inductive even though the cell densities of these biofilms were 7 to 12 times greater (Fig. 1.3). These data indicate that induction of metamorphosis is due to specific chemical characteristics of *P. luteoviolacea* (Huang and Hadfield 2003). Furthermore, production of this metamorphic cue is strain specific; a different strain of *P. luteoviolacea* obtained from the American Type Culture Collection (Manassas, VA) does not induce settlement of larvae of *H. elegans* (unpublished personal observations).

Hydroides elegans is particularly well-suited for use in testing of experimental coatings. The adhesive that secures the calcareous tubes of *H. elegans* appears to be stronger than that of the balanoid barnacles *Balanus eburneus* and *B. amphitrite*, two species often employed in testing of marine coatings. The mean removal force for *H. elegans* that had settled on 6 different silicone coatings in Pearl Harbor, HI was nearly 3 times greater than the mean removal force required to remove *B. eburneus* from replicate panels immersed in the Indian River Lagoon, FL (Fig. 1.4A, Stein et al. 2003).

Due to the ease with which they can be raised in the laboratory and the strength of their attachment adhesives, newly metamorphosed juveniles of *H. elegans* are a good organism to use to rapidly test coatings under laboratory conditions. We used a series of standardized tests to evaluate effectiveness of the foul-release properties of the silicone coating RTV11 (General Electric Co., New York) and the foul-release coating Veridian® (International Coatings, Southampton, England). Both coatings showed poor foul-release characteristics. In the case of RTV11, more spat of *B. amphitrite* are removed from the coating than newly settled juveniles of *H. elegans* after a 4 minute exposure to a wall-

shear force equivalent to 100 Pa (unpublished personal observations presented in Fig. 1.4B) in a turbulent flow apparatus (described in Schultz et al. 2003). The foul-release coating Verdian® also performed poorly in both antifouling and foul-release tests. Glass microscope slides coated with Veridian® did not inhibit the settlement and metamorphosis of *H. elegans*, nor was there a difference in removal of juvenile *H. elegans* from Veridian®-coated microscope slides than from uncoated microscope slides after exposure to a wall-shear force equivalent to 100 Pa (unpublished personal observations presented in Table 1).

Information on the occurrence and biology of *H. elegans* has been published under several taxonomic names (e.g., Edmondson 1944; Wisely 1958). This confusion has been resolved in taxonomic reviews by Zibrowius (1971), ten Hove (1974) and Bastida-Zavala and ten Hove (2003), who concluded that *H. norvegica* is a species of the northern Atlantic Ocean and the Mediterranean Sea and that the similar species in warm seas around the world should be referred to *H. elegans*. There are, of course, other tropical species of *Hydroides*, and they may easily be confused with *H. elegans* without careful observation of the operculum and setae, which are well illustrated in ten Hove (1974), Bailey-Brock (1987) and Bastida-Zavala and ten Hove (2003). According to ten Hove (1974), *H. elegans* is the only *Hydroides* species that forms dense aggregations in warm water bays and estuaries worldwide.

The remainder of this chapter provides a concise summary of methods developed in our laboratory for the culture of *Hydroides elegans* for use in biofouling testing. Our techniques have been used to successfully culture *H. elegans* elsewhere (e.g., Bryan et al. 1997), including areas that do not have access to coastal waters.

Collection and Care of Adults

In Pearl Harbor, HI, larvae of *Hydroides elegans* settle on biofilmed surfaces throughout the year and can reach high densities on both natural and man-made surfaces (Fig. 1). Several different materials have been used as artificial settlement substrata for the field collection of *H. elegans* (Walters et al. 1997; Lau and Qian 2001; McEdward and Qian 2001; Lau et al. 2002; Walters et al. 2003). We prefer to use small pieces of extruded plastic mesh (Vexar, Internet Inc, Minneapolis, MN) as settlement substrata for collecting *H. elegans* in Pearl Harbor. These screens are hung from a pier approx. 1 m

below the mean low tide line, and within 3-4 weeks thousands of recruits have settled on them and grown to reproductive maturity (Fig. 1.1). These dense populations of worms are then transported back to the laboratory and kept in continuously flowing, unfiltered seawater for several weeks without a noticeable decrease in fecundity.

Vexar® is preferred over solid substrata, because: (1) it greatly increases the surface area of the material; (2) it provides crevices that may entrain larvae near the surface of screen facilitating settlement; and, (3), it allows water flow through the mesh to bring food, oxygen, and remove wastes from settled worms (Walters et al. 1997).

Large populations of adult *H. elegans* can be kept in closed-system aquaria containing either natural or artificial seawater. Additionally, individual worms can be reared separately by allowing larvae to settle on small (1 x 1 cm) biofilmed chips of polystyrene, removing all but one juvenile worm from each chip, and maintaining the chips into individual wells of plastic ice cube trays (Eric Holm, pers. com., Miles et al. 2007). In both settings, adult worms survive and continue producing gametes when fed *Isochrysis galbana* at a final concentration of 6×10^4 cells/ml (see Sect. 3.4.5 for culture instructions).

Spawning

Spawning of *H. elegans* can be achieved using either destructive or non-destructive methods. We typically use the destructive spawning method, because large numbers of gravid worms are available to us throughout the year in Hawaii. When using this method, we remove 30-40 worms from a piece of Vexar® and place them in a small glass dish containing 100 ml of 0.22 µm Milipore-filtered seawater (FSW). To induce release of gametes, the calcareous tubes of the worms are broken in half using forceps, and the abdominal segments of the worms are exposed. This process causes release of thousands of small (~45 µm diameter) orange eggs or clouds of sperm from the abdominal segments of the worm. We then repeat this process until all the worms have been removed from their tubes. After 15-20 minutes, the fertilized eggs are separated from the adult worms and debris by passing them through a 200 µm sieve (Nitex®, Small Parts Inc., Miami Lakes, FL) into a 500 ml beaker. Filtered seawater is added to achieve a volume of 200 ml. This addition of seawater dilutes the sperm concentration to prevent

polyspermy. Fertilization occurs within minutes of exposure of eggs to sperm, and first cleavage occurs approximately 1 hr. after fertilization (23-26° C). Using this method it is easy to obtain tens of thousands of embryos at a time.

If it is not possible to sacrifice large numbers of adult worms to obtain gametes, a non-destructive method may be used. In this method, worms whose tubes are still attached to their substratum are placed in dishes containing FSW, and the aperture of the worm's tube is gently broken with fine forceps. This mechanical disturbance causes release of eggs and sperm into the tube, and the worm then expels the gametes from the tube by muscular peristaltic action. Generally, females induced to spawn using this method release fewer eggs than can be obtained with the destructive method. After the worms have spawned, they can be placed back into their individual containers where they will repair the apertures of their tubes, and can be induced to spawn again in 2-3 days (personal observations). We have also noted that when adult worms are kept individually in ice cube trays, they occasionally release gametes spontaneously after the FSW is changed in the wells of the trays.

Feeding and Care of Larvae

Seawater

In our laboratory, natural coastal seawater (salinity 35 ‰) filtered through a 0.22 µm Millipore filter (FSW) is used in larval cultureto minimize bacterial contamination. We have raised larvae of *H. elegans* in "MBL artificial seawater (Cavanaugh 1975; Bidwell and Spotte 1985; Strathmann 1987) with no deleterious effects. Antibiotics (60 µg/ml Penicillin G and 50 µg/ml Streptomycin Sulfate) may be used if larval mortality is high, but this mixture is generally not required to maintain the larvae through metamorphic competence.

Temperature and light

Larval cultures of *H. elegans* are maintained on the bench top at room temperature (23-26° C) and kept under the ambient lighting regime of the laboratory. However, maintaining larval cultures at 25° C in an incubator provides a greater degree of synchrony of early larval stages. At 24-25° C, larvae attain metamorphic competence

after 5 days in culture. Lower temperatures increase time to competence, at 20° C, larvae become competent to metamorphose after 8-10 days in culture (Wisely 1958, as *H. norvegica*).

Culture vessels

All glassware used for larval culture in our laboratory is scrubbed under running tap water, rinsed several times with de-ionized water, and allowed to air dry prior to use. Additionally, all of our glassware is periodically soaked in a strong acid solution (25% HCl and 25% H_2SO_4) to destroy any organic films that may have developed on the interior surfaces of the containers. Adsorbed organic films hasten the development of a biofilm in the culture vessels, which can provide a metamorphic cue for competent larvae and cause a substantial number of larvae to metamorphose on the walls of the glassware and the surface film. In our laboratory, larvae are cultured in 1 or 2 liter beakers at an initial density of 5-10 larvae/ml. Cultures of larval *H. elegans* are maintained without stirring or aeration with high levels of larval survival through attainment of competence. In order to prevent evaporation, beakers are covered with plastic wrap.

Changing water in cultures

After the second day, the larvae are transferred to clean beakers with fresh FSW. To do this, each larval culture is poured into a small plastic beaker whose bottom has been replaced by a piece of 41 µm Nitex® sieve. The beaker is placed in a small bowl of seawater in a sink, and, as the larval culture is poured through the sieve, the old culture water is allowed to run over the top of the bowl, and the larvae are confined above the screen (see Strathmann 1987). The concentrated larvae are then gently washed from the sieve into clean, acid-washed beakers containing fresh FSW and phytoplankton. Care is taken to retain a small volume of water in the sieve to prevent larvae from being crushed against it. This procedure is subsequently repeated daily until larvae attain competence. Once attaining competence, larvae can be maintained in this manner for several weeks (Unabia and Hadfield 1999).

Larval food and its culture

The unicellular alga *Isochrysis galbana* (Tahitian strain) is the most commonly used food source for larvae of *H. elegans* (Hadfield et al. 1994; Carpizo-Ituarte and Hadfield 1998; Holm et al. 1998; McEdward and Qian 2001; Carpizo-Ituarte and Hadfield 2003; Huang and Hadfield 2003; Lau et al. 2005; Shikuma and Hadfield 2006). However, other algal species have been utilized to raise larvae of this species through metamorphosis (Wisely 1958 as *H. norvegica*; Hadfield et al. 1994). We use *I. galbana* at a density of 6 x 10^4 cells/ml. Larval cultures of *H. elegans* are fed *I. galbana* daily by adding aliquots from our working alga cultures; we do not attempt to separate the alga from its culture media.

In our laboratory*, I. galbana* is grown in a commercially produced, modified Guillard's f/2 media (Micro Algae Grow®, Florida Aqua Farms Inc., Dade City, FL). We syringe filter (0.22 μm) Micro Algae Grow and use it at a working concentration of 1:1000 in autoclaved seawater (salinity 25‰). A stock culture of *I. galbana* is maintained in 50 ml screw-top Erlenmeyer flasks and recultured bi-weekly. Algal cultures for larval cultures are started every 3 days and maintained in autoclaved culture containers described in Switzer-Dunlap and Hadfield (1981). These cultures are then used as a larval food source when the algal populations are in the later portion of their growth phase. All cultures are aerated with aquarium pumps and kept in continuous light supplied by 20-W cool white fluorescent bulbs (83 $\mu E/m^2/s$) at room temperature.

Larval Development

Although the embryonic and larval development of *H. elegans* has been previously described (Wisely 1958 as *H. norvegica*), the timing of larval development is highly dependant on the culture conditions. Larvae cultured in our laboratory develop more rapidly due to the higher ambient temperatures of Hawaii. Cell division proceeds rapidly after first cleavage, and larvae hatch after about 4 hrs. Larvae of *H. elegans* begin feeding as early trochophores approximately 9 hrs after fertilization (25° C), and by 12 hrs they are well developed trochophores with an apical sensory organ (ASO), a single eyespot on the right side of the larva (ES), a prototroch (Pro), and a metatroch (Met) (Fig. 1.5A).

Larvae remain in the unsegmented prototroch stage for approximately 60 hrs. longer. Three days after fertilization larvae have developed into metatrochophores with a second eyespot on the left side of the larval episphere, rudiments of the collar (Col), and elements of the first three abdominal segments including setae (Set) (Fig. 1.5B).

Larvae of *H. elegans* become competent to metamorphose 5 days after fertilization (25°C). The hyposphere of the larvae has lengthened considerably and the gut has shifted posteriorly. The larval midgut (discernable by the algal cells within it, visible in Figs. 15A - C) has been almost entirely displaced from the episphere by the differentiating cerebral ganglia (CG, Fig. 1.5C). In competent larvae, the growth and differentiation of the cerebral ganglia is accompanied with a change in a shape of the larval episphere. The lateral margins of the episphere appear to constrict in the region immediately anterior of the prototroch (compare Figs. 1.5B and 1.5C), so that the previously hemispherical episphere becomes conical and provides a morphological landmark for the development of competence.

Metamorphosis

In addition to exposure to biofilm bacteria, larvae of *Hydroides elegans* can be artificially induced to metamorphose by the bath application of the cations K^+ and Cs^+ and the phosphodiesterase inhibitor 3-isobutyl-1-methylxanthine (IBMX, Sigma, St. Louis, MO). IBMX (0.1mM) induces 80% of the larvae exposed to it to undergo metamorphosis (Holm et al. 1998). Potassium ions (50 mM excess in FSW) typically induce metamorphosis in over 70% of larvae, but the response is much slower than the rate of metamorphosis induced by biofilms (Carpizo-Ituarte and Hadfield 1998). Maximal induction by cesium ions (10 mM excess in FSW) occurs when larvae are placed in Cs^+-supplemented seawater for 3.0 - 4.5 hr and then removed to FSW.

Carpizo-Ituarte and Hadfield (1998) described the morphogenic events associated with metamorphosis in larvae of *H. elegans* (Fig. 6). Competent larvae of *H. elegans* may initiate metamorphosis almost immediately after contacting inductive surfaces and begin the process by excreting a sticky thread from their posterior end that serves to tether the larvae to the substratum. Almost immediately after, larvae lie flat on the surface and begin secreting a primary tube from most or all of the segments. They shape

the newly secreted tube by rotating within it as they erect their setae to push the primary tube away from their bodies (Carpizo-Ituarte and Hadfield 1998). The secretion of the primary tube, which can be completed in as little as 10 minutes after contact with a surface, is an irreversible process that permanently attaches a larva to the substratum. As the primary tube is secreted, the collar is everted, the area immediately surrounding the collar constricts, the larval body elongates, and the metatroch is lost. Simultaneously, the pair of lobes that are the precursors to the branchial radioles become apparent on the anterolateral margins of the episphere of the juvenile. The primary tube is never calcified.

Secretion of the calcified secondary tube begins at the anterior margin of the primary tube approximately 2 hrs after the commencement of metamorphosis, after which new material is added to the secondary tube continuously. As the secondary tube is secreted, the prototroch is resorbed, and the branchial radioles begin to differentiate from the anterior lobes. Metamorphosis is complete and juvenile development has commenced by 11-12 hrs post-settlement (Carpizo-Ituarte and Hadfield 1998). Because both the primary tube and the early portions of the secondary tube are transparent, the events of metamorphosis and early juvenile development are easily observed with relatively low power microscopy (Fig. 6).

In summary, the major tropical marine fouler *Hydroides elegans* has proven to be a near perfect laboratory-animal model for studies of biofouling processes. The information provided above should make it possible to employ this organism for studies of biofouling or questions involving the development of polychaete worms in most laboratories. If scientists attempting to use *H. elegans* in their research find problems in its culture, we would be happy to communicate with them to find solutions.

References

Baier RE (1984) Initial events in microbial film formation. In: Costlow JD, Tipper RC (eds) Marine Biodeterioration: an interdisciplinary study. Naval Institute Press, Annapolis, pp 57-62

Bailey-Brock JH (1987) Phylum Annelida. In: Devaney DM, Eldredge LG (eds) Reef and shore fauna of Hawaii. Bishop Museum Press, Honolulu, pp 213-454

Bastida-Zavala JR, ten Hove HA (2002) Revisions of *Hydroides* Gunnerus, 1768 (Polychaeta: Serpulidae) from the Western Atlantic region. Beaufortia 52: 103-178

Bastida-Zavala JR, ten Hove HA (2003) Revisions of *Hydroides* Gunnerus, 1768 (Polychaeta: Serpulidae) from the Eastern Pacific region and Hawaii. Beaufortia 53: 67-110

Bidwell JP, Spotte P (1985) Artificial Seawaters: Formulas and Methods. Bartlett Publishing Inc., Boston

Brady Jr. RF, Singer IL (2000) Mechanical factors favoring release from fouling release coatings. Biofouling 15: 73-81

Bryan PJ, Qian P-Y, Kreider JL, Chia F-S (1997) Induction of larval settlement and metamorphosis by pharmacological and conspecific associated compounds in the serpulid polychaete *Hydroides elegans*. Mar Ecol Prog Ser 146: 81-90 0.22 µm Milipore-filtered seawater (FSW).

Carlton JT, Hodder J (1995) Biogeography and dispersal of coastal marine organisms: experimental studies on a replica of a 16th century sailing vessel. Marine Biology (Berlin) 121: 721-730

Carpizo-Ituarte E, Hadfield MG (1998) Stimulation of metamorphosis in the polychaete *Hydroides elegans* Haswell (Serpulidae). Biol Bull 194: 14-24

Carpizo-Ituarte E, Hadfield MG (2003) Transcription and translation inhibitors permit metamorphosis up to radiole formation in the serpulid polychaete *Hydroides elegans*. Biol Bull 204: 114-125

Cavanaugh GM (1975) Formulae and Methods of the Marine Biological Laboratory Chemical Room. Marine Biological Laboratory, Woods Hole, pp 84

Costerton JW, Stewart PS, Greenberg EP (1999) Bacterial biofilms: A common cause of persistent infections. Science 284: 1318-1322

Edmondson CH (1944) Incidence of fouling in Pearl Harbor. Occasional Papers of Bernice P Bishop Museum 18: 1-34

Godwin LS (2003) Hull fouling of maritime vessels as a pathway for marine species invasions to the Hawaiian Islands. Biofouling 19 (Suppl): 123-131

Gollasch S (2002) The importance of ship hull fouling as a vector of species introductions into the North Sea. Biofouling 18: 105-121

Hadfield MG, Paul VJ (2001) Natural chemical cues for settlement and metamorphosis of marine invertebrate larvae. In: McClintock JB, Baker W (eds) Marine Chemical Ecology. CRC Press, Boca Raton, pp 431-461

Hadfield MG, Strathmann M (1996) Variability, flexibility and plasticity in life histories of marine invertebrates. Oceanologica Acta 19: 323-334

Hadfield MG, Unabia CC, Smith CM, Michael TM (1994) Settlement preferences of the ubiquitous fouler *Hydroides elegans*. In: Thompson MF, Nagabhushanam R, Sarojini R, Fingerman M (eds) Recent Developments in Biofouling Control. Oxford and IBH Pub. Co., New Delhi, pp 450

Harder T, Lam C, Qian P-Y (2002) Induction of larval settlement in the polychaete *Hydroides elegans* by marine biofilms: an investigation of monospecific diatom films as settlement cues. Mar Ecol Prog Ser 229: 105-112

Holm ER, Nedved BT, Carpizo-Ituarte E, Hadfield MG (1998) Metamorphic-signal transduction in *Hydroides elegans* (Polychaeta: Serpulidae) is not mediated by a G-protein. Biol Bull 195: 21-29

Holm ER, Nedved BT, Phillips N, DeAngelis KL, Hadfield MG, Smith CM (2000) Temporal and spatial variation in the fouling of silicone coatings in Pearl Harbor, Hawaii. Biofouling 15: 95-107

Holm ER, Kavanagh CJ, Meyer AE, Wiebe D, Nedved BT, Wendt D, Smith CA, Hadfield MG, Swain G, Darkangelo Wood C, Truby K, Stein J, Montemarano J

(2006) Interspecific variation in patterns of adhesion of marine fouling to silicone surfaces. Biofouling 22: 233-243

Huang S, Hadfield MG (2003) Composition and density of bacterial biofilms determine larval settlement of the polychaete *Hydroides elegans*. Mar Ecol Prog Ser 260: 161-172

Lau SCK, Qian PY (2001) Larval settlement in the serpulid polychaete *Hydroides elegans* in response to bacterial films: An investigation of the nature of putative larval settlement cue. Mar Biol 138: 321-328

Lau SCK, Mak KKW, Chen F, Qian PY (2002) Bioactivity of bacterial strains isolated from marine biofilms in Hong Kong waters for the induction of larval settlement in the marine polychaete *Hydroides elegans*. Mar Ecol Prog Ser 226: 301-310

Lau SCK, Thiyagarajan V, Cheung CK, Qian P-Y (2005) Roles of bacterial community composition in biofilms as a mediator for larval settlement of three marine invertebrates. Aquat Microb Ecol 38: 41-51

Marshall KC (1981) Bacterial adhesion in natural environments. In: Berkeley RCW, Lynch JM, Melling J, Rutter PR, Vincent B (eds) Microbial adhesion to surfaces. Ellis-Horwood, New York, pp 187-196

McEdward LR, Qian PY (2001) Effects of the duration and timing of starvation during larval life on the metamorphosis and initial juvenile size of the polychaete Hydroides elegans (Haswell). J Exp Mar Biol Ecol 261: 185-197

Naldrett MJ, Kaplan DL (1997) Characterization of barnacle (*Balanus eburneus* and *B.crenatus*) adhesive proteins. Mar Biol 127: 629-635

Paul MD (1937) Sexual maturity of some organisms in the Madras Harbor. Curr Sci (Bangalore) 5: 478-479

Schultz MP, Finlay JA, Callow ME, Callow JA (2003) Three Models to Relate Detachment of Low Form Fouling at Laboratory and Ship Scale. Biofouling 19 (Suppl): 17-26

Shikuma NJ, Hadfield MG (2006) Temporal variation of an initial marine biofilm community and its effects on larval settlement and metamorphosis of the tubeworm *Hydroides elegans*. Biofilms 2: 213-238

Smith AM, Callow JA (2006) Biological adhesives. Springer, Berlin, Heidelberg

Stein J, Truby K, Darkangelo Wood C, Stein J, Gardner M, Swain G, Kavanagh C, Kovach B, Schultz M, Wiebe D, Holm E, Montemarano J, Wendt D, Smith C, Meyer A (2003) Silicone foul release coatings: Effect of the interaction of oil and coating functionalities on the magnitude of macrofouling attachment strengths. Biofouling 19 (Suppl): 71-82

Strathmann MF (1987) Reproduction and development of marine invertebrates of the Northern Pacific Coast. University of Washington Press, Seattle

Switzer-Dunlap M, Hadfield MG (1981) Laboratory culture of *Aplysia*. In: Hinegardner RE, Fay R (eds) Marine invertebrates, laboratory animal management. National Academy of Sciences, Washington, D.C., pp 199-216

ten Hove HA (1974) Notes on *Hydroides elegans* (Haswell, 1883) and *Mercierella enigmatic* (Fauvel, 1923), alien serpulid polychaetes introduced to the Netherlands. Bulletin Zoologisch Museum (University of Van Amsterdam) 4: 45-51

Townsin RL (2003) The ship hull fouling penalty. Biofouling 19 (Suppl): 9-15

Unabia CRC, Hadfield MG (1999) Role of bacteria in larval settlement and metamorphosis of the polychaete *Hydroides elegans*. Mar Biol 133: 55-64

Walters LJ, Hadfield MG, del Carmen KA (1997) The importance of larval choice and hydrodynamics in creating aggregations of *Hydroides elegans* (Polychaeta: Serpulidae). Invertebr Biol 116: 102-114

Walters LJ, Smith CM, Hadfield MG (2003) Recruitment of sessile marine invertebrates on Hawaiian macrophytes: Do pre-settlement or post settlement processes keep plants free from fouling? Bull Mar Sci 72: 813-839

Wiegemann M (2005) Adhesion in blue mussels (*Mytilus edulis*) and barnacles (genus *Balanus*): mechanisms and technical applications. Aquat Sci 67: 166–176

Wisely B (1958) The development of a serpulid worm, *Hydroides norvegica*, Gunnerus (Polychaeta). Aust J Mar Freshw Res 9: 351-361

Woods Hole Oceanographic Institution (1952) Marine fouling and its prevention. United States Naval Institute, Annapolis

Zibrowius H (1971) Les espèces Méditerranéennes du genre *Hydroides* (Polychaeta Serpulidae): remarques su le prétendu polymorphisme de *Hydroides uncinata*. Tethys 2: 691-746

Zobell CE, Allen EC (1935) The significance of marine bacteria in the fouling of submerged surfaces. J Bacteriol 29: 239-251

Table 1.1. Settlement and attachment strength of Hydroides elegans to two surfaces. Competent larvae of *H. elegans* were allowed contact with biofilmed test surfaces for 18 hrs before evaluation. The average force required to remove adult tubes of *H. elegans* was determined using a hand-held strain gauge (Holm et al. 2006). In the calibrated flow-cell tests, juvenile worms were exposed to a shear wall-shear force equivalent to 100 Pa for 4 minutes before evaluation.

Coating	Settlement Density (worms/cm^2)	Push-off Force (kPa)	Worms Remaining (%) after Calibrated Flow-Cell test
Veridian®	42.14 $\pm$18.48	224.5 $\pm$ 80	81.3 $\pm$ 18.1
Uncoated Glass	22.41 $\pm$ 12.12	240 $\pm$ 180	77.5 $\pm$ 21.5

Figure 1.1. A dense accumulation of tubes of *Hydroides elegans* on Vexar® after a one-month submersion in Pearl Harbor, Hawaii.

Figure 1.2. Induction of metamorphosis of *Hydroides elegans* by mono-specific biofilms on plastic Petri dishes prepared from isolated bacterial strains. Controls include: (1) dishes similarly treated with filter-sterilized culture medium from each bacterial strain (S1, S2, S3, S4); natural biofilms (NB) developed in flowing seawater; (3) untreated Petri dishes filled with filtered seawater (FSW) and (4) dishes rinsed with fresh culture medium (M). KMB1, *Pseudoalteromonas luteoviolacea*; KMB2, *Flexibacter* sp.; KMB3, *Cytophaga* sp. Inoculation densities of all strains was approx. 10^{-8} cells/ml. Bars represent mean present of larvae that metamorphosed in 24 h + SD (n= 5 replicates per treatment) (reproduced from Huang and Hadfield 2003)

Figure 1.3. Bacterial densities in single-species biofilms (see Fig. 2), counted under fluorescence microscopy after formalin fixation and DAPI staining. Inoculation densities of all strains were approx. 10^{-8} cells/ml. Controls are the same as in Fig. 2. Bars represent bacterial cell numbers x 10^3 mm^{-2} + SD (n=25, consisting of area counts per replicate and 5 replicate dishes per treatment; replicate effects were not significant). (reproduced from Huang and Hadfield 2003).

Figure 1.4. Strength of adhesion of tubeworms and barnacles in the field (A) and a laboratory trial (B). **A**, mean attachment strength of barnacles and tubeworms on test coatings. Data are for *Hydroides dianthus* at Indian River and *H. elegans* at Pearl Harbor, and *Balanus eburneus* at Indian River (reproduced with permission from Stein et al 2003). **B**, percent of juveniles remaining after exposure to a wall shear stress equivalent to 100 Pa for four minutes. Data are for *H. elegans* and *Balanus amphitrite* (previously unpublished data from our laboratory).

Figure 1.5. Differential interference contrast microscopy images of larval development in *Hydroides elegans*. (A) Lateral view of trochophore stage larva (12 hrs. post-fert at 25° C). (B) Ventral view of metatroch stage larva (72 hrs. post-fert). (C) Ventral view of a competent larva (~120 hrs. post-fert). ASO, apical sensory organ; CG, cerebral ganglia; Col, collar; ES, eyespot; Met , metatroch; Pro, prototrochal band; Set, setae. Scale bars = 50 µm.

Figure 1.6. Time course of metamorphosis in *Hydroides elegans*. Photographs represent a competent larva at the moment of metamorphic induction (0 h) and at selected times during the first 11.3 h after induction. P, prototroch; c, collar; b, branchial lobes; it, initiation point of calcareous tube; br, branchial radioles; t, calcareous tube covering the worm (Carpizo-Ituarte and Hadfield 1998).

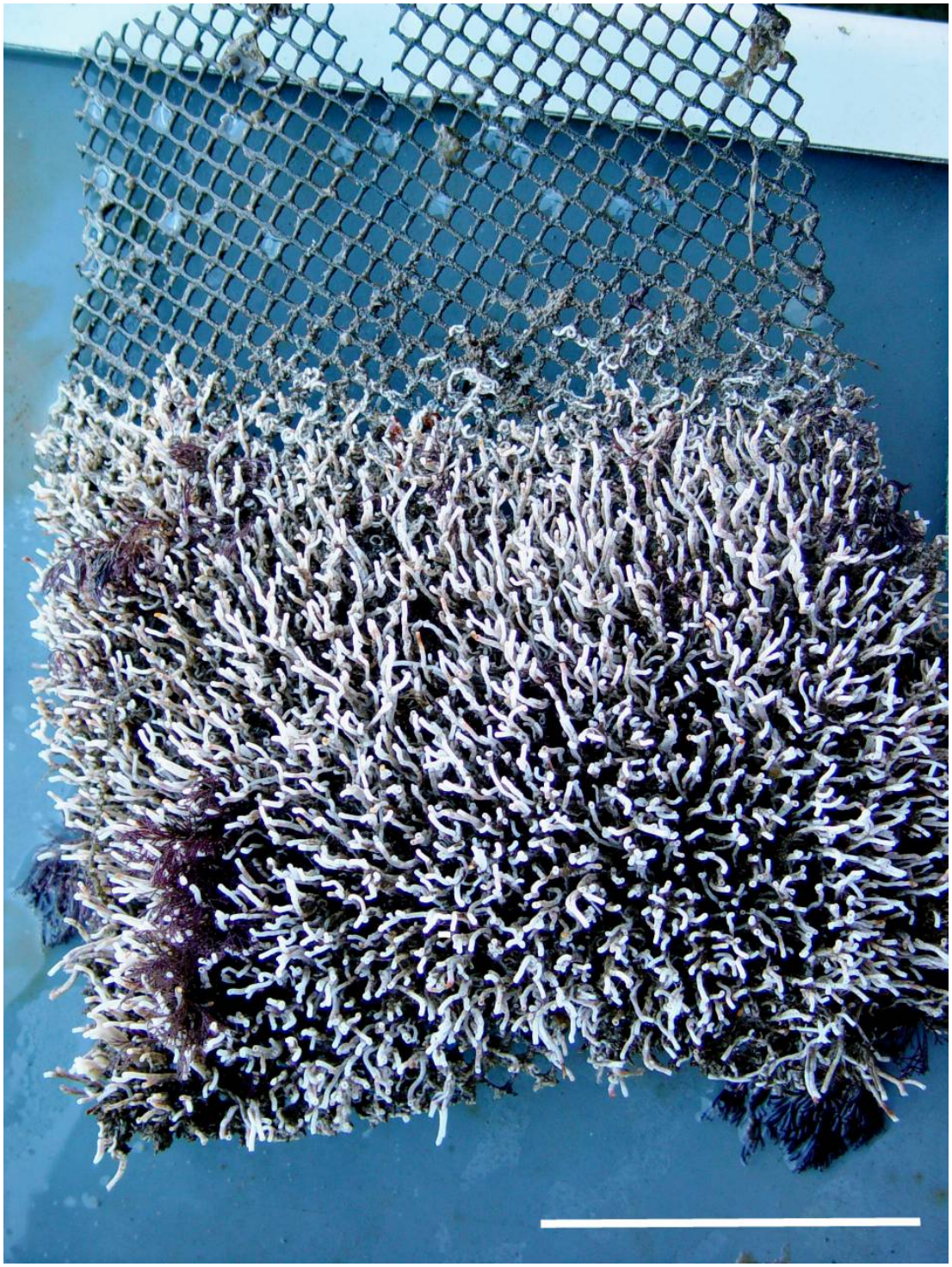

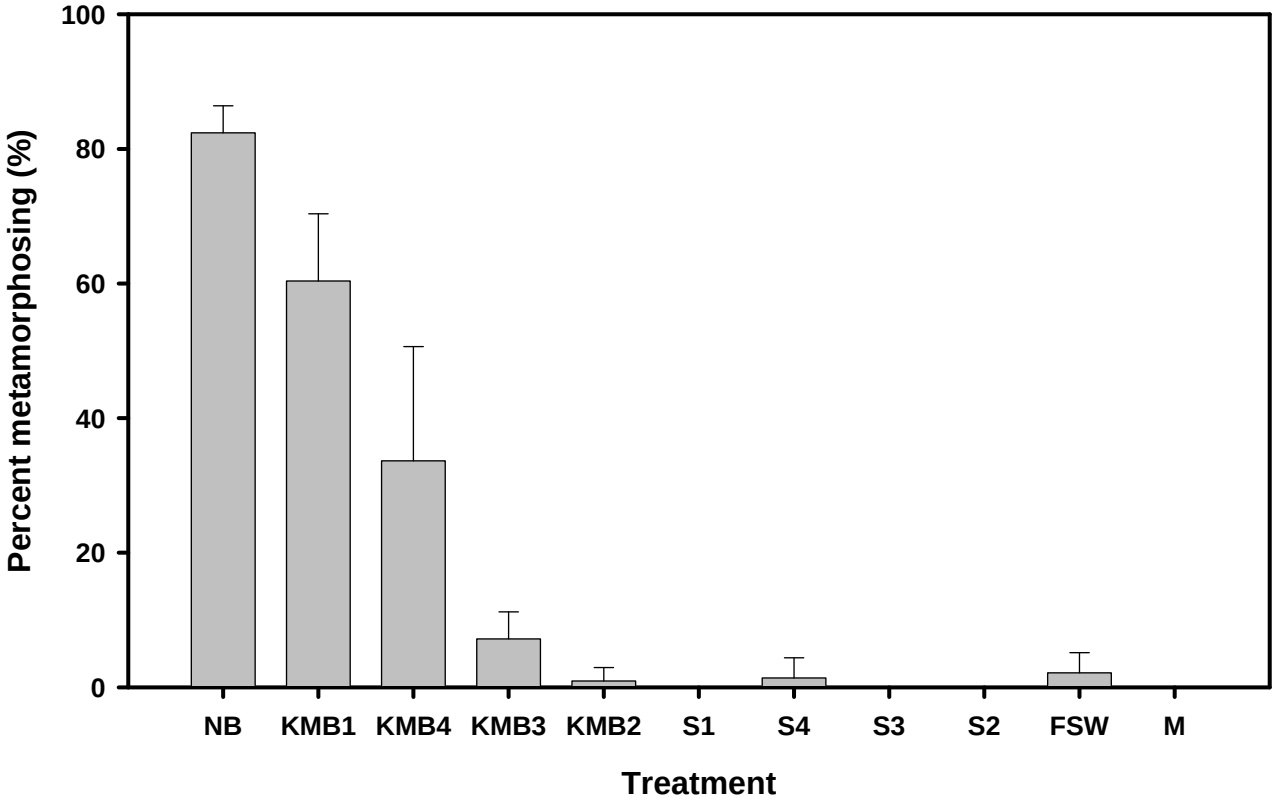
100
80
60
40
20
0
Percent metamorphosing (%)
NB
KMB1
KMB4
KMB3
KMB2
S1
S4
S3
S2
FSW
M
Treatment

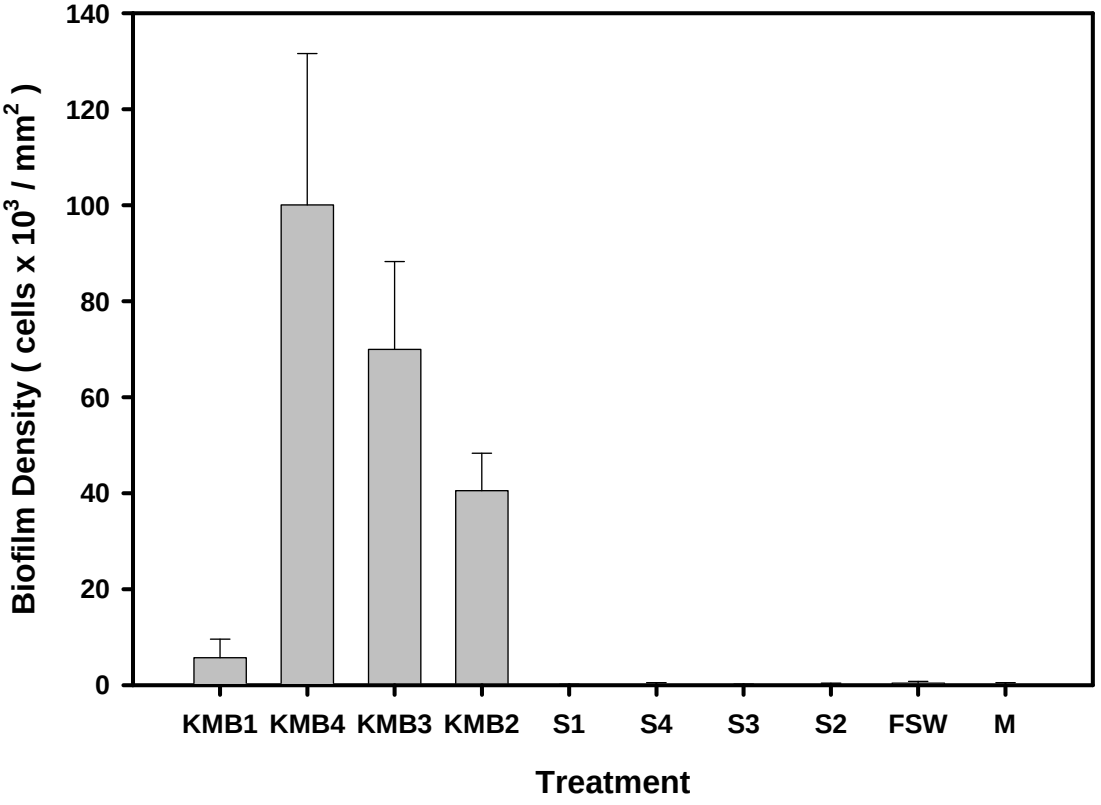
Biofilm Density (cells x 10^3 / mm^2)
140
120
100
80
60
40
20
0
KMB1
KMB4
KMB3
KMB2
S1
S4
S3
S2
FSW
M
Treatment

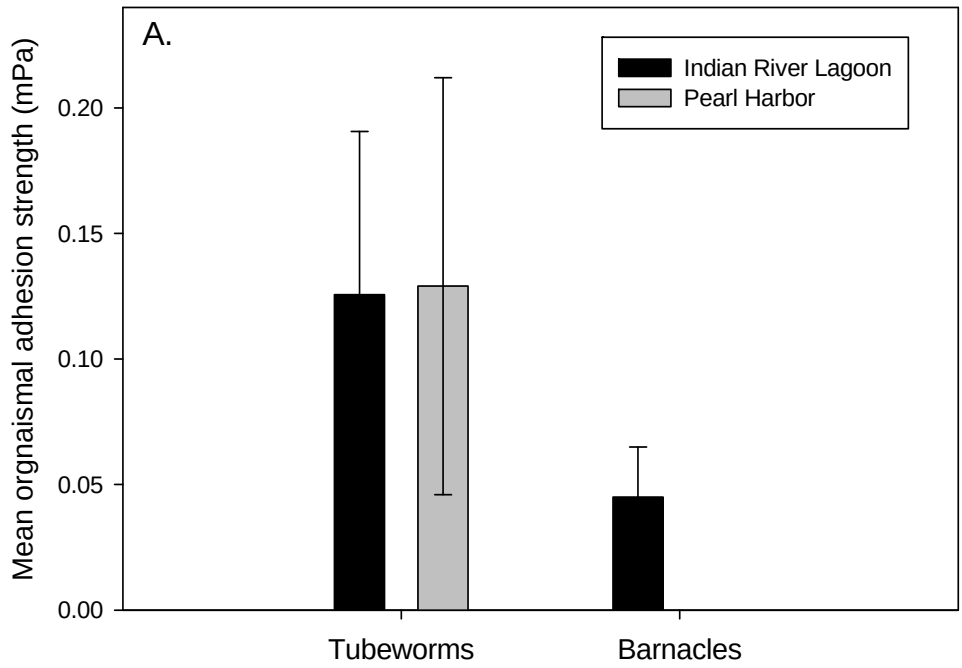
A.
Indian River Lagoon
Pearl Harbor
Mean orgnaismal adhesion strength (mPa)
0.00
0.05
0.10
0.15
0.20
Tubeworms
Barnacles

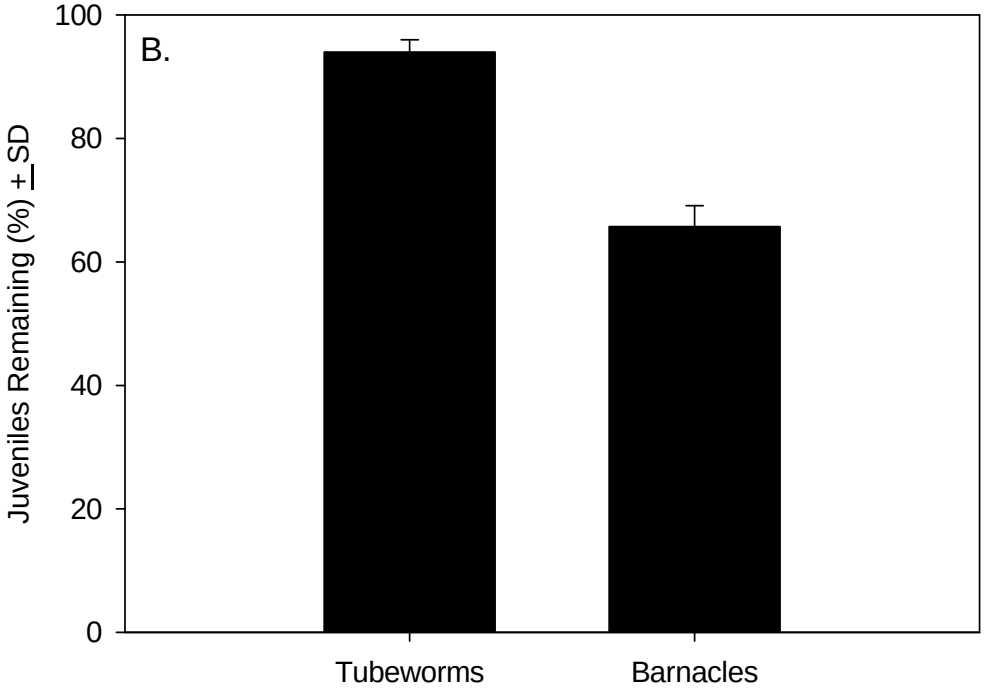
B.
Juveniles Remaining (%) ± SD
0
20
40
60
80
100
Tubeworms
Barnacles

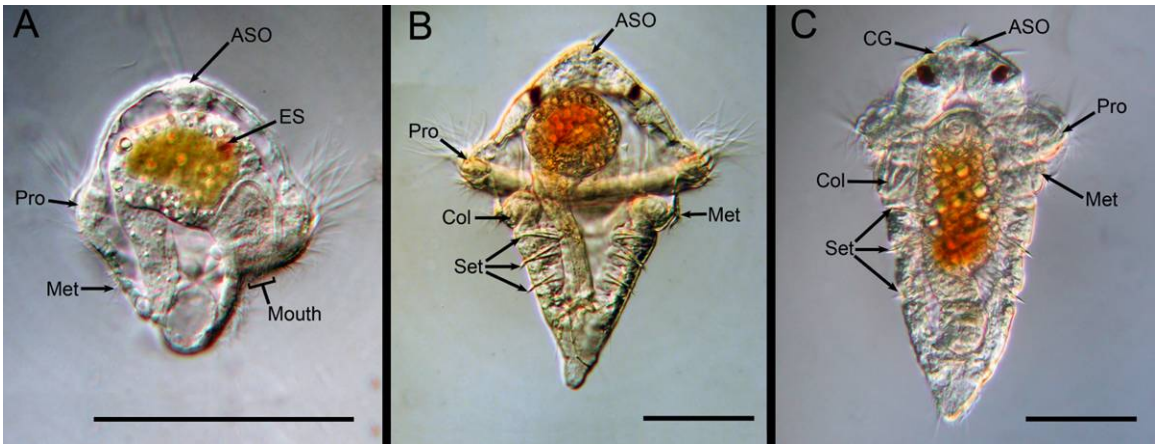
A
ASO
ES
Pro
Met
Mouth
B
ASO
Pro
Col
Set
Met
C
CG
ASO
Pro
Col
Met
Set

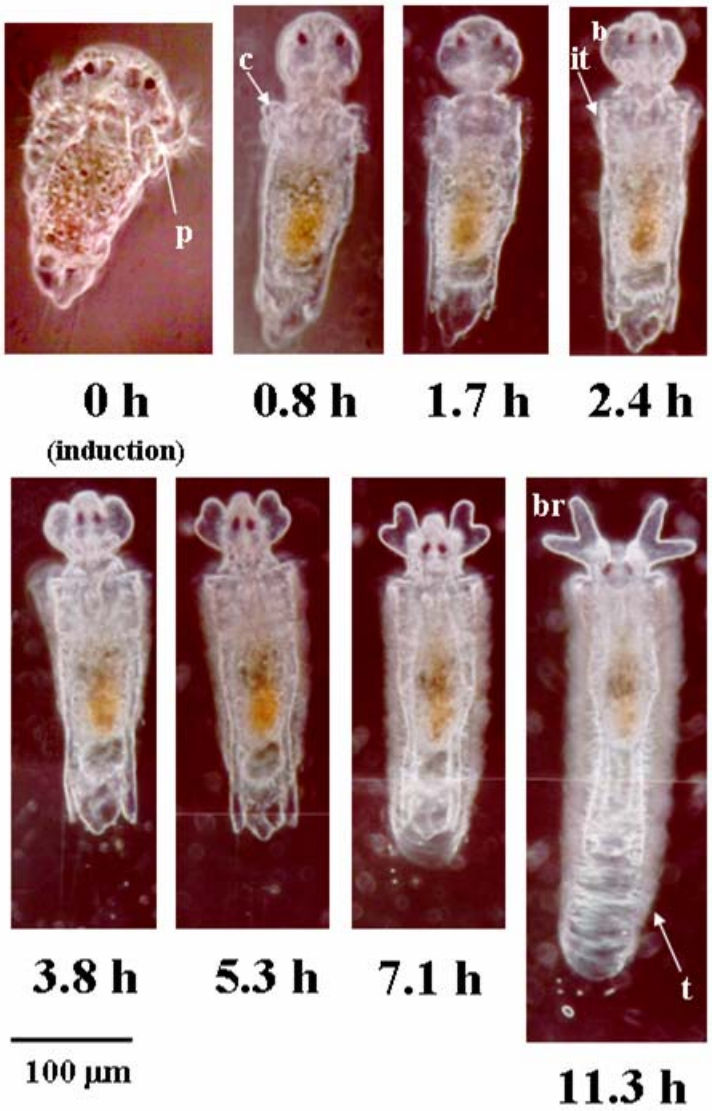
p
c
b
it
0 h
(induction)
0.8 h
1.7 h
2.4 h
br
3.8 h
5.3 h
7.1 h
t
100 µm
11.3 h

Chapter 2.

CONFOCAL LASER SCANNING MICROSCOPE ANALYSIS OF NEUROGENESIS IN THE SERPULID POLYCHAETE HYDROIDES ELEGANS

Introduction

Annelids are a speciose group that occur in wide variety of ecological habitats and display a range of morphologies (Ruppert and Barnes, 1994; Rouse and Pleijel, 2001). While there has been considerable debate over the phylogenetic relationships among the Polychaeta, Hirundinia, and Oligochaeta, it is generally thought that the polychaetes are ancestral for the group but may be paraphyletic (Rousset et al., 2007; Struck et al., 2007; Zrzavy et al., 2009). The indirect developing trochophore larvae of the polychaetes are the may be type larva of the phylum (Lacalli, 1984). Most phylogenetic topologies (Aguinaldo et al., 1997; Giribet et al., 2007; Rousset et al., 2007; Dunn et al., 2008; Kupriyanova et al., 2008) have split the Articulata clade and called for the placement of the annelids within the lophotrochozoans. This split has created an interest in comparative developmental studies that focus on the mechanisms utilized for the construction of the adult body plans (e.g. mechanisms of segmentation in disparate groups like annelids, arthropods, and chordates), and also afford the opportunity for the comparison of development between polychaetes and other lophotrochozoans (Seaver and Shankland, 2000; Seaver et al., 2001; Seaver, 2003; Seaver et al., 2005; Kerner et al., 2006; Seaver and Kaneshige, 2006; Denes et al., 2007; Tessmar-Raible et al., 2007; Arendt et al., 2008; Simionato et al., 2008; Boyle and Seaver, 2009; Meyer and Seaver, 2009; Dray et al., 2010; Tomer et al., 2010).

While there have been extensive studies of the embryology and development of polychaetes (reviewed by Anderson 1966, 1973), there have been surprisingly few thorough descriptions of the development of the nervous system (Lacalli, 1976; 1981; Bhup and Marsden, 1982; Lacalli, 1986; 1988; Hay-Schmidt, 1995; Voronezhskaya et al., 2003; McDougall et al., 2006; Brinkmann and Wanninger, 2008), and most do not provide a consistent description of either early nervous system development or morphology. Kleinenberg (1886) supposed that the early nervous system of polychaete

larvae was composed of a prototroch nerve, four large multi-polar cells in the episphere, developing cerebral ganglia, and a dorsomedial nerve in the hyposphere. In contrast, Meyer (1901) and Butschli (1912) described a complicated orthogon consisting of a prototroch nerve, three nerve rings in the episphere, one ring in the hyposphere, and seven longitudinal nerves. Akesson (1967) later rejected this description and instead described a reticulum of multi-polar cells in the episphere of the larvae of *Lopadorhynchus*. Research by Lacalli (1981, 1984) on the development and ultrastructure of the nervous system of *Spirobranchus polycerus* and *S. giganteus* provided the most complete description of the central nervous system (CNS) in polychaete larvae and is composed of: an apical sensory organ; 2) prototrochal and metatrochal nerves, and 3) the pharyngeal and suboral complexes that innervate the feeding organs of the larva.

Hay-Schmidt (1995) first used antibodies raised against serotonin (5-hydroxytryptamine [5HT]) and the neuropeptide FMRF-amide on polychaete larvae and described a centralized larval nervous system consisting of a well developed apical sensory organ (ASO), circumesophageal connectives, and a suboral, ventral ganglion in *Polygordius lacteus.* These studies supported the consensus opinion that neurodevelopment in polychaete larvae occurred in an anterior to posterior progression (Anderson, 1973).

Veronezhskaya et al. (2003) performed an immunochemical study of neural development in *Phyllodoce maculata* and provided a description of the appearance of the larval CNS in pre-hatching stages. This examination of early larval stages showed that the earliest neural cell body appeared in the posterior of the larva, and that fibers projected from this cell developed in a posterior to anterior direction. Voronezhskaya et al. (2003) suggested that these tracts may serve as a positional framework for elements of the later developing adult CNS. This developmental sequence contradicts the traditionally held notion of an anterior to posterior development of the CNS in polychaetes and is similar to the pattern of neural development observed in molluscs (Croll, 2000).

Dorresteijn et al. (1993) documented neural development in larvae of *Platyneris dumerilli* and showed that neural development proceeded from posterior to anterior, and

that the precursors of the ventral nerve cords (VNC) originated from posteriorly positioned paired cell bodies in *P. dummerilli*. Yet another pattern of early neural development occurred in larvae of *Scolopes armiger* (Orrhage and Müller, 2005) and *Parapionsyllis minuta* (Orrhage and Müller, 2005; Müller, 2006). In larvae of both of these organisms, the earliest appearing immunoreactive cells developed in the dorsolateral regions of the prostomium and their projections developed anteriorly to form a set of cerebral commisures, and after crossing the ventral midline, the axons projected posteriorly into the hyposphere. Additionally, there was a second pair of neurites that originated in the hyposphere and crossed the prototroch at the future location of the circumesophageal connectives. These axons continued to project anteriorly through development, and finally meet to form second commisure within in the developing brain (Orrhage and Müller, 2005).

Yet another pattern of development occurred in larvae of *Sabellaria alveolata*. Serotonergic fibers were the first neuronal elements to appear and were located adjacent to the chaetal sacs in the first larval segment. The growth cones of these fibers proceeded anteriorly in more developed larvae and formed the circumesophageal connectives and terminated in the cerebral commisures of larvae of *S. alveolata* (Brinkmann and Wanninger, 2008).

These studies as well as descriptions of neurogenesis in serpulids *Pomatocerus lamarckii* (McDougall et al., 2006) and *Spirobis* cf. *spirobis* (Brinkmann and Wanninger, 2009) showed that neurogenesis may not always proceed in the classically defined anterior to posterior progression. Orrhage and Müller (2005) postulated a second mode of neurogenesis for polychaetes in which neural development proceeds from both the episphere and hyposphere of the larvae and fibers from both anteriorly and posteriorly positioned neurons form the ventral nerve cords and circumesophageal connectives.

Additionally, McCougall et al (2006) suggested that the mode of larval development may correlate with neuronal development. In lecithotrophic larvae, the authors hypothesized that the rudiments of the adult nervous system develop earlier than the larval CNS. The present paper utilizes immunocytochemistry and confocal laser scanning microscopy to provide a description of the development of both the larval and nascent adult central nervous systems of the microserpulid polychaete *Hydroides elegans*

Hydroides elegans is a common member of the worldwide fouling community in tropical and sub-tropical waters. Due to its absolute requirement of a bacterial inductive cue (Hadfield et al., 1994; Unabia and Hadfield, 1999) as well as the relative ease required for larval culture, the larvae of *H. elegans* are increasingly being used in studies concerned with the induction of metamorphosis (Hadfield et al., 1994; Walters et al., 1996; Walters et al., 1997; Holm et al., 1998; Unabia and Hadfield, 1999; Lau and Qian, 2001; McEdward and Qian, 2001; Harder et al., 2002; Carpizo-Ituarte and Hadfield, 2003; Huang and Hadfield, 2003). Scanning laser confocal microscopy and antibodies raised against 5HT, FMRF-amide, tyrosine hydroxylase (TH) and β-tubulin were used to track neurogenesis and neural development from early in larval development through the attainment of metamorphic competence in *H. elegans.*

Materials and Methods

Larval Culture

Adults of *Hydroides elegans* were collected from Pearl Harbor, Hawaii and kept in running seawater tables at the Kewalo Marine Laboratory. When embryos were needed, several adults were placed in small dishes containing 0.22 μm filtered seawater (FSW), and removed from their tubes to induce spawning of both male and female worms. Fertilization occurred rapidly and embryos were separated from adult worms and debris by passage through a 325 μm nylon mesh (Nitex, Small Parts Inc., Miami Lakes, FL). Larvae were cultured through competence as described in Chapter 1.

Immunohistochemistry

Procedures modified from Croll and Chiasson (1989) and Voronezhskaya et al. (2003) were used to determine the expression of 3 neurotransmitter phenotypes and β-tubulin in the developing larvae of *H. elegans*. Larvae were concentrated by sieving cultures through a 41 μm Nitex sieve and relaxed in 3.7% $MgCl_2$ in FSW for 2-5 minutes at room temperature. Larvae were then fixed for 1 h in either (1) 3.5% formaldehyde in 0.22 μm filtered seawater (4°C) for the detection of 5-HT , FMRF-amide, and β -tubulin

like immunoreactivities, or (2) ice-cold, acidified methanol (addition of glacial acetic acid for a final concentration of 1%) for the detection of tyrosine hydroxylase (TH).

After fixation, larvae were washed (3 X 5 minutes) in phosphate buffered saline (PBS; 50 mM Na_2PO_4, 140 mM NaCl pH 7.4). Larvae were then washed (3 X 30 minutes) in PBT (PBS + 0.01% Triton X100) and further incubated for 20-30 minutes in blocking solution (PBT + 5% v/v heat inactivated normal goat serum). Larvae were incubated for two days at 4°C in one of 4 primary antibodies (Abs), the polyclonal antibodies anti-5-HT (raised in rabbit, DiaSorin, Stillwater, MN) and anti-FMRF-amide (raised in rabbit, DiaSorin), or the monoclonal antibodies anti-TH (raised in mouse, DiaSorin) and anti-β-tubulin (Clone E7, raised in mouse, Developmental Studies Hybridoma Bank, University of Iowa). The polyclonal antibodies were used at a dilution of 1:500 (v/v in blocking solution), while the monoclonal antibodies were used at a working dilution of 1:50 (anti-TH) or 1:5 (anti-β-tubulin).

After incubation in primary antibodies, larvae were subjected to three 2-3 minute washes with PBT, followed by three washes (30 min) in PBT, and then incubated in blocking solution (30 min). Larvae were subsequently incubated for 12-24 hrs at 4 °C in either Alexa Fluor®488 goat anti-rabbit (1:1000 dilution, Molecular Probes,) or in Alexa Fluor® 546 goat anti-mouse (1:1000 dilution, Molecular Probes) secondary antibodies. After incubation in the secondary antibodies, larvae were washed several times in PBS, immersed overnight in 3:1 glycerol: PBS, and mounted on glass microscope slides in the PBS:glycerol solution that included the anti-fading agent 2% n-propyl-gallate (Giloh and Sedat 1982).

In order to visualize the position of labeled nerves within the larvae, a fluorescently tagged phalloidin was used as a counterstain to provide morphological landmarks within larvae. A 1:500 dilution of Alexa Fluor® 594 phalloidin (Molecular Probes) was co-incubated with the secondary antibody solutions. The patterns of muscle development in larvae of *H. elegans* are described in Chapter 5.

Double labeled larvae

For anti-5HT and anti-tubulin double labeling, larvae were processed as usual and then incubated in a mixture of anti-5HT Abs and anti-β-tubulin Abs (Clone E7, raised in mouse, Developmental Studies Hybridoma Bank, University of Iowa, 1:5 in blocking

solution) for 2 days at 4° C, washed as usual and then incubated in a mixture of Alexa Fluor® 488 IgG goat anti-rabbit and Alexa Fluor® 546 goat anti-mouse (Molecular Probes,1:1000) overnight at 4°C. The preparations were then washed and mounted as above.

Controls

As negative controls, larvae were processed without incubation in primary antibodies, and did not exhibit detectable fluorescence. Positive controls included parallel processing of the adult CNS of the nudibranch *Phestilla sibogae* with the anti-5HT, anti-FMRFa, and anti-TH antibodies, which exhibited typical staining as described elsewhere (Croll et al., 2001).

Photography

A minimum of 40-50 whole mount specimens was examined at each developmental stage using a Zeiss LSM 510 scanning confocal microscope (Zeiss, Germany) equipped with the appropriate laser and filter combinations. Digital images of optical sections of the preparations were produced using the LSM 510 imaging software (Version 4) and single plane projections of these images, which have a greater depth of focus than single images, were produced using the same software package. Plates of these images were constructed using Adobe Photoshop CS3 (Adobe Systems, San Jose, CA), and the brightness and contrast of each figure was adjusted to provide consistency within the plate.

Results

Although the embryonic and larval development has previously been described for *H. elegans* (as *H. norvegica,* Wisley, 1958), the timing of larval development is highly dependant on the culture conditions. In this study, a staging system that was similar to that described by Seaver et al. (2005) was used. The staging of development of *H. elegans* has been split into 6 stages: hatching (Stage 1); trochophore (Stage 2); late trochophore (Stage 3); early metatrochopore (Stage 4); precompetent nectochaete (Stage 5); and competent nectochaete (Stage 6). Each stage is illustrated by distinct morphological changes as well as changes in immunoreactive patterns.

Mid Stage 1 (7 hrs post-fertilization)

Mid Stage 1 larvae were motile but non-feeding trochophores. A thickening and cellularization of the apical plate (AP, Fig. 2.1A) as well as the presence of tuft of apical cilia were present in the episphere of the larva. In the hyposphere of the larva, the prototroch (Pro, Fig. 2.1A) had developed, and rudiments of the gut were present. However, neither the lumen within the gut nor the openings of the mouth and anus were visible (Figs. 2.1A and 2.2A). Labeling larvae of this stage with phalloidin also demonstrated the absence of larval muscle fibers.

Serotonin-like Immunoreactivity

A single, serotonin-like-immunoreactive (5HT-LIR) cell was present in the hyposphere of the larva. The soma of this 5HT-LIR posterior cell (S-PC) was positioned dorsal to and just anterior of the future opening of the larval anus (Fig. 2.2A), and a pair of bilaterally symmetrical processes projected anteriorly from each side of the cell. These processes were directed ventrally toward the rudiment of the mouth (Fig. 2.2B) and were the only immunoreactive fibers within the larvae.

Late Stage 1 (9 hrs post-fertilization)

Serotonin-like Immunoreactivity

Coincident with the appearance of the lumen of the midgut, the fibers from the S-PC soma have extended and met above the upper lip of the larval mouth (Fig. 2.2C). Shortly after, a second cell shows serotonin-LIR (5HT-LIR). The soma of this cell (S-SO) was located on the ventral surface of the hydrosphere of the larva and was just posterior of the larval mouth. An additional pair of immunoreactive fibers had extended from this cell body towards anterior lip of the mouth (Fig 2.2C). A second pair of immunoreactive processes have diverged from the fiber tract of the S-PC cell and terminated on the processes of the S-SO cell, interconnecting the tracts of both of these cells.

FMRFamide-like Immunoreactivity

Faint FMRFamide-like immunoreactivity (FMRFa-LIR) was present in the apical sensory organ (ASO), but this labeling had not developed enough to provide resolution of

specific cell bodies or fibers in the early stage trochophores of *H. elegans* (data not shown).

Stage 2 (12 hrs post-fertilization)

Larvae that had developed to Stage 2 were feeding trochophores. In addition to the development of the apical sensory organ (ASO), a single eyespot (ES, Fig 2.1B) had developed on the right side of the episphere of the larva. The larval gut was functional (Fig. 2.1B) and was bounded by numerous muscle fibers (see phalloidin reactive fibers, Fig. 2.2D and 2.2E). The diameter of the midgut had expanded and the anterior portion of the stomach had projected into the episphere (Fig 2.1B). In addition to the prototroch (Pro), a metatrochal ciliary band (Met) and a neurotroch (NT) had also developed in the hyposphere of the larva. A large anal vesicle (AV) that is ventral to the anus has also differentiated by the beginning of Stage 2 (Fig. 2.1B).

Serotonin-like Immunoreactivity

The immunoreactivity of the S-PC and S-SO cells increased in Stage 2 larvae, and a stout, posteriorly-directed projection had developed from the soma of the S-PC cell (Fig. 2.2C). This projection appeared to innervate a posterior cilium that was positioned above the anus of the larva. In addition to the fibers encircling the mouth, two other fibers had developed 5HT-like immunoreactivity. One of these fibers encircled the prototroch, and connected with the oral 5HT-LIR fibers. A second, apically directed fiber had reached the midpoint of the episphere on the right ventral side of the larva (data not shown). In slightly older larvae, this fiber (S-AF) terminated against an immunoreactive perikaryon (S-A1) located within the right side of the ASO (Fig. 2.2D).

Tyrosine Hydroxylase-like Immunoreactivity

The onset of tyrosine hydroxylase-like immunoreactivity (TH-LIR) had occurred in Stage 2 larvae. Six cells closely associated with the larval gut displayed TH-LIR. Three of these cells were positioned within the wall of the pharynx of the larva and are collectively referred to as the TH-LIR stomatogastric cells (T-O1, T-O2, T-O3, Fig. 2.2E). Cell T-O1 has single, laterally-flattened soma, and was positioned below the lower lip of the mouth (Fig. 2.2E). The second cell body (T-O2) was positioned on the

upper left portion of the pharynx, and the third soma was located deeper within the upper left side (T-O3) of the pharynx (Fig. 2.2E)

An additional pair of TH-LIR perikarya (T-M1 and T-M2) was lateral of the larval gut and underlied the metatroch of the larvae (Fig. 2E). The perikaryon of the final TH-LIR cell (T-NT) was ovoid, laterally-flattened, and positioned slightly to the left of the midline of the larva, within the metatroch. Cell T-NT issued an immunoreactive fiber toward the cell T-M2 on the corresponding side of the larva. In addition to this fiber, a number of other fibers had developed from the cell bodies displaying TH-LIR. A fiber originated from each T-M1 and T-M2 cells and terminated above the mouth (Fig. 2.2E). An additional TH-LIR fiber encircled the pharynx, and provided points of contact for each of the TH-LIR cells within the stomatogastric system, but both the origin and termination of this fiber were unclear.

FMRFamide-like Immunoreactivity.

The faint immunoreactivity that was present in the ASO of earlier larval stages increased in intensity and became resolved as single soma showing FMRFa-LIR in the ASO (F-A1, Fig. 2.2F). Additionally, a pair of multi-reticulated cells (Ret) had developed along the dorsal portion of the hyposphere near the transition from the stomach to the intestine (Fig. 2.2F). A short, thin, weakly immunoreactive process served as a point of contact between the RET cell bodies. Figure 2.3 provides a summary of development of larvae of *H. elegans* up to Stage 2 in larval development.

Stage 3 (48 hrs post-fertilization)

Stage 3 larvae had approximately doubled in size, and the larval stomach had expanded and occupied most of the free space within the episphere of the larva (Fig. 1C). The hindgut has also thickened considerably and contracted vigorously as the larvae swam. The hyposphere of the larva has elongated and the ectodermal and mesodermal bands of the hyposphere had thickened within the hyposphere. Within this thickening, immediately posterior of the metatroch, rudiments of the shell glands have begun to develop (see phalloidin reactive fibers, Figs 2.4A and 2.4C).

Serotonin-like Immunoreactivity

In early Stage 3 larvae, an additional pair of cells (S-MC1 and S-MC2) showing 5HT-LIR have appeared in the hyposphere of the larva. The somata of these cells were positioned along the ventral midline of the larva in the presumptive region of sub-esophageal ganglion (Fig. 4A). A pair of slender fibers served as a point of connection between these cells and those fibers of the S-PC cell (Fig. 2.3A).

Slightly later in development, additional processes and cell bodies showed 5HT-LIR. Paired somata (S-TC1 and S-TC2) began to show 5HT-LIR along the ventral midline of the larval hyposphere. These cell bodies are ventral of the perikarya of S-PC and appear to be the first elements of a terminal commisure (Fig. 2.4D). There was asynchronous development of 5HT-LIR in these paired cells, with the right (S-TC1) developing immunoreactivity first (Fig. 2.4D). In addition to these somata, a pair of fibers developed immunoreactivity. These fibers were part of the developing circumesophageal connectives (S-CEC, Fig 2.4D) and appeared to originate from the earlier developing cell bodies of the S-MC 1 and S-MC2. The fiber within the right CEC appears to be independent of the other anteriorly directed fiber on that side of the larval episphere (compare positions of S-CEC and S-AF, Fig. 2.4D).

Tyrosine Hydroxylase-like Immunoreactivity

By Stage 3, another two cells had joined the TH-LIR perikarya in the stomatogastric system. The somata of these cells were vase shaped and projected a short dendrite that terminated on the surface of the gut. These cells (T-O4 and T-O5) were the corresponding pair of presumed sensory cells that were positioned on the left side of the larva in Stage 2, and these cells contacted the immunoreactive fiber encircling the pharynx (Fig. 2.4B).

In addition to these cells, new axons had developed that connected the TH-LIR cells of the metatroch to the stomatogastric system. These cell T-M1 projected fibers contacted both the cell T-O1 as well as a posteriorly projected fiber from the cell T-NT forming a Y-shaped structure (Fig. 2.4B). Additionally, cell T-M2 also extended a fiber that terminated within this fiber network (Fig. 2.4B). Finally, two more cells outside of the stomatogastric complex had developed faint TH-LIR. A pair of cells (T-D1 and T-D2) was located within the dorsolateral region of the metatroch (Fig. 2.4B).

FMRFamide-like Immunoreactivity

The overall pattern of FMRFa-LIR showed little change in Stage 3 larvae other than additional cells in the ASO displayed FMRFa-LIR. By this stage, there were 4 vase-shaped, presumed sensory cells within the ASO that were arrayed around the intensely labeled apical neuropil (F-A1, F-A2, F-A3, F-A4, Figs. 2.4C and 2.4E). An FMRFa-LIR fiber appeared on the right side of the larvae (F-AF), and was directed posteriorly along the right side of the larval episphere (Figs. 2.4C and 2.4E). The reticulated cells (RET) continued to show strong FMRFa-LIR and thin processes from these cells encircled the larval midgut (Fig. 2.2F). Figure 2.5 provides a summary of neural development at this stage of larval development.

Stage 4 (72 hrs post-fertilization)

Stage 4 larvae have increased their overall size and the hyposphere has continued to lengthen. In the episphere of the larva, a second eyespot developed on the left side of the larva. The paired cerebral ganglia continued to develop, filling in the space between the eyespots, and forming a horse-shoe shaped structure with the ASO at its apex (Fig. 2.1D). Within the hyposphere, the ventral ectoderm has thickened considerably, and the first three thoracic segments of the adult body have developed. Each segment contained 2 pairs of simple neuropodial chaetae. The distal tips of these chaetae erupted from the body wall and serve as an easily recognizable marker for each of three segments (Set, Fig. 2.1D). In addition to the thoracic segments, the rudiments of the collar (which is everted early in metamorphosis) began to develop as an in-pocketing of ectoderm that was posterior of the metatroch in larvae of *H. elegans* (Fig 2.1D).

Serotonin-like Immunoreactivity

As the first thoracic segment developed in the hyposphere, several additional cells showed 5HT-LIR in it. The somata of both of the cells were located in the pygidium of the larvae (S-T1 and S-T2) and the axons of these cells were present in the developing ventral nerve cords (S-VNC, Fig. 2.6A). These fibers appeared to overlie the fibers from the S-PC, and the fibers of the S-PC may have served as a framework for the developing VNC in these segments. The 5HT-LIR immunoreactive fibers were still present in the prototrochal nerve, and a single fiber had developed 5HT-LIR in the metatroch (S-Met, Fig. 2.6A). Two additional immunoreactive cells also developed in the sub-esophageal

ganglion, forming a medial cluster of 4 cells (SubEs, Fig. 2.6A). The anteriorly directed fibers from S-MC1 and S-MC2 have progressed through the circumesophageal connectives (CEC) to the developing cerebral ganglion. An additional pair of axons developed in the CEC, but the origin of these fibers was unclear (Fig. 2.6A). Four cells within the developing cerebral ganglion had also developed 5HT-LIR (S-CG1—S-CG 4). These cells directed axons into the cerebral commisure and together with the processes from the CEC formed a tangled network of fibers within the cerebral commisure that was divided into dorsal and ventral fiber tracts (Figs. 2.6A and 2.6B).

Serotonin-LIR cells did not develop synchronously within the segmental ganglia of the larvae of *H. elegans*. In slightly older larvae (Fig 6B) there were a total of eight additional 5HT-LIR immunoreactive somata developed within the ganglia in thoracic segments one and two. Two pairs of 5HT-LIR neurons had developed in both of the first and second thoracic segmental ganglia (Seg 1 and Seg 2, Fig. 2.6B) and the somata of each of the cells were located medial to the VNC. Although there were three segments within the larval hyposphere at this developmental stage, no cells were detectable within the "third segment." A short, thin immunoreactive axon was also present in the developing segmental commisure of the 2nd thoracic segment, but it could not be traced back its cell somata (Fig 2.6B).

Tyrosine Hydroxylase-like Immunoreactivity

In metatrochophore larvae, eight cells showed immunoreactivity in the ASO and developing cerebral ganglia. Four presumed sensory cells developed TH-LIR (T-A1—T-A4 respectively) adjacent to the ASO. These cells occupied positions on the on lateral edges of the dorsal (T-A2 and T-A4) and ventral surfaces (T-A1 and T-A3) of the ASO and projected short axonal processes into an immunoreactive region of the cerebral commisure (Fig. 2.6C). This region consisted of both a neuropil and immunoreactive fibers, and appeared to be positioned posterior of the 5HT-LIR immunoreactive processes in the developing brain (compare Fig. 2.6B and 2.6C). In addition to the immunoreactive cells in the ASO, two pairs of cells have developed immunoreactivity in both the left and right cerebral ganglia (T-CG1 — T-CG4), and also project short processes into the adjacent commisure (Fig. 2.6B). Finally, four additional cells (T-CEC1 – T-CEC4) had

developed TH-LIR in the episphere of the larva. The somata of T-CEC 1 and T-CEC2 are nestled against the immunoreactive fibers of the CEC on the ventral side of the larva (Fig. 2.6C) and projected a short axon into the CEC. The perikarya of T-CEC3 and T-CEC4 occupied a similar position of the dorsal side of CEC and also projected short fibers into the CEC (not shown).

The pharyngeal cells have increased in their immunoreactivity and a metatrochal fiber (T-Met) has developed and served as a point of connection between the ventrally (T-M1 and T-M2) and dorsally (T-D1 and T-D2) positioned cells within the metatroch (Fig. 6C). In addition to the cells surrounding the larval pharynx, a number of other cells had developed TH-LIR in the hyposphere of Stage 4 larvae. Of these newly developed cells, the cells with the strongest immunoreactivity (T-SG1 and T-SG2) are located within what are presumed to be the developing shell glands and projected a short process toward a single immunoreactive fiber (T-VNC) within the ventral nerve cords (Fig 2.6C). This fiber appears to originate from cells that had developed in the nascent terminal ganglion (T-T1 and T-T2) and terminates at the level of the metatroch, amongst the complex of TH-LIR immunoreactive fibers of the stomatogastric system (Fig. 2.6C). An additional pair of cells also developed TH-LIR in the terminal ganglion. The somata of these cells (TH-T3 and TH-T4) are located adjacent to the TH-LIR fiber within the VNC and projected a short process that abuts against this fiber (Fig. 2.6C). Finally, faintly immunoreactive cells were present along mediolateral regions of the first and second thoracic segments. These cells had vase-shaped dendrite that projected to the epithelial surface and due to this morphology, were presumed to be sensory neurons (T-Sen1 – T-Sen4). The axons from these neurons was directed medially and synapsed with the single TH-LIR fiber in the VNC (Fig. 2.4C, only T-Sen2 and T-Sen4 are visible).

FMRFamide-like Immunoreactivity

The most conspicuous additions of FMRF-LIR elements in the segmented larvae were in the episphere of the larvae of *H. elegans*. The immunoreactive region within the cerebral commisure had greatly expanded and showed strong FMRFa-LIR immunoreactivity in the region between the halves of the cerebral ganglia. The neurons

F-A1 – F-A4 (collectively labeled F-Apical in Fig. 2.6D) also showed strong increases in immunoreactivity. In addition to these cells, 4 other cells developed FMRFa-LIR in the brain. One pair of cells was positioned within the lateral edges of the cerebral commisure (F-CG1 and F-CG2) (Fig. 2.6D). The remaining cells were paired, faintly-immunoreactive, sensory cells that projected dendrites to the dorsal epithelium of the larval episphere, and directed an axon into the cerebral commisure (not shown). Finally, 2 pairs of posteriorly directed immunoreactive fibers had developed and extended through the CEC and into both of the ventral nerve cords (F-VNC, Fig. 2.6 D). Figure 2.7 provides a summary of neural development in Stage 4 larvae.

Stage 6 (120 hrs post-fertilization)

Larvae that had developed to Stage 6 have attained metamorphic competence. The cerebral ganglia continued to develop (Fig. 2.1E) and had almost entirely filled in the episphere with cells. The gut has shifted posteriorly and the larval midgut has been almost completely displaced from the episphere. In Stage 6 larvae, a change in shape of episphere accompanied the attainment of metamorphic competence. The lateral margins of the episphere appeared to constrict in the region immediately anterior of the prototroch (compare Figs.1D and 1E). Uncini had developed in the hyposphere but their positions were out of register with the with the parapodial chaetae. There were no uncini in the first thoracic segment and an additional pair of neuropodial uncini was located within the pygidium of competent larvae (Fig. 2.1E). Commissural nerves had developed in each of the thoracic segments, and β-tubulin-like immunoreactivity (tub-LIR) showed that two commissural nerves had developed with in the first thoracic segment (Figs. 2.8A, 2.9A, and 2.10A). The more anterior nerve contained many tub-LIR axons and ran under the subesophageal ganglion (Figs 2.8a and 2.10A). The second commisure contained few axons and was posterior of the first one (Fig 2.10A). The remaining segments only contained a single commisure (Fig. 2.10A)

Serotonin-like Immunoreactivity

In competent larvae, eight cells in the cerebral ganglia showed immunoreactivity to serotonin antibodies. In addition to the cells that had appeared earlier, four more cells

developed 5HT-LIR. These cells were paired across the midline of the brain (S-CG5 -- S-CG8 respectively, Figs. 2.8b, 2.9B, and 2.11B) and each directed a short axon into the cerebral commisure. The perikarya of these cells were smaller in diameter than the earlier developing cells and were closer to the immunoreactive regions within the cerebral commisure (Fig. 11B). The cell within the ASO (S-A1) no longer showed reactivity to the serotonin antibody. The terminal end of the anteriorly directed fiber S-AF (Fig. 2.2D) also no longer showed 5HT-LIR (Figs. 2.8B and 2.11B), and could not be discerned among immunoreactive elements of the cerebral commisure (Fig. 2.8B). Additional fibers had developed in the cerebral commisures of Stage 6 larvae. Three 5HT-LIR fibers were present in the ventral tract of the commisure and two immunoreactive fibers were present in the dorsal tract (Fig. 2.8B).

In the hyposphere of Stage 6 larvae, the number of 5HT-LIR cells had increased in the sub-esophageal and thoracic ganglia. A total of six cells had 5HT-LIR in the subesophageal ganglion and the perikarya of these newly developed cells were nestled around S-MC1 and S-MC2 within the ganglion (Figs. 2.8B and 2.10B) Axons from these cells contributed to the numerous fibers in more anterior commisure in the first segment. (Figs. 2.8B and 2.10B). The three immunoreactive cells in the each thoracic ganglion in the first segment were present, but their immunoreactivity was diminished (Figs. 2.8B, 2.9A and C). There were three pairs of 5HT-LIR cells within the ganglia of the second segment (Figs 2.8B and 2.10B), and four 5HT-LIR somata in the third segmental ganglia with 2 weakly immunoreactive cells present in each ganglion (Fig 10B). Perikarya of these cells were medial to the 5HT-LIR of the VNC. Additionally, there were 5HT-LIR fibers in each of the commisures, including a single weakly immunoreactive fiber in the more posterior commisure of the first segment and two 5HT-LIR fibers in the both the second and third segmental commisures (Fig 2.10B). The VNC of competent larvae had a minimum of three 5HT-LIR axons in each cord and several more axons adjacent to each of the segmental ganglia (Fig. 2.10B). The cell S-PC also was present and had maintained its position above the anal vesicle, but the immunoreactivity of the perikarya and its fibers had diminished (Figs. 2.8B and 2.11B). A summary of 5HT-LIR in Stage 6 larvae is shown in Figures 2.9A and C.

TH-like immunoreactivity

Overall, few new cells showed TH-LIR in competent larvae and the greatest difference between Stage 4 and Stage 6 larvae was an increase in immunoreactivity in all of the earlier developing cells. A single pair of new cells showed TH-LIR in the cerebral ganglia (T-CG5 and T-CG6, Figs. 8C, 9C, 11C), these cells possessed weakly immunoreactive perikarya, were positioned medial to the cell bodies of T-CG3 and T-CG4 within the cerebral ganglia, and projected a short axon into the TH-LIR cerebral commisure (Figs. 8C and 10C).

The remaining cells that had developed TH-LIR were located in the larval hyposphere and within the collar rudiment and lateral portions of thoracic segments. Two pairs of moderately immunoreactive cell bodies developed within each of the collar rudiments, (T-Col1 -- T-Col4, Figs. 2.8C and 2.9C). The remaining pair of TH-LIR perikarya was located in lateral region third segment and projected an axon to the region of the third segmental ganglia (T-Sen 3 and T-Sen4, Figs 2.8C, 2.9B, and D). These cells appeared to the homologs of the presumed sensory cells T-Sen1 and T-SEN2. Additionally, an immunoreactive fiber originating from the cell (T-NT) had projected beneath the neurotroch and terminated in the pygidium of the larva (Fig. 2.8C). Figures 2.9B and E summarize the pattern of TH-LIR in Stage 6 larvae.

FMRFamide-like Immunoreactivity

A large number of cells developed FMRFa-LIR in the episphere of Stage 6 larvae. In addition to the cells within the ASO, and 16 -20 new cells developed immunoreactivity (Fig. 2.11D and E). The perikarya of the majority of these cells were arrayed close to the ventral sides of cerebral ganglia, had long tapering dendrites and sent short process into the FMRFa-LIR region of cerebral commisure (Figs 2.10D, 2.10E, 2.12C, 2.12F). In addition to these ventrally located cells, three pairs of FMRF-LIR cell bodies had developed just below the dorsal epithelium of the episphere of competent larvae of *H, elegans* (Fig. 2.11E). Immunoreactivity also intensified in the 2 pairs of FMRFa-LIR fibers within the CEC and VNC. Both sets of fibers showed numerous varicosities with punctuate labeling (Figs. 2.5D and Fig 2.7D). There also was strong immunoreactivity within the VNC in areas lateral to the segmental ganglia (Fig 2.10C.) Further, there were

at least two FMRFa-LIR axons within the first and third segmental commisures, but no FMRFa-LIR axons were present in the second commisure (Fig. 2.10C). The only FMRFa-LIR perikarya in the hyposphere of Stage 6 larvae were are located in the third segment (Figs. 2.8D and 2.10C). These cell bodies were peripheral of the VNC and sent a single fiber into the third segmental ganglion. Figures 2.9C and F provide a summary of the number and relative position of FMRF-LIR in Stage 6 larvae.

Discussion

There have been multiple investigations of the general architecture and development the nervous system in the polychaetes. The earliest studies suggested a central nervous system consisting of multiple, evenly-spaced nerves running from the larval episphere to the hyposphere and multiple commisures running between these nerves to form orthogonal arrangement of neuronal fibers within the larva (Myer, 1901 Wolereck, 1904). However, later studies in larvae of *Lopadorhynchus* sp. (Åkesson, 1967) and *Polygordius laectus* (Hay-Schmidt, 1995) disproved this idea. These studies and multiple others of polychaete larvae demonstrated that the ground plan for the central nervous system in segmented larvae consisted of an anterior, dorsally-positioned cerebral ganglion, paired ventral nerve cords, circumesophageal connectives, a prototrochal nerve, and an apical sensory organ (Anderson, 1966; Lacalli, 1981; Bhup and Marsden, 1982; Lacalli, 1984; 1986; 1988; Hay-Schmidt, 1995; Orrhage and Müller, 2005; McDougall et al., 2006; Müller, 2006; Brinkmann and Wanninger, 2008; Brinkmann and Wanninger, 2009; Wanninger et al., 2009; Brinkmann and Wanninger, 2010b; a).

The current study revealed the sequence of appearance and interconnection of the elements of both larval and adult central nervous system (CNS) during the larval development in the serpulid polychaete *Hydroides elegans*. Here, the larval central nervous system is defined as the apical sensory organ (ASO), apical nerves, nerves underlying the ciliated trochal bands, and innervation of the larval stomatogastric system. Further, the adult central nervous system is defined as paired cerebral ganglia, circumesophageal connectives ventral nerve cords (VNC), and segmental ganglia within the hyposphere of larvae of *H. elegans.* There were subpopulations of cells within all of

these structures that were immunoreactive to at least one of the antibodies used in this study.

Early developing immunoreactive cells in polychaetes

Neural development in polychaetes was classically thought to have occurred in an anterior to posterior progression during larval development with fibers originating in the larval episphere forming the ventral nerve cords (VNC) (Bhup and Marsden, 1982; Lacalli, 1984; Hay-Schmidt, 1995; Orrhage and Müller, 2005). This pattern of early neural development does not appear to be well conserved throughout the polychaetes and several other patterns of early neuronal development have been described in disparate groups (Struck et al., 2007; Zrzavy et al., 2009) of polychaete larvae.

The earliest detectable elements of the larval nervous system did not develop within the larval CNS of *H. elegans* (Fig. 2.2A), but instead, a posteriorly-positioned serotonin-like-immunoreactive (5HT-LIR) cell in the periphery of the larvae of *H. elegans* (Fig 2.2A) developed first. The morphology, position, transmitter phenotype and trajectory of the neurites of the S-PC cell in *H. elegans* suggest that it may be homologous to the 5HT-LIR cells "sp1" in *Phylodoce maculata* (Voronezhskaya et al., 2003) and "psc" in the serpulid *Pomatoceros lamarckii* (McDougall et al., 2006). These authors hypothesized that the early appearing cells and their processes act as scaffolding for the later developing ventral nerve cords. Subsequent development of the VNC on top of these fibers in larvae of in *H. elegans* (Fig. 2.4A) and the persistence of S-PC and its fibers through competence (Figure 2.5B and 2.7B) support this supposition.

While neurogenesis appears to be similar between, *Hydroides elegans* and another serpulid, *Pomatoceros larmarckii*, this pattern of neural development may not be shared by all members of the Serpulidae. A recent paper detailing the neural development of the spirobid polychaete *Spirorbis* cf. *spirorbis* did not describe any posterior 5HT-LIR-positive cells in early stage embryos (Brinkmann and Wanninger, 2009). Instead the earliest appearance in the nervous system occurred in the VNC of the un-hatched larvae (Brinkmann and Wanninger, 2009). Perhaps the differences in developmental modes, brooding (*S.* cf *spirorbis)* vs. planktonic development (*H. elegans*), influences early neuronal development in the Serpulidae. As phylogenies of polychaetes become better

resolved, it will be interesting to determine an ancestral pattern of early neural development within the polychaetes.

Immunoreactivity in apical sensory organs (ASO) in polychaetes

The apical sensory organ (ASO) is a common larval organ within the polychaetes (Ruppert and Barnes, 1994), and the ancestral polychaete is thought to possess an ASO in its episphere (Wanninger, 2008). There is a great diversity in the number, position, and transmitter phenotype of immunoreactive cells in the ASO of polychaetes (Hay-Schmidt, 1995; Voronezhskaya et al., 2003; McDougall et al., 2006; Brinkmann and Wanninger, 2008; Wanninger, 2008; Brinkmann and Wanninger, 2009; Wanninger, 2009). Larvae of *Phyllodoce maculata* have seven immunopositive cells, four FMRFa-LIR and three 5HT-LIR cells, respectively, in the ASO at the time of hatching (Voronezhskaya et al., 2003).

Yet another pattern was observed by Brinkmann and Wanninger (2008) in larvae of *Sabellaria alveolata.* In these larvae, the ASO had neither 5HT-LIR nor FMRFa-LIR cells and only had an immunoreactive apical ring that coalesced into the cerebral connectives in older segmented larvae. Within the serpulids, the ASO is present in competent larvae but the number and diversity of immunoreactive cells is as variable as in more distantly related polychaetes. Larvae of *Filogana implexa* have no cells showing *FMRFa-LIR* or 5HT-LIR in the ASO at competence. McDougall (2006) described the presence of FMRFa-LIR immunoreactive cells in the ASO of *Pomatoceros lamarckii*, but fail to provide a count of the number of cells. There are variable numbers (3-7) of 5HT-LIR neurons in competent larvae *Spirorbis* cf. *spirorbis* (Brinkmann and Wanninger, 2009), while competent larvae of *H. elegans* had eight to nine flask shaped cells immunoreactive to FMRFa in their ASO (Fig. 2.5D and 2.6D).

In an attempt to make comparisons of neurogenesis and the larval nervous systems among annelids and other lophophorates, Wanninger (2008) postulated that the last common ancestor (LCA) of the annelids had four serotonergic immunoreactive cells in its ASO. The pattern of innervation of the ASO *H. elegans* certainly does not comply with this pattern and most closely resembles the in number but not transmitter phenotype of larvae of polyplacophoran molluscs (Friedrich et al., 2002; Voronezhskaya et al., 2002).

The stomatogastric system and trochal nerves in polychaetes

Unlike other polychaete larvae (Orrhage and Müller, 2005; Brinkmann and Wanninger, 2008), the stomatogastric system of *H. elegans* was not innervated by either 5HT-LIR or FMRFa-LIR fibers. Instead, the current study revealed an undescribed subpopulation of neurons that have of tyrosine hydroxylase-like immunoreactivity and innervate the stomatogastric system (Figs 2.2E 2.5B, and E). These TH-LIR elements persist and proliferate through larval development and are thus present in competent larvae of *H. elegans*. The location of these cells closely resembles the position of cells within the pharyngeal and suboral complexes of larvae of *Spirobranchus polycerus* (Lacalli, 1984), and may be homologous them. Hopefully, other studies will be undertaken to determine if TH-LIR cells in the gut is an innovation in *H. elegans* or common within other polychaete larvae.

Innervation of the trochal bands in polychaetes

Two immunoreactive fibers are present beneath the trochal bands of larvae of *H. elegans.* Tyrosine hydroxylase immunoreactive fibers were present in the prototroch, metatroch, and as a single fiber underneath the neurotroch in larvae *H. elegans* (Figs 2.6C and 2.8D). The presence of these fibers and their interconnection with the TH-LIR elements of the stomatogastric system probably suggests that parts TH-LIR nervous system may be involved with the control of feeding in *H. elegans.* However, the morphology of the TH-LIR cells in other peripheral tissues (i.e. the collar rudiments and the segmental sensory cells) may suggest that TH-LIR cells may have broader sensory functions as well.

Additionally, 5HT-LIR fibers are present in both the metatrochal and prototrochal nerves of precompetent and competent larvae (Fig 6B and 8B). The presence of a serotonergic fiber associated with the prototroch appears to be a shared character among the annelids (Wanninger et al., 2005; Brinkmann and Wanninger, 2008; Wanninger, 2008; Brinkmann and Wanninger, 2009; Wanninger, 2009).

The adult central nervous system in polychaetes

Serotonergic-LIR, FMRFa-LIR, and TH-LIR were present in both the ventral nerve cords (VNC) and circumesophageal connectives in both precompetent and competent larvae of *H. elegans* (Figs. 2.6 – 2.10). The presence of both FMRFa-LIR and

5HT-LIR fibers in the ventral nerve cords appeared to be a shared character among the polychaete larvae studied thus far (Voronezhskaya et al., 2003; Wanninger et al., 2005; Brinkmann and Wanninger, 2008; Wanninger, 2008; Brinkmann and Wanninger, 2009; Wanninger, 2009). The development of the circumesophageal connectives in *H. elegans* appeared to be bi-directional, with cell bodies in both the cerebral ganglia and segmental ganglia projecting axons through the CEC. Orrhage and Müller (2005) predicted a similar pattern of development for the ventral nerve cords and CEC in other polychaetes. Posteriorly and anteriorly directed axons would develop simultaneously and would give rise to two pairs of nerves within the ventral nerve cords, a pair of main ventral nerves and a pair of paramedical nerves, respectively. These nerves would remain separate from one another and with fibers from the median nerve (i.e. fibers the neurotroch) would form a proposed penta-neural pattern within the segments of polychaete larvae. However, the development of the CEC in *H. elegans* differed from the proposed ground pattern of development in several ways. First, there is a substantial temporal decoupling between the development of anteriorly and posteriorly directed axons. Unlike the proposed model, the anteriorly directed axons reach their targets in the developing cerebral ganglia approximately 12 h before the posteriorly directed fibers reach the pygidium (Fig. 2.4D and 2.6C). Additionally, there is only one nerve in each of the nerve cords (Fig 2.10A) instead of two separated axonal bundles. Finally, the median fiber tract only consists of a single TH-LIR fiber that is lost after metamorphosis (data not shown). Instead of a penta-neural pattern, competent larvae of *H. elegans* only have two major nerves running along the anterior-posterior axis.

Only a few cell bodies within the segmental ganglia showed immunoreactivity to the antibodies used in this study. These cell bodies showed 5HT-LIR and were confined to the suboral and first segmental ganglia in competent larvae of *H. elegans*. This appears to be a common pattern in the segmented stages of polychaete larvae, and development of 5HT-LIR neurons in segmental ganglia must occur after metamorphosis (Hessling et al., 1999; Orrhage and Müller, 2005; Müller, 2006).

The cerebral ganglia of *Hydroides elegans* that began developing in Stage 4 larvae do not have numerous immunoreactive cells at metamorphic competence (Stage 6), but the cerebral commisures showed high immunoreactivity for all of the antibodies

tested (Figs 2.8-12). Only a total of 14 cells in the cerebral ganglia were immunoreactive to the antibodies tested. The four pairs of cells having 5HT-LIR their soma (S-CG1-S-CG8) were dorsally positioned with in the cerebral ganglia and extended a short process into the heavily labeled cerebral commisure (Fig 2.6A). Unlike the serotonergic cells, the TH-LIR cell bodies (T-CG3-T-CG6) were located more ventrally within the each ganglion and were much closer to the cerebral commisures (Fig. 6B), and six FMRFa-LIR neurons were nestled against both the ventral and dorsal cerebral commisures (See Fig 2.12 for summary). In addition to the cells within the cerebral ganglia, there were numerous other cells in the episphere that showed either FMRFa-LIR or TH-LIR in competent larvae of *H. elegans.* At least 12 cells were immunoreactive to FMRFa antibodies. All had tapering dendritic processes and the perikarya were positioned both dorsal and ventral of the cerebral ganglia (Figs. 2.11D, E, and 12) and from this morphology, may be sensory. Six of these cell bodies were positioned immediately below the dorsal epithelium in two paired clusters (Fig. 2.11E), and their position within the episphere of the larvae may be adjacent to a series of gland cells in the dorsal epithelium of larvae of *H. elegans* (as *H. norvegica,* Wisely, 1958) and *Pomatoceros triqueter (Segrove, 1941)*. An additional two pairs of cells were positioned directly below the below the larval eye spots (Fig 2.6D) and due to their position and immunoreactivity, may be similar to putative photoreceptor cell in *Platyneries dumerilli* (Jekely et al., 2008). Numerous FMRFa-LIR cells were also described in the episphere of larvae of *Polygordius lacteus* (Hay-Schmidt, 1995), but the author made no distinction between neurons that were in the ASO and those within the cerebral ganglia.

Eight additional neurons had TH-LIR and had dendritic processes projecting to the surface of the larvae (Fig 2.6C). Four of these cells (TH-A1 – TH-A4) are of particular interest because they are immediately adjacent to the larval ASO (Figs. 2.8C, 2.11C, and 2.12), and may be involved in the sensation of the metamorphic cues.

In summary, the results of this study indicate that complex developmental pathways lead to the development of both larval and adult nervous systems in larvae of *H*. elegans These neuronal circuits develop in close spatial proximity to each other and are not independent of one another as suggested by Lacalli (1984). Additionally, Orrhage and Müller, (2005) postulated that the mode of larval development effects the timing of

the development of the adult precursors in polychaete larvae. For example, the adult nervous system develops later in larval development in planktotrophs than in lecithotrophs. Early neuronal development in *H. elegans* supports this supposition because the earliest neuronal cell that develops in Stage 1 larvae actually is not a rudiment of the developing adult CNS , but a larval neuron that provides a potential framework (Fig. 2B, 2C) for the later development of VNC (Fig.2.4A).

References

Aguinaldo AMA, Turbeville JM, Linford LS, Rivera MC, Garey JR, Raff RA, Lake J. 1997. Evidence for a clade of nematodes, arthropods and other moulting animals. Nature 387:489-493.

Åkesson B. 1967. On the nervous system of the *Lapadohynchus* larva (Polychaeta). Arkiv for Zoologi 20(2):55-78.

Anderson DT. 1966. The comparative embryology of the polychaeta. Acta Zool 47:1-42.

Anderson DT. 1973. Embryology and phylogeny of annelids and arthropods. New York: Pergamon Press.

Arendt D, Denes AS, Jekely G, Tessmar-Raible K. 2008. The evolution of nervous system centralization. Philos Trans R Soc Lond B Biol Sci 363(1496):1523-1528.

Bhup R, Marsden JR. 1982. The developement of the central nervous system in *Capitella capitata* (Polychaeta, Annelida). Can J Zool 60:2284-2295.

Boyle MJ, Seaver EC. 2009. Evolution, development and ecology of Capitella sp. I: a waxing model for polychaete studies. Zoosymposia 2:317-328.

Brinkmann N, Wanninger A. 2008. Larval neurogenesis in *Sabellaria alveolata* reveals plasticity in polychaete neural patterning. Evolution & Development 10(5):606-618.

Brinkmann N, Wanninger A. 2009. Neurogenesis suggests independent evolution of opercula in serpulid polychaetes. BMC Evol Biol 9(1):270.

Brinkmann N, Wanninger A. 2010a. Capitellid connections: contributions from neuromuscular development of the maldanid polychaete *Axiothella rubrocincta* (Annelida). BMC Evol Biol 10(1):168.

Brinkmann N, Wanninger A. 2010b. Integrative analysis of polychaete ontogeny: cell proliferation patterns and myogenesis in trochophore larvae of *Sabellaria alveolata*. Evolution & Development 12(1):5-15.

Carpizo-Ituarte E, Hadfield MG. 2003. Transcription and translation inhibitors permit metamorphosis up to radiole formation in the serpulid polychaete *Hydroides elegans*. Biol Bull 204:114-125.

Croll RP. 2000. Insights into early molluscan neuronal development through studies of transmitter phenotypes in embryonic pond snails. Microsc Res Tech 49(6):570-578.

Croll RP, Boudko DV, Hadfield MG. 2001. Histochemical survey of transmitters in the central ganglion of the gastropos mollusc *Phestilla sibogae*. Cell Tissue Res 305:417-432.

Croll RP, Chiasson BJ. 1989. Post-embryonic development if serotonin-like immunoreactivity in the central nervous system of the snail, *Lymnea stagnalis*. J Comp Neurol 280:122-142.

Denes AS, Jekely G, Steinmetz PRH, Raible F, Snyman H, Prud'homme B, Ferrier DEK, Balavoine G, Arendt D. 2007. Molecular Architecture of Annelid Nerve Cord

Supports Common Origin of Nervous System Centralization in Bilateria. Cell 129(2):277-288.
Dorresteijn AWC, O'Grady B, Fischer A, Porchet-Hennere E, Boilly-Marer Y. 1993. Molecular specification of cell lines in the embryo of *Platyneris* (Annelida). Roux's Arch Dev Biol 202:260-269.
Dray N, Tessmar-Raible K, Le Gouar M, Vibert L, Christodoulou F, Schipany K, Guillou A, Zantke J, Snyman H, Behague J, Vervoort M, Arendt D, Balavoine G. 2010. Hedgehog Signaling Regulates Segment Formation in the Annelid *Platynereis*. Science 329(5989):339-342.
Dunn CW, Hejnol A, Matus DQ, Pang K, Browne WE, Smith SA, Seaver E, Rouse GW, Obst M, Edgecombe GD, Sorensen MV, Haddock SHD, Schmidt-Rhaesa A, Okusu A, Kristensen RM, Wheeler WC, Martindale MQ, Giribet G. 2008. Broad phylogenomic sampling improves resolution of the animal tree of life. Nature 452(7188):745-749.
Friedrich S, Wanniger A, Bruckner M, Haszprunar G. 2002. Neurogenesis in the mossy chiton, *Mopalia muscosa* (Gould) (Polyplacophora): evidence against molluscan metamerism. J Morphol 253:109-117.
Giribet G, Dunn CW, Edgecombe GD, Rouse GW. 2007. A modern look at the Animal Tree of Life. Zootaxa 1668:61-79.
Hadfield MG, Unabia CC, Smith CM, Michael TM. 1994. Settlement preferences of the ubiquitious fouler *Hydroides elegans*. In: Thompson MF, Nagabhushanam R, Sarojini R, Fingerman M, editors. Recent Developments in Biofouling Control. New Delhi: Oxford and IBH Pub. Co. p 450.
Harder T, Lam C, Qian P-Y. 2002. Induction of larval settlement in the polychaete *Hydroides elegans* by marine biofilms: an investagation of monospecific diatom films as settlement cues. Mar Ecol Prog Ser 229:105-112.
Hay-Schmidt A. 1995. The larval nervous system of *Polygordius lacteus* Scheinder, 1868 (Polygordiidae, Polychaeta): Immunocytochemical data. Acta Zool 76(2):121-140.
Hessling R, Mueller MCM, Westheide W. 1999. CLSM analysis of serotonin-immunoreactive neurons in the central nervous system of *Nais variabilis*, *Slavina appendiculata* and *Stylaria lacustris* (Oligochaeta: Naididae) Hydrobiologia 406:223-233.
Holm ER, Nedved BT, Carpizo-Ituarte E, Hadfield MG. 1998. Metamorphic-signal transduction in *Hydroides elegans* (Polychaeta: Serpulidae) is not mediated by a G-Protein. Biol Bull 195:21-29.
Huang S, Hadfield MG. 2003. Composition and density of bacterial biofilms determine larval settlement of the polychaete Hydroides elegans. Mar Ecol Prog Ser 260:161-172.
Jekely G, Colombelli J, Hausen H, Guy K, Stelzer E, Nedelec F, Arendt D. 2008. Mechanism of phototaxis in marine zooplankton. Nature 456(7220):395-399.
Kerner P, Zelada Gonzalez F, Le Gouar M, Ledent V, Arendt D, Vervoort M. 2006. The expression of a hunchback ortholog in the polychaete annelid Platynereis dumerilii suggests an ancestral role in mesoderm development and neurogenesis. Dev Genes Evol 216(12):821-828.

Kupriyanova EK, Bastida-Zavala R, Halt MN, Lee MSY, Rouse GW. 2008. Phylogeny of the *Serpula-Crucigera-Hydroides* clade (Serpulidae:Annelida) using molecular and morphological data: implications for operculum evolution. Invertebrate Systematics 22(4):425-437.

Lacalli TC. 1976. A reticulum of nerve-like cells from trochophores of *Phyllodoce mucosa* (Polychaeta). Experientia 33(7):952-954.

Lacalli TC. 1981. Structure and development of the apical organ in trochophores of *Spirobranchus polycerus, Phyllodoce maculata*, and *Phyllodoce mucosa* (Polychaeta). Proceedings of the Royal Soceity of London B 212:381-402.

Lacalli TC. 1984. Structure and organization of the nervous system in the trochophore larvae of *Spirobranchus*. Philos Trans RSoc Lond B 306:79-135.

Lacalli TC. 1986. Prototroch structure and innervation in the trochophore larva of *Phyllodoce* (Polychaeta). Can J Zool 64(176-184).

Lacalli TC. 1988. The larval reticulum in *Phyllodoce* (Polychaeta, Phyllodocida). Zoomorphologie 108:61-68.

Lau SCK, Qian PY. 2001. Larval settlement in the serpulid polychaete Hydroides elegans in response to bacterial films: An investigation of the nature of putative larval settlement cue. Mar Biol 138(2):321-328.

McDougall C, Chen WC, Shimeld SM, Ferrier DE. 2006. The development of the larval nervous system, musculature and ciliary bands of *Pomatoceros lamarckii* (Annelida): heterochrony in polychaetes. Front Zool 3:16.

McEdward LR, Qian PY. 2001. Effects of the duration and timing of starvation during larval life on the metamorphosis and initial juvenile size of the polychaete Hydroides elegans (Haswell). J Exp Mar Bio Ecol 261(2):185-197.

Meyer NP, Seaver EC. 2009. Neurogenesis in an annelid: Characterization of brain neural precursors in the polychaete Capitella sp. I. Dev Biol 331(2):463.

Müller MCM. 2006. Polychaete nervous systems: Ground pattern and variations--cLS microscopy and the importance of novel characteristics in phylogenetic analysis. Integrative and Comparative Biology 46(2):125-133.

Orrhage L, Müller MCM. 2005. Morphology of the nervous system of Polychaeta (Annelida). Hydrobiologia 535-536:79-111.

Rouse GW, Pleijel F. 2001. Polychaetes. Oxford: Oxford University Press. 354 p.

Rousset V, Pleijel F, Rouse GW, Erséus C, Siddall ME. 2007. A molecular phylogeny of annelids. Cladistics 23(1):41-63.

Ruppert EE, Barnes RD. 1994. Invertebrate Zoology. Orlando, Florida: Saunders College Publishing, Harcourt Brace and Company.

Seaver E, Paulson D, Irvine SQ, Martindale MQ. 2001. The spatial and temporal expression of *Ch-en*, the *engrailed* gene in the polychaete *Chaetopterus* does not support a role in body axis segmentation. Dev Biol 236:195-209.

Seaver E, Shankland M. 2000. Leech Segmental repeats develop normally in the absence of signals from either anterior or posterior segements. Dev Biol 224:339-352.

Seaver EC. 2003. Segmentation: mono- or polyphyletic? International Journal of Developmental Biology 47:583-595.

Seaver EC, Kaneshige LM. 2006. Expression of 'segmentation' genes during larval and juvenile development in the polychaetes *Capitella sp. I* and *H. elegans*. Dev Biol 289(1):179-194.

Seaver EC, Thamm K, Hill SD. 2005. Growth patterns during segmentation in the two polychaete annelids, *Capitella sp*. I and *Hydroides elegans*: comparisons at distinct life history stages. Evol Dev 7(4):312-326.

Segrove F. 1941. The development of the serpulid *Pomatoceros triqueter* L. Quarterly Journal of Microscopy Science 82:467-540.

Simionato E, Kerner P, Dray N, Le Gouar M, Ledent V, Arendt D, Vervoort M. 2008. atonal- and achaete-scute-related genes in the annelid *Platynereis dumerilii*: insights into the evolution of neural basic-Helix-Loop-Helix genes. BMC Evol Biol 8:170.

Struck TH, Schult N, Kusen T, Hickman E, Bleidorn C, McHugh D, Halanych KM. 2007. Annelid phylogeny and the status of Sipuncula and Echiura. BMC Evol Biol 7:57.

Tessmar-Raible K, Raible F, Christodoulou F, Guy K, Rembold M, Hausen H, Arendt D. 2007. Conserved sensory-neurosecretory cell types in annelid and fish forebrain: Insights into hypothalamus evolution. Cell 129(7):1389-1400.

Tomer R, Denes AS, Tessmar-Raible K, Arendt D. 2010. Profiling by Image Registration Reveals Common Origin of Annelid Mushroom Bodies and Vertebrate Pallium. Cell 142(5):800-809.

Unabia CRC, Hadfield MG. 1999. Role of bacteria in larval settlement and metamorphosis of the polychaete *Hydroides elegans*. Mar Biol 133:55-64.

Voronezhskaya EE, Tsitrin EB, Nezlin LP. 2003. Neuronal development in larval polychaete *Phyllodoce maculata* (Phyllodocidae). J Comp Neurol 455:299-309.

Voronezhskaya EE, Tyurin SA, Nezlin LP. 2002. Neuronal development in larval chiton *Ischnochiton hakodadensis* (Mollusca: Polyplacophora). J Comp Neurol 444:25-38.

Walters LJ, Hadfield MG, A del Carmen K. 1997. The importance of larval choice and hydrodynamics in creating aggregations of *Hydroides elegans* (Polychaeta: Serpulidae). Invert Biol 116(2):102-114.

Walters LJ, Hadfield MG, Smith CM. 1996. Waterborne chemical comounds in tropical macroalgae: positive and negative cues for larval settlement. Mar Biol 126:383-393.

Wanninger A. 2008. Comparative lophotrochozoan neurogenesis and larval neuroanatomy: Recent advances from previously neglected taxa. Acta Biol Hung 59(Supplement 2):127-136.

Wanninger A. 2009. Shaping the Things to Come: Ontogeny of Lophotrochozoan Neuromuscular Systems and the Tetraneuralia Concept. Biol Bull 216(3):293-306.

Wanninger A, Koop D, Bromham L, Noonan E, Degnan BM. 2005. Nervous and muscle system development in Phascolion strombus (Sipuncula). Development Genes and Evolution 215(10):509-518.

Wanninger A, Kristof A, Brinkmann N. 2009. Sipunculans and segmentation. Commun Integr Biol 2(1):56-59.

Wisely B. 1958. The Development of a Serpulid Worm, *Hydroides norvegica*, Gunnerus (Polychaeta). Aust J Mar Freshwater Res 9:351-361.

Zrzavy J, Riha P, Pialek L, Janouskovec J. 2009. Phylogeny of Annelida (Lophotrochozoa): total-evidence analysis of morphology and six genes. BMC Evol Biol 9(1):189.

Figure Legends

Figure 2.1. Larval development of *Hydroides elegans*. A. Right lateral view of a mid-Stage1 larva (7 hpf). Larva has developed a prototroch but can not yet feed because the lumen of the gut has not yet expanded. The apical plate had not differentiated into the apical sensory organ. B. Right lateral view of a Stage 2 (12 hpf) trochophore larva. Gut is functional. Apical sensory organ, and an eyespot developed in the larval episphere. In addition to the prototroch, a metatroch and neurotroch had also developed. A large anal vesicle was conspicuous in the in the hyposphere. C. Right dorso-lateral view of a Stage 3 (48 hpf). Larval stomach occupies most of the space of the free space within the episphere. The epidermis of both the episphere and hydrosphere has thickened as the precursors of both the cerebral and segmental ganglia have developed.
D. Ventral view of Stage 4 (72 hpf) larva. The first three thoracic segments have developed and setigers in each of the segments had erupted through the body wall. Rudiments of the collar also began to develop. A second larval eyespot developed in the episphere. The larval mouth is out of the plane of focus. E. Ventral view of a Stage 6 (120 hpf) larvae. Rudiments of the cerebral ganglia had developed and occupy a considerable space within the episphere. The hyposphere of the larva has elongated and the segments have further developed. Stage 6 larvae have attained metamorphic competence. Anterior is up in all photos. Scale 50 µm, hours post-fertilization (hpf). Shows the apical plate (AP), apical sensory organ (ASO), prototroch (Pro), metatroch (Met), neurotroch (NT), eye spot (ES), cerebral ganglia (CG), anal vesicle (AV), rudiments of the collar (Col), and setigers (Set).

Figure 2.2. Neural development in Stage 1 and 2 larvae of *H. elegans.*
A. Right-lateral and (B.) oral views of serotonin-like immunoreactivity (5HT-LIR) in mid-Stage 1 larva (7 hpf). The earliest developing 5HT-LIR cell (S-PC) projected fibers towards prototroch. Stomadeum not yet fully opened (arrowheads). C. Oral view of 5HT-LIR in late-Stage 1 (9 hpf) larva. Anteriorly directed fibers reached prototroch, and proceeded to the upper lip of the mouth (large arrowheads). Additional fibers completely encircled the mouth and made contact with a second immunoreactive cell(S-SO) (small arrowheads). D. Serotonin-LIR in Stage 2 (12 hpf) larvae, right lateral view. Cell in

apical sensory organ (S-A1) synapsed with an apically directed fiber (S-AF), prototroch completely innervated by fiber (S-PRO). E. Tyrosine hydroxylase-like immunoreactivity (TH-LIR) in Stage 2 larva. Ventral view, tilted to right. TH-LIR cells in pharynx (T-O1-T-O3), underlying neurotroch (T-NT), and in metatroch (T-M1, T-M2). Cells in metatroch project fibers to anterior lip of mouth. F. Right-lateral view of FMRFamide-like immunoreactivity (FMRFa-LIR) in Stage 2 larva. FMRFa-LIR in single cell in ASO (F-A1) and in small fibers at the junction of larval stomach and intestine (Ret). Anterior is up. Scale =50 µm. All plates are maximum-intensity confocal projections. Phalloidin (red) double label in A-D, F.

Figure 2.3. Summary diagrams of neuronal development in Stage 2 larvae of *H. elegans.* A and D serotonin-like immunoreactivity (5HT-LIR). B. and E. tyrosine hydroxylase-like immunoreactivity (TH-LIR). C and F. FMRF-amide-like immunoreactivity (FMRFa-LIR). A-C are ventral views D-F are lateral views. Labeling is the same as in Fig. 2.

Figure 2.4. Neuronal development in Stage 3 larvae of *H. elegans*. A. Right lateral view of serotonin-LIR (5HT-LIR) in larva. Two cells developed in subesophageal ganglion (S-MC1 and S-MC2). Posterior cell (S-PC) remained as did fibers in prototroch (S-Pro). B. Ventral view of tyrosine hydroxylase-LIR (TH-LIR). Two fibers and five cells in larval pharynx now immunoreactive (T-O1-T-O5). Cells in metatroch (T-M1 and T-M2) and cell under neurotroch (T-NT) remain. C. Ventral view of FMRFamide-LIR (FMRFa-LIR) in larva. Shows four cells immunoreactive in ASO (F-A1-FA4), highly immunoreactive apical neuropil, and a posteriorly directed fiber (F-AF) in the apical nerve. D. Ventral view of 5HT-LIR in late Stage 3 larva. In addition to earlier developed cell and fibers, two anteriorly directed fibers developed in circumesophageal connectives (S-CEC). Also shows earliest developing 5HT-LIR cell (S-PC), immunoreactive cell posterior of mouth (S-SO), cells in subesophageal ganglion (S-MC1 and S-MC2), fiber in prototroch (S-Pro), cell in ASO (S-A1) and fiber in apical nerve (S-AF). E. Magnified image of FMRFa-LIR cells in ASO of Stage 3 larva. * were position of nuclei. F. Magnified image of FMRFa-LIR in reticulated cells. Two cell bodies had developed

immunoreactivity. Anterior is up. Scale = 50 µm. All plates are maximum-intensity confocal projections. Phalloidin (red) double label in A, C-F.

Figure 2.5. Summary diagram of neuronal development in Stage 3 larvae of *H. elegans.* A and D serotonin-like immunoreactivity (5HT-LIR). B and E tyrosine hydroxylase-like immunoreactivity (TH-LIR). C and F FRMF-amide-like immunoreactivity (FMRFa-LIR). A-C are ventral views, D-F are lateral views, labeling is the same as in Fig. 4.

Figure 2.6. Neuronal development in Stage 4 larvae of *H. elegans*. A.Ventral view of serotonin-like immunoreactivity (5HT-LIR) in an early Stage 4 larva. Four cells developed immunoreactivity in the cerebral ganglion (S-CG1-S-CG4). Two fibers were present in the circumesophageal connectives (S-CEC) and a fiber developed in the metatroch (S-Met). Two additional cells developed in subesophageal ganglion (Seg 1), the perikarya were located next to the earlier developing cells (S-MC1 and S-MC2) in the ganglion. A pair of cells developed in the pygidium (S-T1and 2). Also shows earliest developing 5HT-LIR cell (S-PC), immunoreactive cell posterior of mouth (S-SO), immunoreactive cell in ASO (S-A1), fiber in prototroch (S-Pro), and fiber in apical nerve (S-A1). B. Ventral view of 5HT-LIR in mid-Stage 4 larva. Two additional cells developed immunoreactivity in the ganglia of first thoracic segment (Seg 1) and the two pairs of developed in second thoracic segment (Seg 2). Also shows earliest developing 5HT-LIR (S-PC), immunoreactive cell posterior of mouth (S-SO), cells in cerebral commisure(S-CG1 – S-CG 4) and ASO (S-A1), cells in pygidium (S-T1 and 2), fibers in apical nerve (S-AF), and ventral nerve cords (S-VNC). C. Tyrosine hydroxylase-like immunoreactivity (TH-LIR) in Stage 4 larva. Ventral view, tilted to left. Ten cells were immunoreactive in the episphere of the larva. Four cells were in the cerebral ganglia (T-CG1 – T-Cg4) and projected axons into cerebral commisure. Four cells were directly adjacent to the ASO (T-A1 – T-A4), and an additional pair of cells developed slightly anterior of the prototroch on ventral side of the larva (T-CEC1 and 2). New immunoreactive cells also developed in the dorsal portions of the metatroch (T-D2), shell glands (T-SG1 and 2), and two pairs of cells in the pygidium (T-T1 – T-T4). Immunoreactive fibers were present in prototroch (T-Pro), metatroch (T-Met), and a

single fiber in the ventral nerve cords (T-VNC). Additional cells developed in the rudiments of the collar (arrowhead) and peripheral sensory cells (T-Sen2) in the second segment of the larva. The immunoreactive cells in the stomatogastric system remained but not labeled. D. Ventral view of FMRF-amide-like immunoreactivity (FMRFa-LIR). Intensity of fluorescence increased in the four cells in the ASO (F-Apical) and cerebral commisures. A pair of cells (F-CG1 and 2) developed in the lateral portions cerebral commisures. A weakly immunoreactive fiber also developed in the ventral nerve cords (F-VNC). Also shows a short fiber in the apical nerve (F-AP). Anterior is up, scale = 50 μm, all plates are maximum-intensity confocal projections. Phalloidin (red) double label in A, C-D.

Figure 2.7. Summary diagram of neuronal development in Stage 4 larvae of *H. elegans.* A and D serotonin-like immunoreactivity (5HT-LIR). B and E tyrosine hydroxylase-like immunoreactivity (TH-LIR). C and F FRMF-amide-like immunoreactivity (FMRFa-LIR). A-C are ventral views, D-F are lateral views. Labeling is the same as in Fig. 6.

Figure 2.8. Neuronal development in Stage 6 larvae of *H. elegans*. A. Ventral view of β-tubulin-LIR in Stage 6 larva. Shows numerous immunoreactive fibers in the apical sensory organ (ASO), cerebral commisures (CC), circumesophageal connectives (CEC), and ventral nerve cords (VNC). Also shows two immunoreactive fiber bundles in first thoracic segment (Seg 1) and a single bundle of fibers in the second (Seg 2) and third (Seg 3) thoracic segments. B. Ventral view of serotonin-like immunoreactivity (5HT-LIR) in a Stage 6 larva. Shows immunoreactive cells in the cerebral ganglia (S-CG1 – S-CG4), all three thoracic segments (Seg 1 -3), 5-HT-LIR cells in pygidium (S-T1 and 2), and the earliest developing 5HT-LIR cell (S-PC). Serotonin-LIR in fibers including, apical nerve (S-AF1), prototroch (S-Pro), metatroch (S-Met). C. Ventral view of TH-LIR in a Stage 6 larva. Numerous cells showed TH-LIR including cells adjacent to ASO (T-A1 – T-A4), in the cerebral ganglia (T-CG1 – T-CG6), circum esophageal connective (T-CEC1 and 2), shell glands (T-SG1 and 2), pygidium (T-T1 – T-T4), and two pairs of peripheral sensory neurons (T-Sen1 – T-Sen4). A medial fiber underlying the neurotroch also developed (T-NF). D. Ventral view of FMRFa- LIR in a Stage 6 larva. Strong

immunoreactivity in the ASO (F-Ap) cerebral commisures and ventral nerve cords. Immunoreactive fibers were present in the more anterior commisure of the first segment (Sub-Es) and third (Seg 3) commisures of the segmental ganglia. Anterior is up, scale = 100 µm, all plates are maximum-intensity confocal projections. Phalloidin (red) double label in B and D.

Figure 2.9. Summary diagram of neuronal development in Stage 6 larvae of *H. elegans.* A and D serotonin-like immunoreactivity (5HT-LIR). B and E tyrosine hydroxylase-like immunoreactivity (TH-LIR). C and F FRMF-amide-like immunoreactivity (FMRFa-LIR). A-C are ventral views, D-F are lateral views, labeling is the same as in Figs. 6 and 8

Figure 2.10. Ventral nerve cords of Stage 6 larvae. A. β-tubulin-like immunoreactivity in ventral nerve cords. Numerous immunoreactive fibers were present in the ventral nerve cords as well as the commisures in all three thoracic segments (Seg 1 – Seg 3). Cilia of the neurotroch were also immunoreactive to the antibody. B. Serotonin-like immunoreactivity (5HT-LIR) in ventral nerve cords. Immunoreactive cells were present in both the segmental and subesophageal ganglia in the first thoracic segment as well as in the segmental ganglia of the second (Seg 2) and third (Seg 3) thoracic segments. 5HT-LIR fibers were also present in all three commisures. Also shows 5HT-LIR cells in pygidium (S-T1, 2) and the posterior cell that had 5HT-LIR earliest in development. C. FMRF-amide-like immunoreactivity (FMRFa-LIR) in ventral nerve cords. Numerous varicosities were present in the ventral nerve cords between the first commisure (Sub-ES) of the ganglia of the first thoracic segment and the commisure in the third thoracic segment (Seg. 3). Only one pair of somata in segmental ganglia of the third thoracic segment (Seg 3) had FMRFa-LIR. Anterior is up, scale = 100 µm, all images are maximum-intensity confocal projections. Phalloidin (red) double label in B and C.

Figure 2.11. Neuronal development in episphere of a Stage 6 larva of *H. elegans*. A. β-tubulin-LIR in episphere of Stage 6 larva. Numerous immunoreactive fibers were present in the apical sensory organ (ASO), cerebral commisures (CC) and circumesophageal connectives (CEC). B. Serotonin-like immunoreactivity (5HT-LIR) in episphere of a

Stage 6. larva. Eight cells had 5HT-LIR in the cerebral ganglia. Four neurons (S-Cg1 – S-CG4) had larger somata and projected a fiber into the dorsal portion of the cerebral commisure. The remaining four neurons had smaller sized somata and were closer to the cerebral commisure. Maximum intensity projection of 15 z-stack (1μm) confocal images C. Tyrosine hydroxylase-like immunoreactivity (TH-LIR) in episphere of Stage 6 larva. Twelve cells had TH-LIR. Two pairs of cells were positioned on the dorsal and ventral margins of the ASO (T-A1 – T-A1), six cells were part of the cerebral ganglia (T-CG1-T-CG6) and projected processes into the cerebral commisure (T-CG3-T-CG6) or circumesophageal connectives (T-CG1 and T-CG2). Two additional cells (T-CEC1 and T-CEC2) were more posteriorly positioned on top of the circumesophageal connectives. Preparation was dorso-ventrally flattened. Maximum intensity projection of 33 z-stack (1μm) confocal images. D. and E. FMRF-amide-like immunoreactivity (FMRFa-LIR) in episphere of a Stage 6 larva. Over 20 cells had FMRFa-LIR in the episphere of a Stage 6 larvae. In ventral regions (D.) of the episphere cells of the apical sensory organ (F-apical) and 2 additional pairs of sensory cells had FMRFa-LIR. The more laterally positioned sensory cells (small arrows) were positioned underneath the larval eyespots. Three pairs (arrowheads) of cells had FMRFa-LIR and projected dendrites to the dorsal epithelium of the larva. D. and E. are maximum intensity projections of the same larva. D. was constructed from 19 z-stack (1μm) confocal images. The first image in this stack was the ventral limit of immunoreactivity of the cerebral commisure. E. was constructed from nine z-stack (1 μm thickness) confocal images and the first image immediately followed (D.). Anterior is up in all images, scale 50 μm, Phalloidin (red) double label in B, D, and E.

Figure 2.12. Summary diagram of Serotonin-like immunoreactivity (5HT-LIR), FMRF-amide-like immunoreactivity (FMRFa-LIR) and tyrosine hydroxylase-LIR (TH-LIR) in the episphere of a Stage 6 larva of *H. elegans.* Shows FMRFa-LIR in apical sensoruy organ (ASO), FMRFa-LIR in dorsally positioned sensory neurons (black arrowhead) and sensory neurons (grey arrows) positioned beneath the larval eyespots (ES), TH-LIR in sensory cells bordering the ASO (T-A1-TA4). 5HT-LIR (red), TH-LIR (blue), FMRFa-LIR (green), outline of cerebral ganglia (dotted lines).

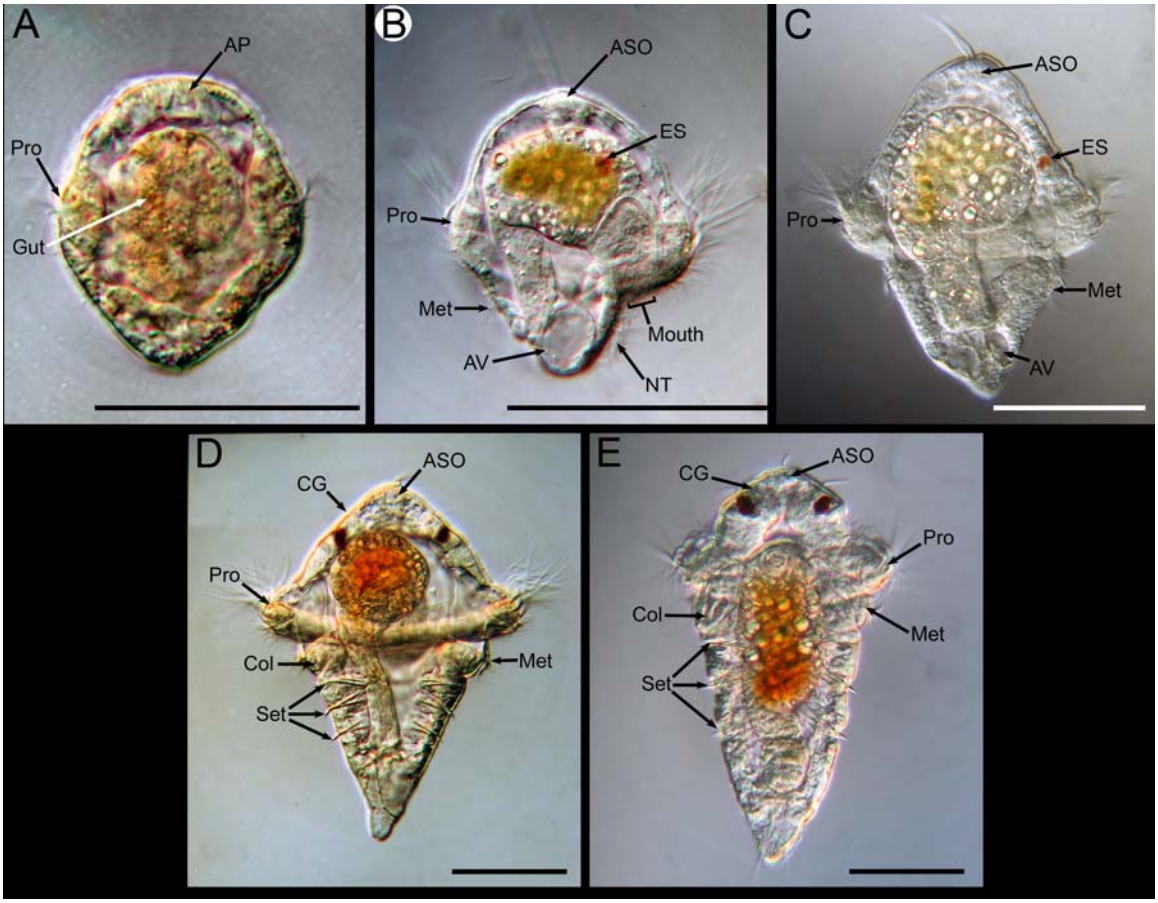
A
AP
Pro
Gut
B
ASO
ES
Pro
Met
Mouth
AV
NT
C
ASO
ES
Pro
Met
AV
D
ASO
CG
Pro
Col
Met
Set
E
CG
ASO
Pro
Col
Met
Set

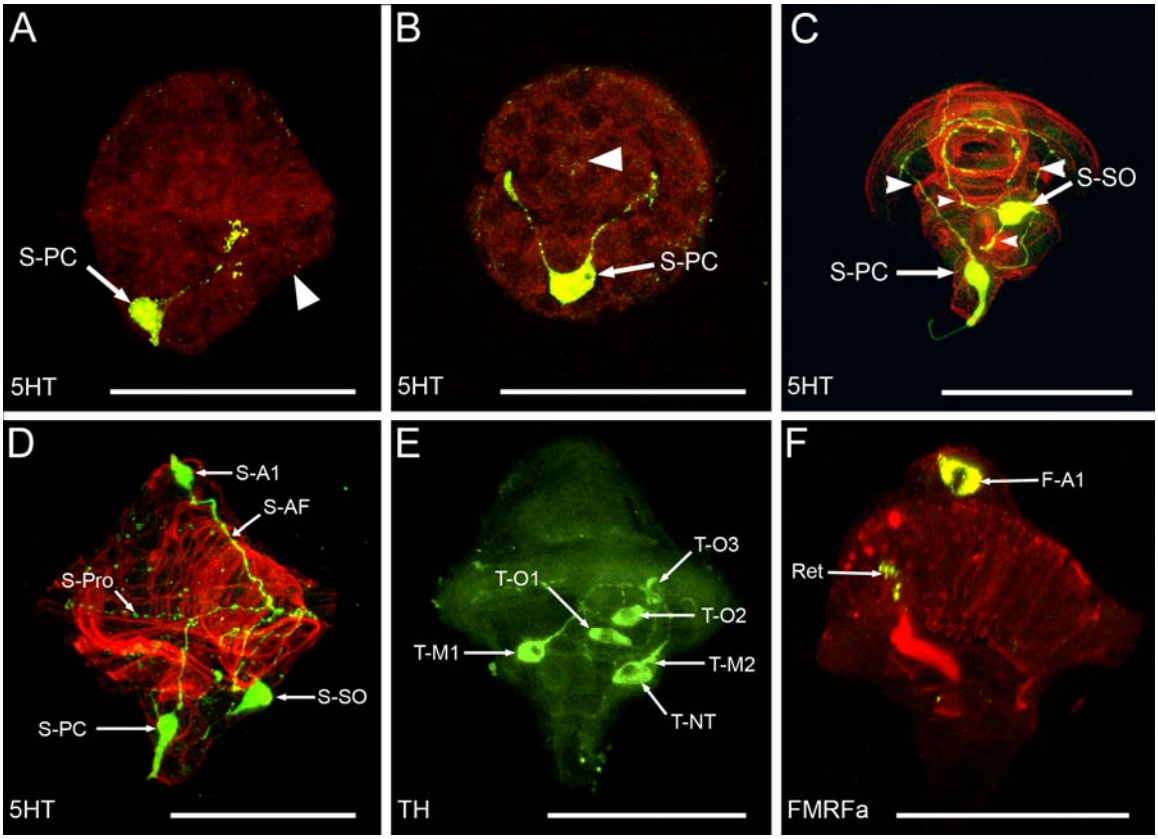
A
S-PC
5HT
B
S-PC
5HT
C
S-SO
S-PC
5HT
D
S-A1
S-AF
S-Pro
S-SO
S-PC
5HT
E
T-O3
T-O1
T-O2
T-M1
T-M2
T-NT
TH
F
F-A1
Ret
FMRFa

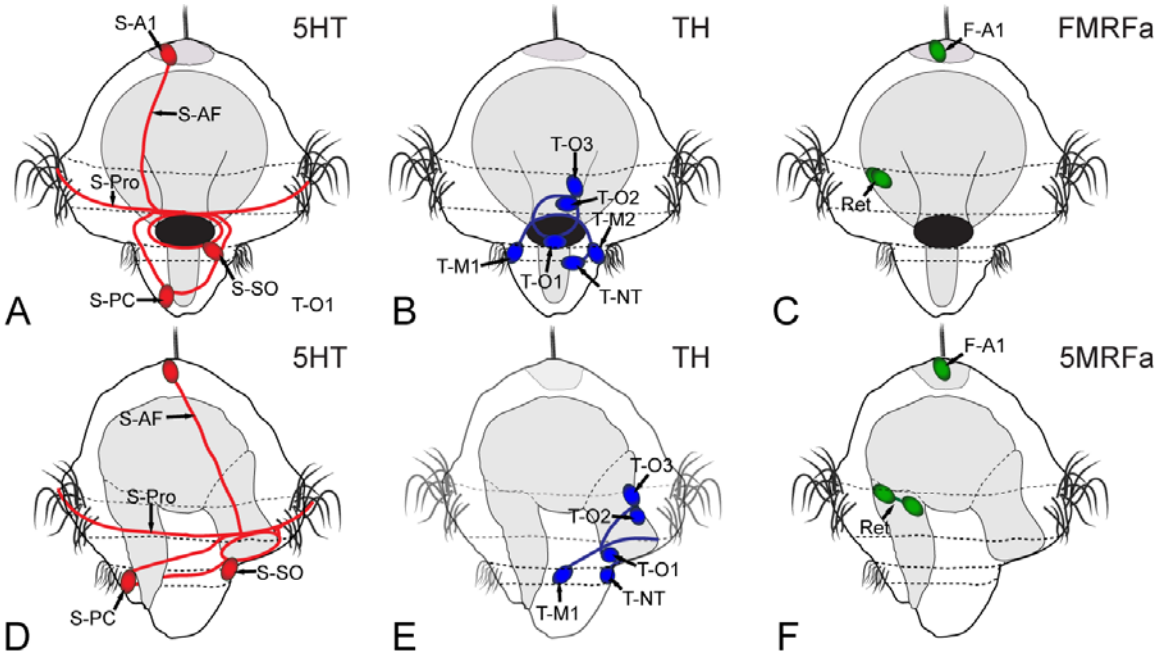
S-A1
5HT
S-AF
S-Pro
S-PC
S-SO
T-O1
A
TH
T-O3
T-O2
T-M2
T-M1
T-O1
T-NT
B
F-A1
FMRFa
Ret
C
5HT
S-AF
S-Pro
S-SO
S-PC
D
TH
T-O3
T-O2
T-O1
T-NT
T-M1
E
F-A1
5MRFa
Ret
F

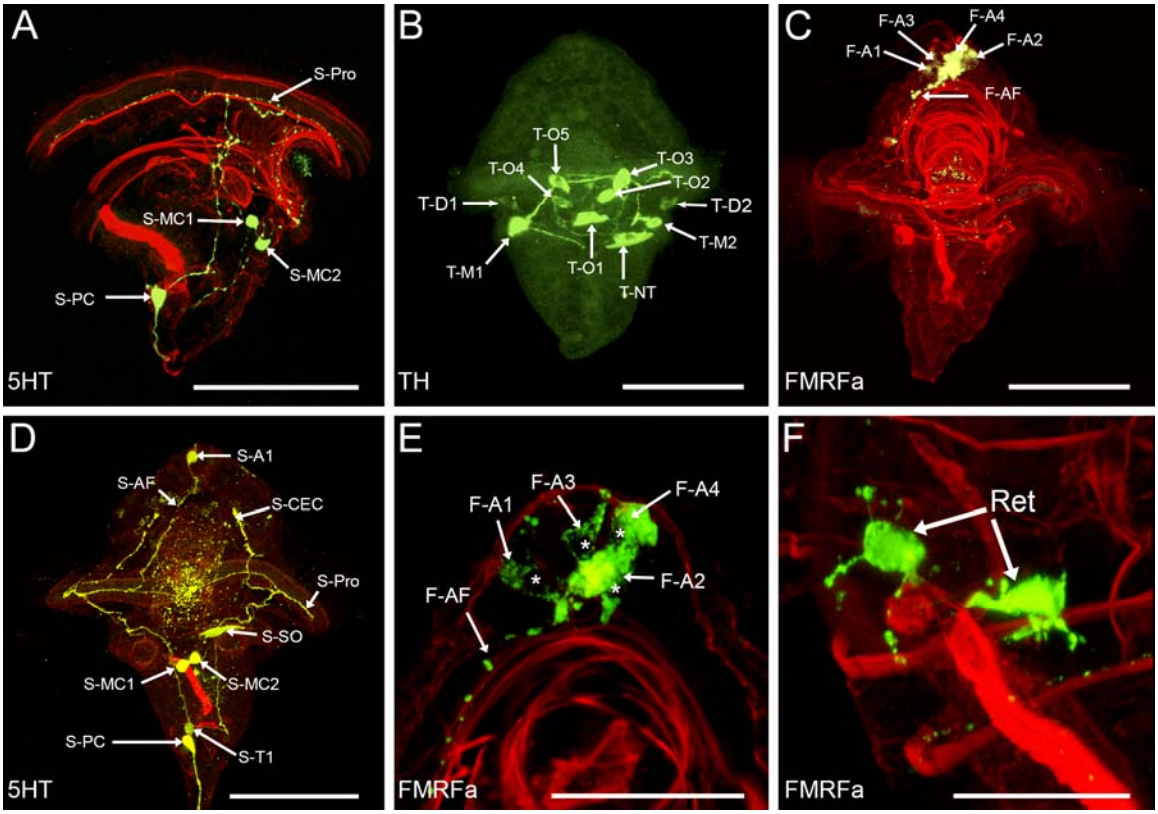
A
S-Pro
S-MC1
S-MC2
S-PC
5HT
B
T-O5
T-O4
T-O3
T-O2
T-D1
T-D2
T-M2
T-M1
T-O1
T-NT
TH
C
F-A3
F-A4
F-A1
F-A2
F-AF
FMRFa
D
S-A1
S-AF
S-CEC
S-Pro
S-SO
S-MC1
S-MC2
S-PC
S-T1
5HT
E
F-A3
F-A4
F-A1
F-A2
F-AF
FMRFa
F
Ret
FMRFa

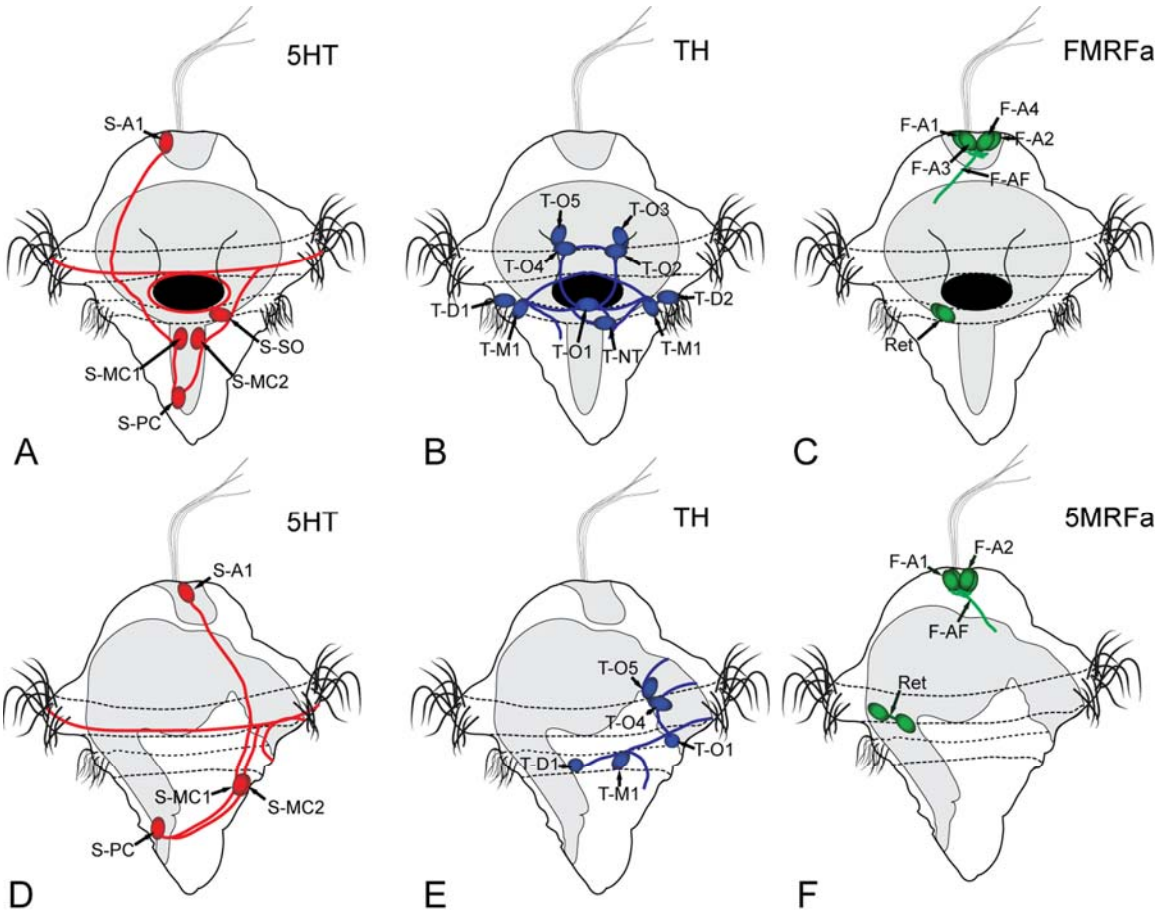
5HT
S-A1
S-SO
S-MC1
S-MC2
S-PC
A
TH
T-O5
T-O3
T-O4
T-O2
T-D1
T-D2
T-M1
T-O1
T-NT
T-M1
B
FMRFa
F-A1
F-A4
F-A2
F-A3
F-AF
Ret
C
5HT
S-A1
S-MC1
S-MC2
S-PC
D
TH
T-O5
T-O4
T-O1
T-D1
T-M1
E
5MRFa
F-A1
F-A2
F-AF
Ret
F

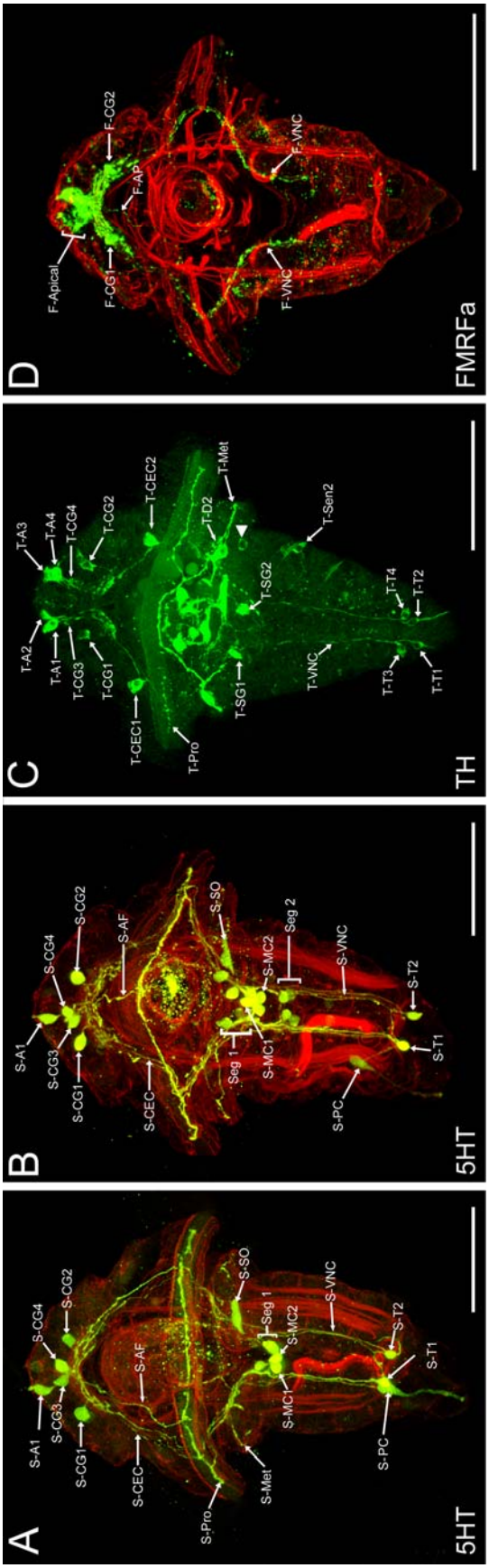
A
5HT
S-A1
S-CG4
S-CG3
S-CG2
S-CG1
S-AF
S-CEC
S-Pro
S-Met
S-SO
Seg 1
S-MC1
S-MC2
S-VNC
S-PC
S-T2
S-T1
B
5HT
S-A1
S-CG4
S-CG3
S-CG2
S-CG1
S-AF
S-CEC
S-SO
Seg 1
S-MC1
S-MC2
Seg 2
S-VNC
S-PC
S-T2
S-T1
C
TH
T-A3
T-A4
T-A2
T-CG4
T-A1
T-CG3
T-CG2
T-CG1
T-CEC2
T-CEC1
T-D2
T-Met
T-Pro
T-SG1
T-SG2
T-Sen2
T-VNC
T-T4
T-T3
T-T2
T-T1
D
FMRFa
F-Apical
F-CG2
F-CG1
F-AP
F-VNC
F-VNC

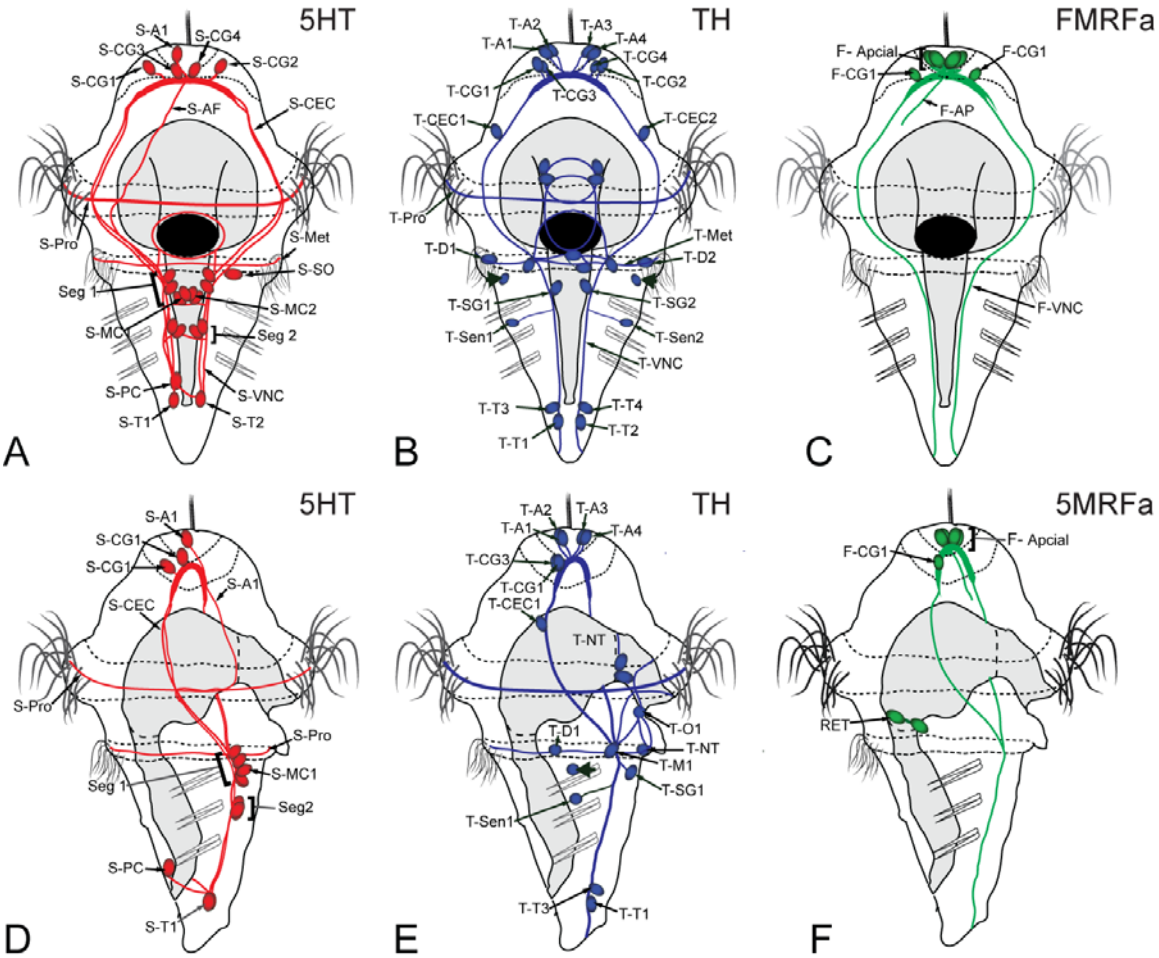
5HT
S-A1
S-CG4
S-CG3
S-CG2
S-CG1
S-AF
S-CEC
S-Pro
S-Met
S-SO
Seg 1
S-MC2
S-MC
Seg 2
S-PC
S-VNC
S-T1
S-T2
A
TH
T-A2
T-A3
T-A1
T-A4
T-CG4
T-CG2
T-CG1
T-CG3
T-CEC1
T-CEC2
T-Pro
T-Met
T-D1
T-D2
T-SG1
T-SG2
T-Sen1
T-Sen2
T-VNC
T-T3
T-T4
T-T2
T-T1
B
FMRFa
F- Apcial
F-CG1
F-CG1
F-AP
F-VNC
C
5HT
S-A1
S-CG1
S-CG1
S-A1
S-CEC
S-Pro
S-Pro
S-MC1
Seg 1
Seg2
S-PC
S-T1
D
TH
T-A2
T-A3
T-A1
T-A4
T-CG3
T-CG1
T-CEC1
T-NT
T-D1
T-O1
T-NT
T-M1
T-SG1
T-Sen1
T-T3
T-T1
E
5MRFa
F-CG1
F- Apcial
RET
F

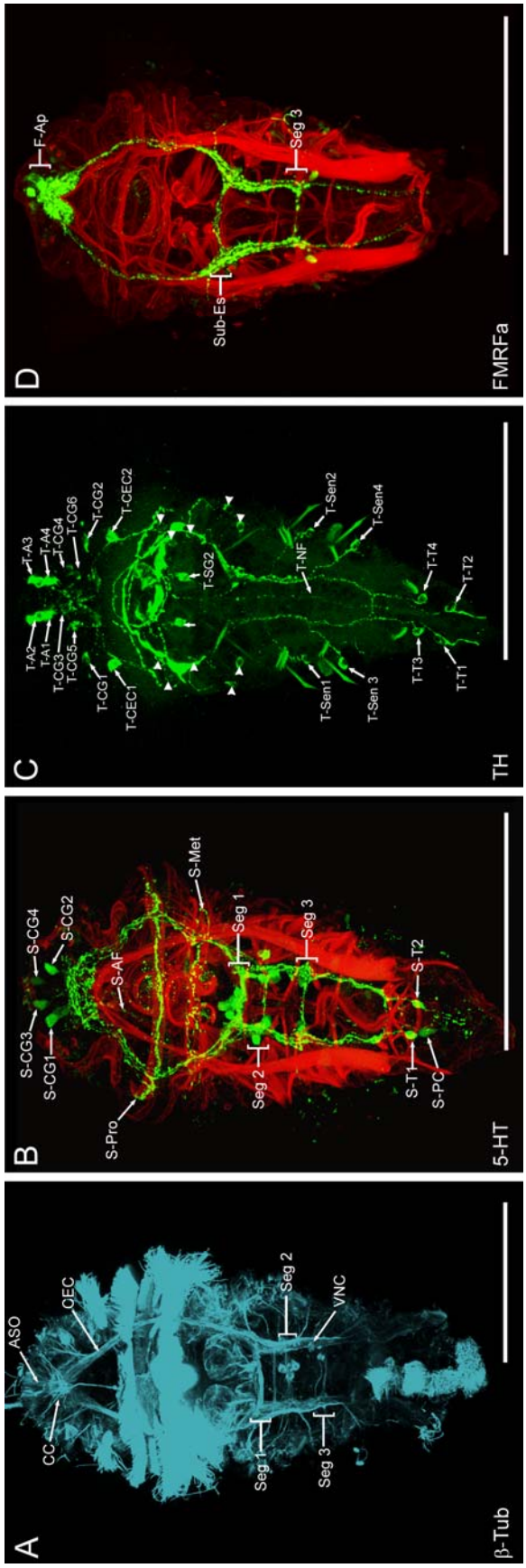
A
ASO
CC
CEC
Seg 1
Seg 2
Seg 3
VNC
β-Tub
B
S-CG3
S-CG4
S-CG1
S-CG2
S-Pro
S-AF
S-Met
Seg 1
Seg 2
Seg 3
S-T1
S-T2
S-PC
5-HT
C
T-A2
T-A3
T-A1
T-A4
T-CG3
T-CG4
T-CG5
T-CG6
T-CG1
T-CG2
T-CEC1
T-CEC2
T-SG2
T-NF
T-Sen1
T-Sen2
T-Sen 3
T-Sen4
T-T3
T-T4
T-T1
T-T2
TH
D
F-Ap
Sub-Es
Seg 3
FMRFa

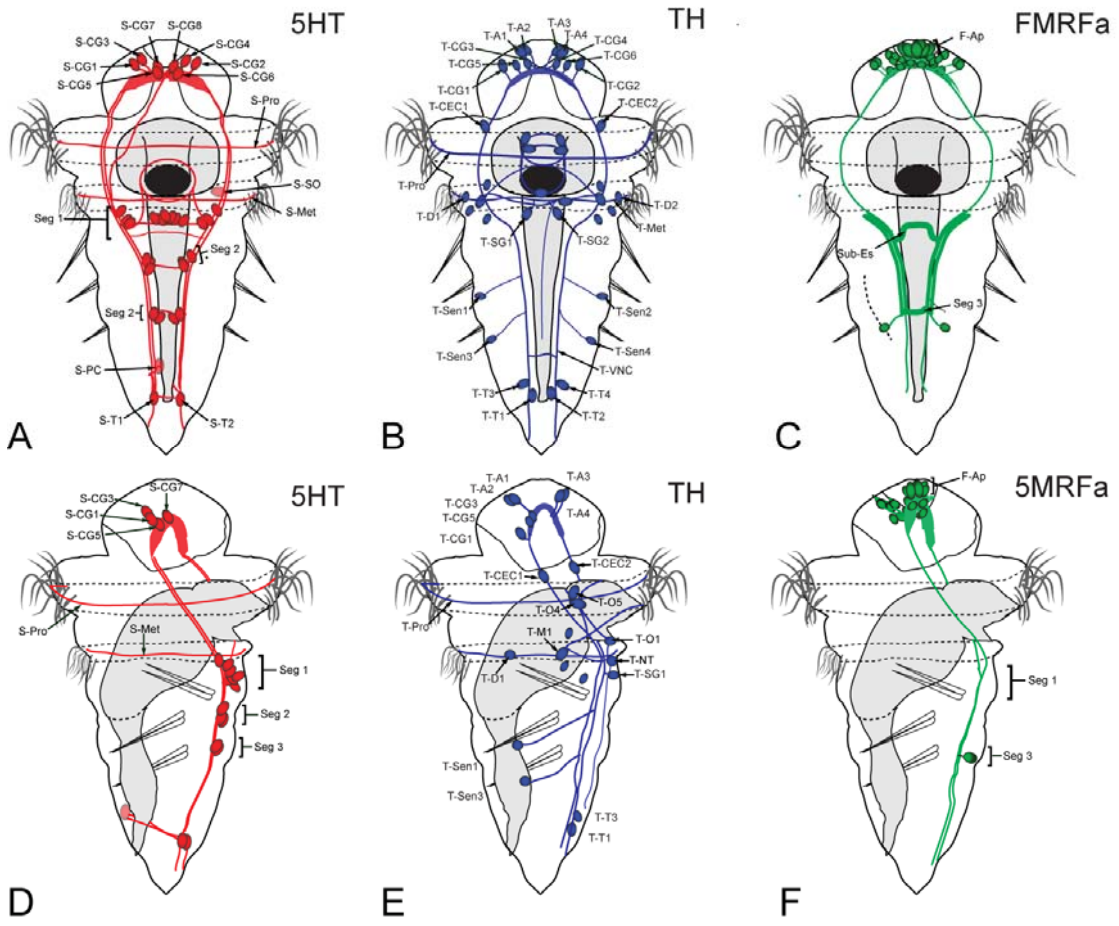
5HT
S-CG7
S-CG8
S-CG3
S-CG4
S-CG1
S-CG2
S-CG6
S-CG5
S-Pro
S-SO
S-Met
Seg 1
Seg 2
Seg 2
S-PC
S-T1
S-T2
A
TH
T-A1
T-A2
T-A3
T-A4
T-CG3
T-CG4
T-CG5
T-CG6
T-CG1
T-CG2
T-CEC1
T-CEC2
T-Pro
T-D1
T-D2
T-Met
T-SG1
T-SG2
T-Sen1
T-Sen2
T-Sen3
T-Sen4
T-VNC
T-T3
T-T4
T-T1
T-T2
B
FMRFa
F-Ap
Sub-Es
Seg 3
C
5HT
S-CG3
S-CG7
S-CG1
S-CG5
S-Pro
S-Met
Seg 1
Seg 2
Seg 3
D
TH
T-A1
T-A3
T-A2
T-CG3
T-CG5
T-A4
T-CG1
T-CEC1
T-CEC2
T-O4
T-O5
T-Pro
T-M1
T-O1
T-NT
T-D1
T-SG1
T-Sen1
T-Sen3
T-T3
T-T1
E
5MRFa
F-Ap
Seg 1
Seg 3
F

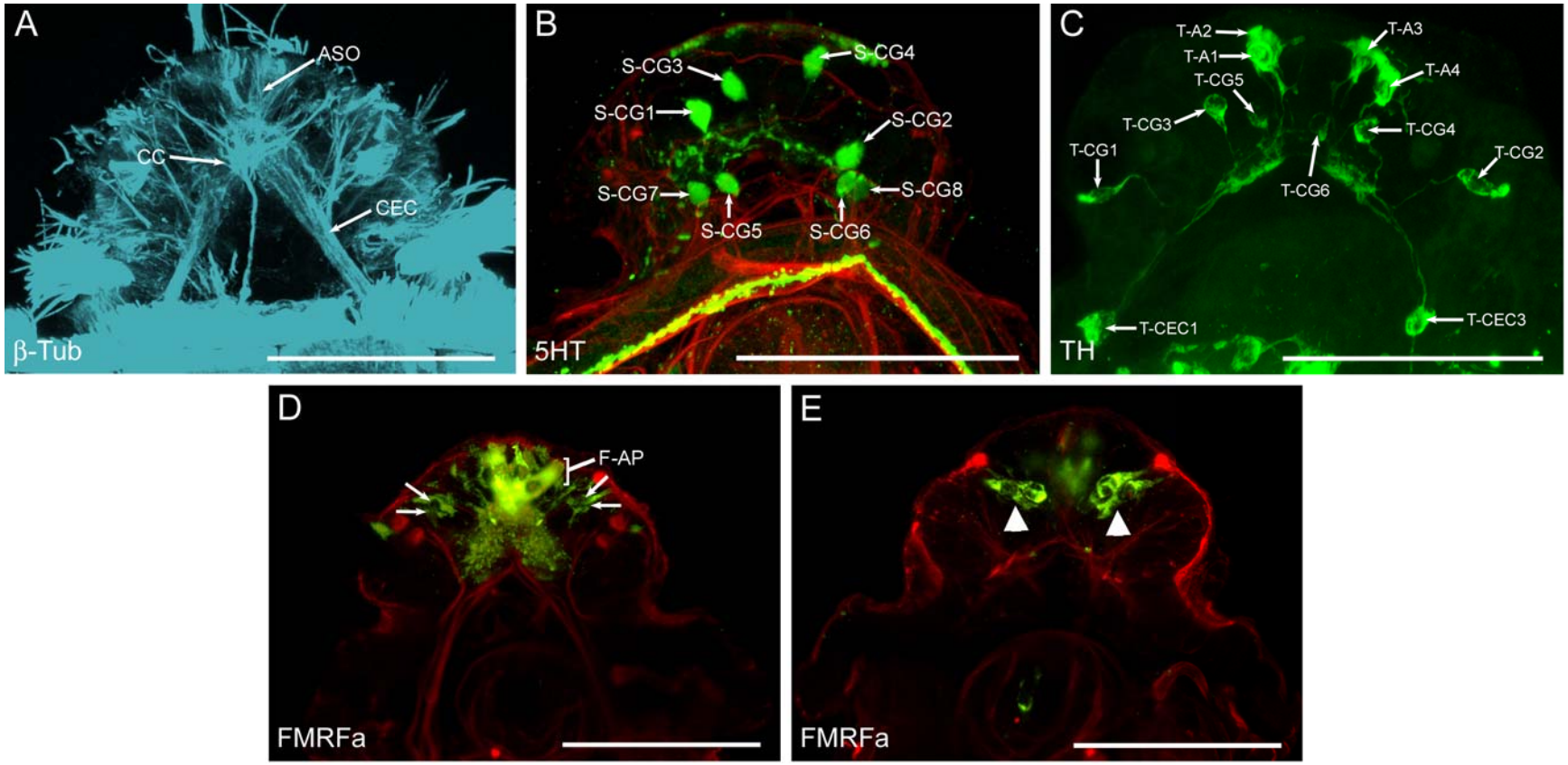
A
ASO
CC
CEC
β-Tub
B
S-CG3
S-CG4
S-CG1
S-CG2
S-CG7
S-CG8
S-CG5
S-CG6
5HT
C
T-A2
T-A3
T-A1
T-A4
T-CG5
T-CG3
T-CG4
T-CG1
T-CG2
T-CG6
T-CEC1
T-CEC3
TH
D
F-AP
FMRFa
E
FMRFa

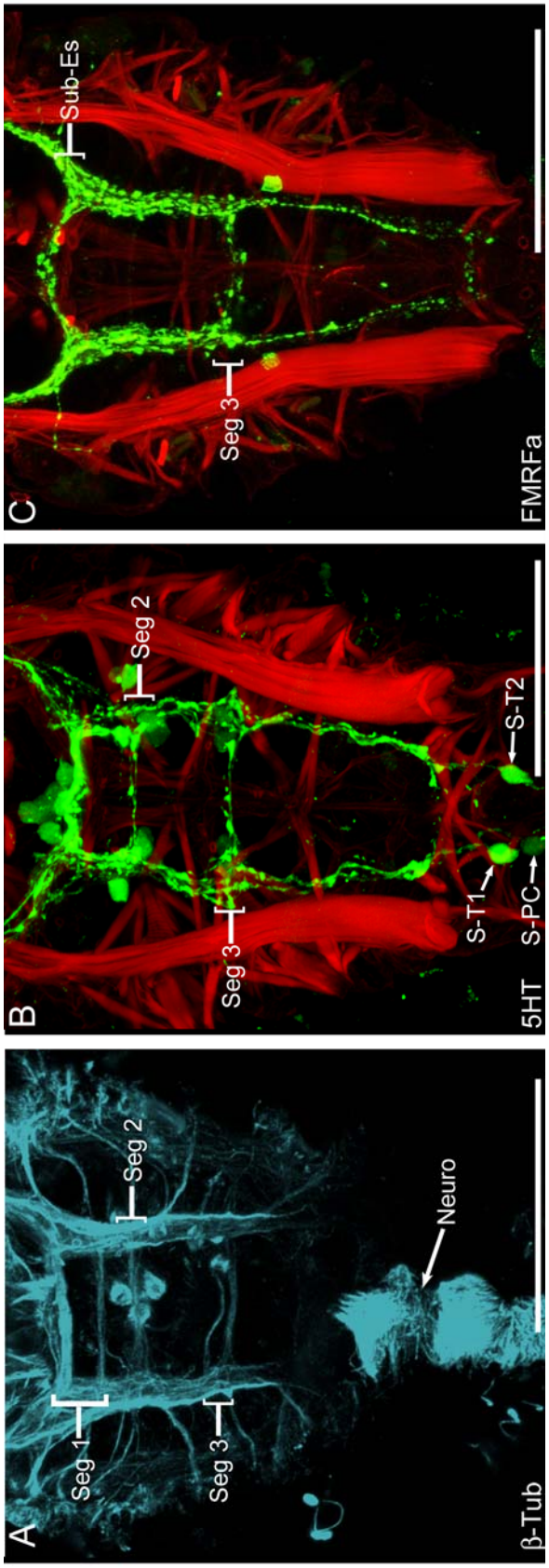
A
Seg 1
Seg 2
Seg 3
Neuro
β-Tub
B
Seg 2
Seg 3
S-T1
S-PC
S-T2
5HT
C
Sub-Es
Seg 3
FMRFa

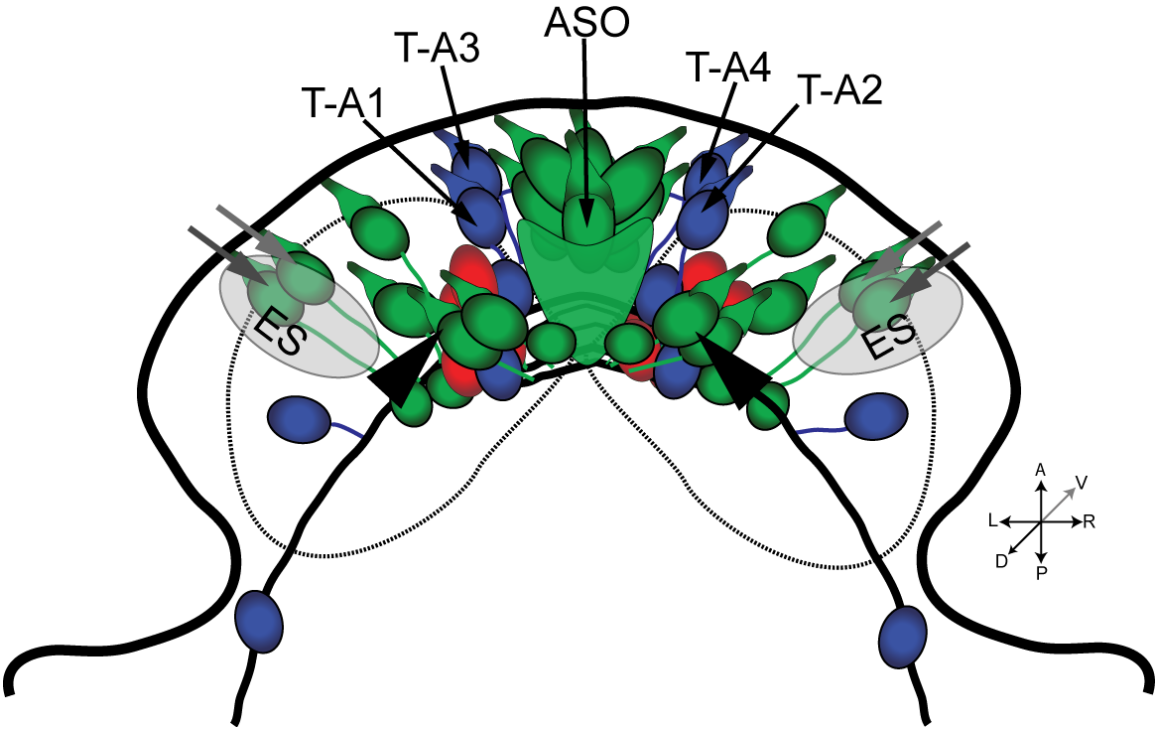
ASO
T-A3
T-A4
T-A1
T-A2
ES
ES
A
V
L
R
D
P

CHAPTER 3

ROLE OF SEROTONIN IN THE COORDINATION AND CONTROL OF METAMORPHOSIS OF *H. ELEGANS*

Introduction

Most marine invertebrates have biphasic life cycles consisting of free-swimming, pelagic larvae and benthic juvenile-adults The transition from the first of these life stages to the second is dependent upon the sensation of an external inductive cue (for reviews see: Crisp, 1974; Pawlik, 1992; Hadfield and Paul, 2001), and the propagation of a morphogenic signal from sensory structures to the responding tissues (Hadfield, 2000) coordinates this process. Due to the speed of metamorphosis and the propensity of small cations to act as artificial inducers of metamorphosis in many invertebrate larvae, presumably acting by depolarizing membranes of excitatory cells (Hadfield, 2000), the nervous system serves to coordinate and control metamorphosis in these larvae (Hadfield, 2000; Kimura et al., 2003). Serotonin (5-hydroxytryptamine [5-HT]) is expressed in the central nervous systems (CNS) of most larvae in the animal kingdom (Hay-Schmidt, 2000), and may act as a neurotransmitter or a neuromodulator of metamorphosis in marine larvae.

Serotonin release has been implicated as a controlling mechanism for many complex physiological functions (Berger et al., 2009) such as: aggressive behavior in mice and crayfish (Gerhardt, 1996); swimming behavior in an amphipods (Guler and Ford, 2010); ciliary beat in gastropod molluscs (Braubach et al., 2006); feeding behaviors in pulmonate mollucs (Gerhardt, 1996); motor output in a number of invertebrate taxa including annelids (Anctil et al., 1984; Diaz-Miranda et al., 1992; Emanuelsson, 1992); and the regulation of neuronal plasticity and long term potentiation in the marine gastropod *Aplysia californica* (Bailey et al., 1997; Martin et al., 1997).

Serotonin has also been implicated in the induction of metamorphosis in a wide range of marine invertebrate taxa, including cnidarians, ecdysozoans, and lophotrochozoans. McCauley (1997) showed that bath application of 5-HT induces

larvae of the anemone *Phialidium gregarium* to undergo the early events of metamorphosis without contact with a natural cue. Additionally, he demonstrated that application of 5-HT receptor antagonists or compounds that cause a global decrease of serotonin inhibited metamorphosis of larvae that have been exposed to natural inductive cues.

Serotonin has also been implicated as inducer of settlement but not metamorphosis in barnacle larvae. The application of L-tryptophan and related compounds, including serotonin, caused cyprid larvae of the barnacle *Balanus amphitrite* to settle from the water column and begin searching substrata for suitable sites for metamorphosis, but metamorphosis did not occur. (Kon-Ya et al., 1995; Yamamoto et al., 1996).

Several studies have demonstrated that 5-HT may play a role in the metamorphosis of molluscan larvae. 5-HT is weakly inductive in the bivalve *Crassostrea gigas* (Beiras and Widdows, 1995) and the gastropod *Hermissenda crassicornis* (Avila et al., 1996), but strongly inductive to larvae of the mud snail *Ilyanssa obsoleta*. Both bath applications (Couper and Leise, 1996; Leise et al., 2001; Leise et al., 2004;) and microinjections of 5-HT and compounds that modulate the 5-HT signaling pathway affect metamorphosis (Couper and Leise, 1996).

Although there is a growing number of studies that document distribution of serotonergic cells within the central nervous systems of polychaete larvae (Westheide, 2002; Nezlin and Voronezhskaya, 2003; Voronezhskaya et al., 2003; Forest, 2005; Müller, 2006; Brinkmann and Wanninger, 2008; Forest and Lindsay, 2008; Müller and; Winchell et al., 2010), there has been little research on the role that serotonin plays in the induction of metamorphosis of these larvae. Only a single study has demonstrated that bath application of serotonin induces metamorphosis in the polychaete larvae (Biggers and Laufer, 1992). The objective of the present study is to determine the role that 5-HT plays in the metamorphosis of the serpulid polychaete *Hydroides elegans.*

H. elegans is a common member of the fouling community throughout tropical and subtropical seas, and due to ease of culture and the rapid rate of larval development, is increasingly being utilized as a model system for understanding metamorphosis of marine invertebrate larvae and biofouling (Chapter 1). Larvae of *H. elegans* are induced

to metamorphose by bacterial biofilms (Hadfield et al., 1994). They then undergo rapid metamorphosis characterized by; secretion of a proteinaceous primary tube; eversion of the collar and constriction of tissues adjacent to it; loss of trochal cilia; and secretion of a calcified secondary tube. These processes are initiated only after physical contact with biofilm-bacterial cells or their associated extracellular polymeric substances (EPS) (Huang and Hadfield, 2003). While the molecular structure of the inductive cue remains unidentified, numerous studies have identified families of bacteria or specific bacterial strains of that induce metamorphosis (Unabia and Hadfield, 1999; Hadfield and Paul, 2001; Lau and Qian, 2001; Huang and Hadfield, 2003; Lau et al., 2005; Shikuma and Hadfield, 2006; Zardus et al., 2008; Huggett et al., 2009; Hung et al., 2009) and ongoing research is focused the molecular makeup of inductive cues for *H. elegans* (Hadfield, in press). Additionally, previous studies have examined the morphogenic and cellular processes triggered by the induction of metamorphosis in *H. elegans* (Carpizo-Ituarte and Hadfield, 1998; 2003; Wang and Qian, 2010), but the integration between sensing a bacterial cue and the initiation of metamorphic morphogenesis remains poorly resolved (Holm et al., 1998; Hadfield, in press). Because competent larvae of *H. elegans* have a well developed serotonergic nervous system (Chapter 2) that innervates both the cerebral ganglia and larval structures fated to be lost during metamorphosis, seven different compounds (Table 3.1) involved in both the biosynthesis of 5-HT and those altering 5-HT signaling pathways to were tested determine if release of 5-HT coordinates and controls metamorphosis of *H. elegans.*

Materials and Methods

Larval Culture

Dense aggregations of adult *H. elegans* were collected from Pearl Harbor, Hawaii, transported to the Kewalo Marine Laboratory, and kept in flowing seawater tables at. Gametes were obtained from clumps of adult worms and embryos, and larvae were cultured through competence as described in Chapter 1.

Neuropharmacological Agents

Seven compounds were tested for their effects on metamorphosis of *H. elegans.* These substances were chosen, because they directly affect the amount of serotonin

available for release by presynaptic cells and in the synapse or they act as receptor agonists and antagonists in post-synaptic cells (Table 1). Experiments using the compounds serotonin (5-HT), 5-hydroxy-tryptophan (5-HTP), α-methyl-serotonin (α-methyl-5HT) and fluoxetine were performed to determine if they could induce metamorphosis of *H. elegans* in the absence of an inductive bacterial cue. Additional experiments were conducted to determine if fluoxetine potentiates metamorphosis of *H. elegans* in the presence of a sub-optimal bacterial cue. Finally, experiments were performed with three compounds, p-chlorophenylalanine (p-CPA), mianserin, and gramine, to determine if they would inhibit metamorphosis of the larvae of *H. elegans* in the presence of an inductive bacterial cue. All compounds were purchased from Sigma (St. Louis, MO). Stock solutions of all the compounds except gramine were made in 0.22 μm-filtered seawater (FSW). Stock solutions of gramine were made in ethanol. All stock solutions were freshly made on the day of the experiment and subsequently diluted in FSW.

Experiments testing if 5-HT, 5-HTP, α-methyl-5-HT, and fluoxetine induce metamorphosis

Four ml of each test solution were pippetted into 35 x 10 mm polystyrene Petri dishes (Fisher Scientific, Pittsburgh, PA). Competent larvae of *H. elegans* were collected from their culture beakers by sieving (41 μm mesh size) and then washed from the sieves into small beakers containing 40-50 ml of FSW. Larvae were added to each Petri dish by pippetting 40 μl of concentrated larvae into each dish, resulting in 20 to 145 larvae/dish. Four replicate dishes of each chemical treatment and the appropriate controls were included in each experiment. Each experiment was repeated two times and the data were combined for analysis. Experiments were conducted in the dark to minimize oxidation of the test compounds and at room temperature. All experiments were allowed to run for 24 h.

Experiments testing if pCPA, mianserin and gramine inhibit metamorphosis

The experimental procedures were the same as that described above, except that, after 30 minutes, marine biofilms were added to each dish. Marine biofilms were obtained by placing small pieces of extruded plastic mesh (Vexar®) in sea tables with

constantly flowing seawater for a minimum of 10 days. Previous studies have shown that microbial biofilms form on this surface and high percentages of larvae quickly metamorphose on them (Hadfield et al., 1994; Holm et al., 1998; Unabia and Hadfield, 1999). Gramine stock solutions were diluted 100 fold before use. Each experiment was repeated two times and the data were combined for analysis.

Experiments testing if fluoxetine potentiates metamorphosis

The experimental procedure used to determine if fluoxetine potentiates metamorphosis was the same as the procedure used to determine if fluoxetine induces metamorphosis of *H. elegans*, except that a piece of Vexar coated with a one-day biofilm was added to each dish to provide a sub-optimal inductive cue. Metamorphosis of *H. elegans* is positively correlated with biofilm age and bacterial density (Hadfield et al., 1994; Huang and Hadfield, 2003), and a low percentage of larvae metamorphose on one day-old-biofilms. A compound that potentiates metamorphosis should produce an increase the percentage of larvae to a sub-optimal cue. Each experiment was repeated two times and the data were combined for analysis.

Controls

Positive and negative controls were included with every experiment. Biofilmed pieces of Vexar were used as positive controls in all experiments to ensure that larvae had attained metamorphic competence. A negative control of FSW was included in each experiment to test for spontaneous metamorphosis, which is rare for larvae of *H. elegans*. An additional control was included in the gramine experiments to ensure that the carrier did not inhibit metamorphosis.

Assessing toxic effects of the test compounds

Metamorphosis of larvae was scored 24 hrs after continuous exposure to the test compounds. Some concentrations of experimental compounds produced toxic effects in juveniles and larvae such as reduced swimming rates or complete cessation of swimming. Larvae were considered to have metamorphosed if they: (1) permanently attached to the surface of the Petri dish or the biofilmed substrata by secreting a primary tube, (2) secreted a calcified secondary tubes, and (3) showed normal differentiation of the branchial crown (Carpizo-Ituarte and Hadfield, 1998). Juvenile worms showing these abnormal morphologies were not counted as metamorphosed.

Statistical analysis

The proportion of metamorphosed juveniles in each replicate dish was determined and subjected to the angular transformation (Sokal and Rohlf, 1981). Data sets were tested for normality and homogeneity of variance using Analyse-it for Microsoft Excel (version 2.20). Normally distributed data were compared statistically by ANOVA, and heteroscedastic data assessed by the non-parametric Kruskal-Wallis ranks test. In both tests, multiple comparisons of experimental treatments against the appropriate controls were made using the Bonferroni correction (Analyse-it Software, Ltd. http://www.analyse-it.com/; 2009). A two-sample t-test was used to compare inhibition of metamorphosis by the compound gramine, that is, each concentration of the drug was compared against its ethanol control. Untransformed proportional data were converted to percentage data, and the untransformed means and standard errors were plotted using SigmaPlot 11 (SysStat Software, Inc. San Jose, CA)

Results

Effects of 5-HTP, 5-HTP and pCPA on metamorphosis

Both serotonin (5-HT) and an its immediate precursor 5-hydroxytryptophan (5-HTP) induced larvae of *H. elegans* to metamorphose in the absence of a biofilm (Fig. 3.1A, B). However, only the highest concentration of 5-HT induced metamorphosis (1mM, Fig. 1A). Concentrations of 5-HTP at10 nM, 1 μM and 10 μM significantly induced metamorphosis of *H. elegans* (Kruskal-Wallis test, $\chi^2 = 22.64$, p =0.01), but the mean metamorphosis (62.6 % $\pm$ 29.8) induced by exposure to 10 μM concentrations of 5-HTP was still much less than the percentage of larvae metamorphosed in response to natural biofilms (99.6% + 0.1, Fig. 3.1B).

P-Chlorophenylalanine (pCPA), which should reduce the amount of 5-HT available for release by irreversibly binding to the enzyme tryptophan hydroxylase, inhibited larval metamorphosis (Kruskal-Wallis test, χ^2=53.81, $p < 0.0001$). Over 90 % of larvae metamorphosed with the biofilm controls, but chronic exposures of 1 μM and 10 μM resulted in reduction of metamorphosis to 64% ($\pm$18) and 10% ($\pm$10), respectively (Fig. 3.2). The highest concentration of pCPA (100 μM) tested was toxic.

At all other concentrations larvae continued to swim normally and developed into juveniles that showed no signs of abnormal metamorphosis.

Effects of fluoxetine on metamorphosis

The selective serotonin-reuptake inhibitor fluoxetine did not induce larvae to metamorphose in the absence of a biofilm (data not shown). However, fluoxetine did potentiate competent larvae of *H. elegans* to metamorphose in higher proportions (ANOVA, $F_{(6,46)}$=46. 12, $p < 0.001$) when exposed to both the drug and a suboptimal inductive cue (1d bacterial biofilm). One-day old bacterial biofilms were poor inducers of *H. elegans* and only about 17% of the larvae metamorphosed in this control treatment. Chronic exposure to both 10 nM and 100 nM fluoxetine significantly increased metamorphosis of larvae to 49% ($\pm$ 12) and 37% ($\pm$ 12), respectively (Fig. 3.3). Higher concentrations of fluoxetine were toxic and caused both abnormal swimming behaviors (1 μM) and death of larvae (10 μM).

Effect of 5-HT receptor agonists and antagonists on metamorphosis

The receptor agonist α-methyl-serotonin (α-m-5-HT) induced larvae of *H. elegans* to metamorphose in the absence of natural inducers (Kruskal-Wallis test, $\chi^2 = 56.33$, $p< 0.0001$). More than 46% of larvae exposed to 100 μM of α-m-5-HT metamorphosed after 24 hrs of exposure to the drug (Fig. 3.4). However, α-m-5-HT did not perform as well as a bacterial biofilm as a metamorphic inducer. More than 90% of larvae had metamorphosed in the positive control treatment containing FSW and biofilm.

Serotonin-receptor antagonists inhibited metamorphosis of *H. elegans*. The antagonist mianserin inhibited metamorphosis when larvae were exposed to both it and a well-developed biofilm (Kruskal-Wallis test, $\chi^2 = 38.96$, $p < 0.0001$). Only about 27% of larvae metamorphosed in the 1 μM mianserin treatment, a level of metamorphosis similar to the FSW controls (Fig. 3.5A). Higher concentrations of the drug caused toxic effects toxic effects. Exposure to concentrations of gramine greater than 40 μM significantly inhibited metamorphosis (Table 3.2), and exposure of larvae to 100 μM concentrations of gramine almost completely inhibited metamorphosis (Fig. 3.5B).

Discussion

A general disadvantage of using pharmacological agents as inducers and inhibitors of metamorphosis of marine invertebrate larvae is the inherent uncertainty that a compound whose effects are defined by exposure to vertebrate nervous systems will function in the manner intended on whole larvae. Fortunately, the clinical relevance of serotonin in the treatment of human depression and other psychiatric illnesses has driven the discovery of many compounds that effect serotonin biosynthesis and its actions on target cells (see Murphy et al., 2004). The seven compounds (Table 3.1) used in this study appear to have similar function in lophotrochozoans as they have in mammals.

Serotonin is synthesized in vertebrate brains (Borue et al., 2009; Liuzzi et al., 1977) and other nervous tissues and has been shown to be synthesized in the central nervous systems of leeches (Henderson, 1983; Lent, 1985). Furthermore, 5-HT has been to shown to act as a neurotransmitter or neuromodulator in isolated body wall musculature of the polychaete *Sabellastarte magnifica* (Diaz-Miranda et al., 1992) and the intestine of *Chaetopterous variopedatus* (Anctil et al., 1984). 5-hydroxytryptophan (5-HTP) is an intermediate in the biosynthesis of serotonin and is converted to 5-HT in vertebrate and most invertebrate systems (Cooper et al., 1996). 5-HTP has been indentified in the scallop *Placopectin magellanicus* using HPLC (Pani and Croll, 1998). It has also been isolated from leech tissues and shown to be converted to 5-HT in Retzius cells of *Hirudo intestinalis* (Henderson, 1983). p-Chlorophenylalanine depletes 5-HT by inactivating the enzyme tryptophan hydroxylase in vertebrates (Jequier et al., 1967; Cooper et al., 1996), and appears to have a similar function in molluscs (Pani and Croll, 1998) and polychaetes. Anctil et al (1989) showed that pCPA depleted serotonin in isolated elytra of the polynoid polychaetes *Harmothoe imbricata* and *H. lunulata*. These data suggest that the biosynthetic pathway of 5-HT is similar between vertebrates and lophotrochozoans. Accordingly, bath applications of both 5-HT and 5-HTP, should cause a global increase in 5-HT in larval tissues, and this increase should induce metamorphosis of *H. elegans.* Additionally, exposure of larvae to pCPA should inhibit the activity of tryptophan hydroxylase and cause a global decrease in 5-HT in larval tissues. The depletion of serotonin within the CNS of larvae should inhibit metamorphosis if *H. elegans* is using it as a neurotransmitter or neuromodulator during metamorphosis.

The receptor agonist and antagonists used in the present study have well-defined actions. α- Methyl-serotonin functions as a receptor agonist in both vertebrate (Chaouch-Teyara et al., 1993) and invertebrate nervous systems (Walker, 1986), and probably acts in a similar manner on *H. elegans.* Both gramine and mianserin are 5-HT receptor antagonists in vertebrates (Segal, 1976; Maj et al., 1978; Sah and Matsumoto, 1987;) and have similar functions in molluscs (Katz and Frost, 1995; Kamardin et al., 1999;). Because these compounds are both present and have similar functions in lophotrochozoans, gramine and mianserin should act as antagonists against serotonin receptors in larvae of *H. elegans.*

Fluoxetine is a selective reuptake inhibitor (SSRI), which functions by inhibiting serotonin transporters that remove 5-HT from the synaptic cleft in mammals and invertebrates (Henderson, 1983; Bruns et al., 1993), and has been shown to act as a selective reuptake inhibitor (SSRI) in leeches (Bruns et al., 1993; Calvino et al., 2005). Additionally, injections of the drug into larvae of *Ilyanasa obsoleta* induced metamorphosis of the larvae in the absence of natural inducers (Couper and Leise, 1996). Fluoxetine is expected to have a similar function in larvae of *H. elegans* because of its functions as a SSRI in the tissue of other invertebrates and because it induces metamorphosis of other kinds invertebrate larvae (Couper and Leise, 1996).

The hypothesis that release of serotonin controls and coordinates metamorphosis of in the serpulid polychaete *Hydroides elegans* is supported by the data presented here. If serotonin is involved in controlling metamorphosis, exposure of competent larvae of *H. elegans* to both it and its immediate precursor, 5-HTP, should induce competent larvae to metamorphose without stimulation by bacterial biofilms. Bath applications of both compounds induced high percentages of metamorphosis in larvae of *H. elegans* (Fig. 3.1A and B). Additionally, exposure of larvae to pCPA should reduce 5-HT in cells within *H. elegans* and inhibit metamorphosis. As expected, exposure of larvae to pCPA inhibited larvae of *H. elegans* to metamorphose in the presence of bacterial biofilms (Fig. 2). Further the receptor agonist α-m-5-HT induced metamorphosis (Fig. 3.4), and the receptor antagonists gramine and mianserin inhibited metamorphosis (Fig 3.5A and 3.5B), suggesting that larvae of *H. elegans* express 5-HT receptors and can respond to 5-

HT during metamorphosis. Finally, fluoxetine, a SSRI, potentiated the metamorphosis of larvae of *H. elegans* to a suboptimal metamorphic cue (Fig. 3.3).

The selective serotonin reuptake inhibitor fluoxetine was predicted to induce metamorphosis of *H.* elegans but instead it potentiated metamorphosis. While this final experimental outcome was not identical to the predicted outcome, the mode of action of the drug and its effect on *H. elegans* support the conclusions drawn from the other metamorphic assays. When externally applied, it causes the accumulation of spontaneously-released extracellular 5-HT in the synaptic cleft of leech neurons (Henderson, 1983; Bruns et al., 1993; Bruns et al., 2000; Calvino et al., 2005;), and should act in a similar way in the CNS of *H. elegans*. However, the amount of spontaneously released 5-HT by fluoxetine was not enough to trigger metamorphosis without an additional cue, but pre-exposing larvae of *H. elegans* fluoxetine and then challenging them with a sub-optimal metamorphic cue (1d biofilm) potentiates metamorphosis (Fig. 3.3). Perhaps induction of metamorphosis is only triggered after an increase in the rate of action potentials generated in the postsynaptic target cells. When larvae contact a suboptimal natural cue (i.e. a biofilm with less than optimal bacterial cell density), they do not encounter surface bound inducers frequently enough to cause the necessary rate increase and initiate metamorphosis, but exposure of larvae to both fluoxetine and a suboptimal may increase the frequency that the post synaptic cell fires and induce metamorphosis.

The high concentrations of serotonin and its analog α-methyl-serotonin required to induce metamorphosis of *Hydroides elegans* may be of concern. However, the 1mM of 5-HT that induces larvae of *H. elegans* falls well within the 100 μM - 5 mM inductive concentration ranges other species, (Biggers and Laufer, 1992; Leise, 1996; McCauley, 1997; Leise et al., 2001; Leise et al., 2004; Zega et al., 2007; Zega et al., 2005). Additionally, the concentrations of 5-HT that are typically used in electrophysiological studies of isolated ganglia and nerve cells of both vertebrates and invertebrates are between 10 μM – 100 μM (Andrade and Nicoll, 1987; Beato and Nistri, 1998; Katz and Frost, 1995; Marinesco and Carew, 2002). Marinesco and Carew (2002) estimated that the effective concentration of exogenous 5-HT reaching the synaptic region of the partially dissected CNS of *Aplysia californica* was diluted 50 times because of diffusion

barriers and active serotonin-transport mechanisms. The effective concentration of 5-HT that actually reaches the CNS of larvae of *H. elegans* may be even lower since it must also diffuse across a larval cuticle before penetrating epidermal cells.

Potential models for the mode of action of serotonin during metamorphosis

McCauley(1997) demonstrated that 5-HT is involved in the metamorphosis of larvae of *Phialidium gregarium* and functions as an early metamorphic signal in a multi-step process. Bath applied 5-HT induces metamorphosis of larvae, and recordings from epithelial cells of larvae of revealed that 5-HT controlled increases of both the amplitude and frequency of Ca2+ transients (McCauley, 1997), and these transients must occur for induction metamorphosis in *P. gregarium* by biofilm (Freeman and Ridgway, 1987). Calcium ions may act as a second messenger in activation protein kinase C (PKC). Protein kinase C was implicated in the metamorphosis of *P. gregarium* because the phorbal ester PMA, an activator of PKC, induced metamorphosis of larvae of *P. gregarium* in the absence of other cues. Additionally, an inhibitor of PKC, H7, blocked the metamorphosis of larvae of *P. gregarium* that had been induced by 5-HT. Taken together these results suggest that 5-HT may function upstream of PKC in the metamorphic pathway of *P. gregarium*. The model suggested by McCauley (1997) postulates that contact of larvae of *Phialidium gregarium* with a bacterial cue releases 5-HT into the environment, where it then acts on external receptors, causing membrane depolarization, calcium influx, and activation the metamorphic program through the activation of PKC.

The model proposed by McCauley is probably not the mode of action of 5-HT during metamorphosis of *H. elegans* because phorbal esters do not induce metamorphosis of *H. elegans* (Holm et al., 1998) as they do in *P. gregarium*. Additionally, the majority of 5-HT positive cells are neither in the epithelium of competent larvae of *H. elegans*, nor do most 5-HT positive cell bodies project processes to the larval surface (see Chapter 2). Although there is pair of cells in the pygidium of competent larvae of *H. elegans* that has surface processes, it is difficult to imagine how release of 5-HT at the posterior end of the larvae could diffuse over a distance of at least 150 um, the length of a competent larva, and remain concentrated enough to depolarize a second set of chemoreceptors in the presumed region of chemoreception at the anterior pole of the larva.

Larvae of *Ilyanassa obsoleta* metamorphose when exposed to either bath-applied or directly injected 5-HT (Leise, 1996). These results suggest that 5-HT acts downstream of metamorphic chemoreception. If 5-HT acts as an external cue on the epithelial cells or the dendrites of the metamorphic chemoreceptors, direct injection of 5-HT or the appropriate receptor agonists and antagonists into the hemolymph of larvae of *Ilyanassa obsoleta* should produce lower levels of metamorphosis or disrupt the normal timing of metamorphic events. This is not the case: both the timing and the level of metamorphosis were the same regardless of the mode of application of the drugs (Leise et al., 2001). Leise et al. (2004) also infer that one of the downstream targets 5-HT may be the molecule nitric oxide synthase (NOS) within the apical ganglion (AG) of the larva. The inhibition of NOS causes a decrease of nitric oxide (NO), which in turn, may trigger apoptosis of the larval AG (Leise et al., 2004, Gifondorwa and Leise, 2006;). While there is no concrete data to suggest that apoptosis of AG of *I. obsoleta* triggers metamorphosis, if larvae were kept for several weeks in culture, these larvae begin to spontaneously metamorphose (Leise et al., 2004), and apoptosis was occurring in the AG of these larvae (Gifondorwa, 2002; Leise et al., 2004). It is uncertain if 5-HT has a similar mode of action during metamorphosis of *H. elegans*. Serotonin-like reactive cells are not present in the apical sensory organ (ASO) of competent larvae of *Hydroides elegans* (Chapter 2), and therefore, release of serotonin from the ASO can not act as a trigger for the initiation of apoptosis of ASO and induction of metamorphosis.

Clearly, serotonin is required for the induction of metamorphosis of *Hydroides elegans,* but its mode of action within the metamorphic process is not well understood. It can neither act as an environmental stimulus of metamorphosis nor can it be utilized by the primary chemoreceptors to convey the metamorphic signal to the rest of the CNS. Serotonin has not be shown to be produced by marine bacteria, and even if it was being secreted into the environment by bacteria, larvae of *H. elegans* do not respond to dissolved bacterial cues of either multi-species (Hadfield, in press) or single strain biofilms (Unabia and Hadfield, 1999; Huang and Hadfield, 2003). Additionally, it is probably not being used as a neurotransmitter by the primary chemosensory cells (the apical sensory organ) that induce metamorphosis, because 5-HT is not produced by those cells (Chapter 2). It must therefore act at least one step downstream of chemoreception,

but the cellular targets of the release of serotonin are not known. The serotonergic neurons seem to be mostly confined to the CNS of competent larvae of *H, elegans,* but it is strongly expressed in the nerves that underlie the larval prototroch and metatroch (Chapter 2). Both of these of these organs are lost during metamorphosis, and the release of serotonin may trigger the cascade that causes the loss of these tissues. Alternatively, serotonin may act as neuromodulator, and the release of serotonin into the hemolymph may affect tissues quite distant from the serotonergic nervous system. Experiments using antibodies raised against serotonin receptors may help to uncover the cells being affected by the release of serotonin during metamorphosis of *H. elegans* and their proximity to tissues that are remodeled during metamorphosis.

References

Anctil M, Bassot J-M, Nicolas M-t. 1989. Effects of monoamines and related drugs on the bioluminescence of scale-worm elytra (Polychaeta, Polynoidae). Comp Biochem and Physiol C: Comparative Pharmacology 93(1):127-135.

Anctil M, Laberge M, Martin N. 1984. Neuromuscular pharmacology of the anterior intestine of Chaetopterus variopedatus, a filter-feeding polychaete. Comp Biochem Physiol C 79(2):343-351.

Andrade R, Nicoll R. 1987. Pharmacologically distinct actions of serotonin on single pyramidal neurons of the rat hippocampus recorded in vitro. J Physiol 394:99–124.

Avila C, Tamse CT, Kuzirian AM. 1996. Induction of Metamorphosis in *Hermissenda crassicornis* larvae (Mollusca: Nudibranchia) by GABA, choline and Serotonin. Inv Rep Develop 29(2):127-141.

Bailey CH, Kaang B-K, Chen M, Martin KC, Lim C-S, Casadio A, Kandel ER. 1997. Mutation in the phosphorlation sites of MAP kinase blocks learning-related interalization of apCAM in *Aplysia* sensory neurons. Neuron 18:913-924.

Beato M, Nistri A. 1998. Serotonin-induced inhibition of locomotor rhythm of the rat isolated spinal cord is mediated by the 5-HT1 receptor class. Proceedings of the Royal Society B: Biological Sciences 265:2073–2080.

Beiras R, Widdows J. 1995. Induction of metamorphosis in larvae of the oyster *Crassostrea gigas* using neuroactive compounds. Mar Biol 123(2):327-334.

Berger M, Gray JA, Roth BL. 2009. The Expanded Biology of Serotonin. Annu Rev Med 60(1):355-366.

Biggers WJ, Laufer H. 1992. Chemical induction of settlement and metamorphosis of *Capitella capitata* Sp.I (Polychaeta) larvae by juvenile hormone-active compounds. Inv Rep Develop 22(1-3):39-46.

Bishop CD, Pires A, Norby S-W, Boudko D, Moroz LL, Hadfield LL. 2008. Analysis of nitric oxide-cyclic guanosine monophosphate signaling during metamorphosis of

the nudibranch *Phestilla sibogae* Bergh (Gastropoda: Opisthobranchia). Evolution & Development 10(3):288-299.
Borue X, Cooper S, Hirsh J, Condron B, Venton BJ. 2009. Quantitative evaluation of serotonin release and clearance in Drosophila. J Neurosci Methods 179(2):300-308.
Braubach OR, Dickinson AJG, Evans CCE, Croll RP. 2006. Neural control of the velum in larvae of the gastropod, Ilyanassa obsoleta. J Exp Biol 209(23):4676-4689.
Brinkmann N, Wanninger A. 2008. Larval neurogenesis in *Sabellaria alveolata* reveals plasticity in polychaete neural patterning. Evolution & Development 10(5):606-618.
Bruns D, Engert F, Lux HD. 1993. A fast activating presynaptic reuptake current during serotonergic transmission in identified neurons of Hirudo. Neuron 10(4):559-572.
Bruns D, Riedel D, Klingauf J, Jahn R. 2000. Quantal Release of Serotonin. Neuron 28(1):205-220.
Calvino MA, Iscla IR, Szczupak L. 2005. Selective Serotonin Reuptake Inhibitors Induce Spontaneous Interneuronal Activity in the Leech Nervous System. J Neurophysiol 93(5):2644-2655.
Carpizo-Ituarte E, Hadfield MG. 1998. Stimulation of Metamorphosis in the Polychaete *Hydroides elegans* Haswell (Serpulidae). Biol Bull 194:14-24.
Carpizo-Ituarte E, Hadfield MG. 2003. Transcription and translation inhibitors permit metamorphosis up to radiole formation in the serpulid polychaete *Hydroides elegans*. Biol Bull 204:114-125.
Chaouch-Teyara K, Fournier B, M.Safar, Dabire H. 1993. Vascular and cardiac effects of alpha-methyl-5-HT and DOI are mediated by different 5-HT receptors in the pithed rat. Europoean Journal of Pharmacology 250:67-75.
Cooper JR, Bloom FE, Roth RH. 1996. The biochemical basis of neuropharmacology. New York: Oxford University Press. 518 p.
Couper JM, Leise EM. 1996. Serotonin injections induce metamorphosis in larvae of the gastropod mollusc *Ilyanassa obsoleta*. Biol Bull 191:178-186.
Crisp DJ. 1974. Factors influencing the settlement of marine invertebrate larvae. In: Mackie PGaA, editor. Chemoreception in Marine Organisms. London: Academic Press. p 177-265.
Diaz-Miranda L, de Motta GE, Garcia-Arraras JE. 1992. Monoamines and neuropeptides as transmitters in the sedentary polychaete *Sabellastarte magnifica*: actions on the longitudinal muscle of the body wall. J Exp Zool 263(1):54-67.
Emanuelsson H. 1992. Autoradiographic localization in polychaete embryos of tritiated mesulergine, a selective antagonist of serotonin receptors that inhibits early polychaete development. International Journal of Developmental Biology 36(2):293-302.
Forest DL. 2005. The nervous systems of spionid polychaetes: structure, composition, and effects of serotonin on behavior: University of Maine. 90 p.
Forest DL, Lindsay SM. 2008. Observations of serotonin and FMRFamide-like immunoreactivity in palp sensory structures and the anterior nervous system of spionid polychaetes. J Morphol 269(5):544-551.
Freeman G, Ridgway EB. 1987. Endogenous photoproteins, calcium channels and calcium transients during metamorphosis. Roux's Arch Dev Biol 196:30-50.

Froggett SJ, Leise EM. 1999. Metamorphosis in the marine snail *Ilyanassa obsoleta*, Yes or No. Biol Bull 196:57-62.
Gerhardt CC. 1996. Molecular cloning and functional characterization of serotonin and octopamine receptors present in the central nervous system of *Lymnaea stagnalis* [Ph. D. dissertation]. Amsterdam: Vrije Universiteit. 136 p.
Gifondorwa DJ. 2002. Programmed cell death in the apical ganglion during metamorphosis of the marine mollusc *Ilyanassa obsoleta*. Greensboro: University of North Carolina Greensboro.
Gifondorwa DJ, Leise EM. 2006. Programmed cell death in the apical ganglion during larval metamorphosis of the marine mollusc Ilyanassa obsoleta. Biol Bull 210(2):109-120.
Guler Y, Ford AT. 2010. Anti-depressants make amphipods see the light. Aquat Toxicol 99(3):397-404.
Hadfield MG. 2000. Why and how marine-invertebrate larvae metamorphose so fast. Seminars in Cell & Developmental Biology 11:437-443.
Hadfield MG. in press. Biofilms and marine invertebrate larvae: what bacteria produce that larvae use to choose settlement sites. Annual Reviews of Marine Science 3.
Hadfield MG, Paul VJ. 2001. Natural chemical cues for settlement and metamorphosis of marine invertebrate larvae. In: McClintock JB, Baker W, editors. Marine Chemical Ecology: CRC Press. p 431-461.
Hadfield MG, Unabia CC, Smith CM, Michael TM. 1994. Settlement preferences of the ubiquitious fouler *Hydroides elegans*. In: Thompson MF, Nagabhushanam R, Sarojini R, Fingerman M, editors. Recent Developments in Biofouling Control. New Delhi: Oxford and IBH Pub. Co. p 450.
Hay-Schmidt A. 2000. The evolution of the serotonergic nervous system. Proceedings of the Royal Soceity of London B 267:1071-1079.
Henderson LP. 1983. The role of 5-hydroxytryptamine as a transmitter between identified leech neurones in culture. The Journal of Physiology 339(1):309-324.
Hens MD, Fowler KA, Leise EM. 2006. Induction of Metamorphosis Decreases Nitric Oxide Synthase Gene Expression in Larvae of the Marine Mollusc Ilyanassa obsoleta (Say). Biol Bull 211(3):208-211.
Holm ER, Nedved BT, Carpizo-Ituarte E, Hadfield MG. 1998. Metamorphic-signal transduction in *Hydroides elegans* (Polychaeta: Serpulidae) is not mediated by a G-Protein. Biol Bull 195:21-29.
Huang S, Hadfield MG. 2003. Composition and density of bacterial biofilms determine larval settlement of the polychaete Hydroides elegans. Mar Ecol Prog Ser 260:161-172.
Huggett MJ, Nedved BT, Hadfield MG. 2009. Effects of initial surface wettability on biofilm formation and subsequent settlement of Hydroides elegans. Biofouling 25(5):387-399.
Hung OS, Lee OO, Thiyagarajan V, He HP, Xu Y, Chung HC, Qiu JW, Qian PY. 2009. Characterization of cues from natural multi-species biofilms that induce larval attachment of the polychaete Hydroides elegans. Aquat Biol 4(3):253-262.
Jequier E, Lovenberg W, Sjoerdsma A. 1967. Tryptophan hydroxylase Iinhibition: the mechanism by which p-chlorophenylalanine depletes rat brain serotonin. Mol Pharmacol 3(3):274-278.

Kamardin N, Szucs A, Rozsa KS. 1999. Distinct responses of osphradial neurons to chemical stimuli and neurotransmitters in *Lymnaea stagnalis* L. Cell Mol Neurobiol 19(2):235-247.

Katz PS, Frost WN. 1995. Intrinsic neuromodulation in the *Tritonia* swim CPG: serotonin mediates both neuromodulation and neurotransmission by the dorsal swim interneurons. J Neurophysiol 74(6):2281-2294.

Kimura Y, Yoshida M, Morisawa M. 2003. Interaction between noradrenaline or adrenaline and the [beta]1-adrenergic receptor in the nervous system triggers early metamorphosis of larvae in the ascidian, Ciona savignyi. Dev Biol 258(1):129-140.

Kon-Ya K, Shimidzu N, Adachi K, Miki W. 1995. L-Tryptophan and related compounds induce larval settlement of the barnacle *Balanus amphitrite* Darwin. Fisheries Sci 61:800-803.

Lau SCK, Qian PY. 2001. Larval settlement in the serpulid polychaete Hydroides elegans in response to bacterial films: An investigation of the nature of putative larval settlement cue. Mar Biol 138(2):321-328.

Lau SCK, Thiyagarajan V, Cheung CK, Qian P-Y. 2005. Roles of bacterial community composition in biofilms as a mediator for larval settlement of three marine invertebrates. Aquatic Microbial Ecology 38(1):41-51.

Leise EM. 1996. Selective retention of the fluorescent dye DASPEI in a larval gastropod mollusc after paraformaldehyde fixation. Microsc Res Tech 33(6):496-500.

Leise EM, Kempf SC, Durham NR, Gifondorwa DJ. 2004. Induction of metamorphosis in the marine gastropod Ilyanassa obsoleta: 5HT, NO and programmed cell death. Acta Biol Hung 55(1-4):293-300.

Leise EM, Thavaradhara K, Durham NR, Turner BE. 2001. Serotonin and Nitric Oxide Regulate Metamorphosis in the Marine Snail Ilyanassa obsoleta. Am Zool 41(2):258-267.

Lent CM. 1985. Serotonergic modulation of the feeding behavior of the medicinal leech. Brain Res Bull 14(6):643-655.

Liuzzi A, Foppen FH, Saavedra JM, R. Levi-Montalcini I, Kopin J. 1977. Gas chromatographic-mass spectrometric assay of serotonin in rat superior cervical ganglia. Effects of nerve growth factor and 6-hydroxydopamine. Brain Res 133:354-357.

Maj J, Mogilnicka E, Klimek V. 1978. The influence of mianserin and danitracen, 5--hydroxytryptamine receptor blockers, on the 5--hydroxytryptamine disappearance induced by h22/54 in the rat brain. Pol J Pharmacol Pharm 30(2-3):413-420.

Marinesco S, Carew TJ. 2002. Serotonin Release Evoked by Tail Nerve Stimulation in the CNS of Aplysia: Characterization and Relationship to Heterosynaptic Plasticity. J Neurosci 22(6):2299-2312.

Martin KC, Casadio A, Zhu H, E Y, Rose JC, Chen M, Bailey CH, Kandel ER. 1997. Synapse-specific, long-term facilitation of *Aplysia* to sensory to motor synapses: A function for local protein synthesis in memory storage. Cell 91:927-938.

McCauley DW. 1997. Serotonin plays an early role in the metamorphosis of the Hydrozoan *Phialidium gregarium*. Dev Biol 190:229-240.

Müller MCM. 2006. Polychaete nervous systems: Ground pattern and variations--cLS microscopy and the importance of novel characteristics in phylogenetic analysis. Integrative and Comparative Biology 46(2):125-133.
Müller MCM, Westheide W. 2002. Comparative analysis of the nervous systems in presumptive progenetic dinophilid and dorvilleid polychaetes (Annelida) by immunohistochemistry and cLSM. Acta Zoologica Stockholm 83(1):33-48.
Murphy DL, Lerner A, Rudnick G, Lesch K-P. 2004. Serotonin Transporter: Gene, Genetic Disorders, and Pharmacogenetics. Molecular Interventions 4(2):109-123.
Nezlin LP, Voronezhskaya EE. 2003. Novel, posterior sensory organ in the trochophore larva of *Phyllodoce maculata* (Polychaeta). Proceedings of the Royal Society of London Series B: (Suppl) Biology Letters:159-162.
Pani A, Croll RP. 1998. Pharmacological analysis of monoamine synthesis and catabolism in the scallop *Plactopecten magellanicus*. Gen Pharmacol 31(1):67-73.
Pawlik JR. 1992. Induction of Marine Invertebrate Larval Settlement: Evidence for Chemical Cues. In: Paul VJ, editor. Ecological roles of marine natural products. ithaca: Cornell Univ. Press. p 189-236.
Sah DW, Matsumoto SG. 1987. Evidence for serotonin synthesis, uptake, and release in dissociated rat sympathetic neurons in culture. J Neurosci 7(2):391-399.
Segal M. 1976. 5-HT antagonists in rat hippocampus. Brain Res 103(1):161-166.
Shikuma NJ, Hadfield MG. 2006. Temporal variation of an initial marine biofilm community and its effects on larval settlement and metamorphosis of the tubeworm *Hydroides elegans*. Biofilms 2(4):231-238.
Sokal RR, Rohlf FJ. 1981. Biometry :the principles and practice of statistics in biological research: W. H. Freeman.
Unabia CRC, Hadfield MG. 1999. Role of bacteria in larval settlement and metamorphosis of the polychaete *Hydroides elegans*. Mar Biol 133:55-64.
Voronezhskaya EE, Tsitrin EB, Nezlin LP. 2003. Neuronal development in larval polychaete *Phyllodoce maculata* (Phyllodocidae). J Comp Neurol 455:299-309.
Walker RJ. 1986. Transmitters and Modulators. In: Wilbur KM, editor. The Mollusca. New York: Academic Press. p 279-452.
Wang H, Qian P-Y. 2010. Involvement of a novel p38 mitogen-activated protein kinase in larval metamorphosis of the polychaete *Hydroides elegans* (Haswell). Journal of Experimental Zoology Part B: Molecular and Developmental Evolution 314B(5):390-402.
Winchell C, Valencia J, Jacobs D. 2010. Confocal analysis of nervous system architecture in direct-developing juveniles of *Neanthes arenaceodentata* (Annelida, Nereididae). Frontiers in Zoology 7(1):17.
Yamamoto H, Tachibana A, Kawaii S, Matsumura K, Fusetani N. 1996. Serotonin involvement in larval settlement of the barnacle, *Balanus amphitrite*. The Journal of Experimental Zoology 275(5):339-345.
Zardus JD, Nedved BT, Huang Y, Tran C, Hadfield MG. 2008. Microbial biofilms facilitate adhesion in biofouling iInvertebrates. Biol Bull 214(1):91-98.
Zega G, Pennati R, Fanzago A, De Bernardi F. 2007. Serotonin involvement in the metamorphosis of the hydroid *Eudendrium racemosum*. International Journal of Developmental Biology 51:307-313.

Zega G, Pennati R, Groppelli S, Sotgia C, Bernardi FD. 2005. Dopamine and serotonin modulate the onset of metamorphosis in the ascidian *Phallusia mammillata*. Dev Biol 282(1):246-256.

. **Table 3.1**. Compounds tested for effects of metamorphosis on larvae of *Hydroides elegans*

Compound	Proposed Mode of Action	Expected Effect on Metamorphosis
5-HT	Taken up by serotonergic cells and augments amount of 5-HT available for release	Induce metamorphosis
5-HTP	Immediate precursor of 5-HT. Taken up by serotonergic cells and immediately converted to serotonin	Induce metamorphosis
PCPA	Irreversibly binds to tryptophan hydroxylase and disrupts the synthesis of 5-HT	Inhibit metamorphosis
Alpha-Methyl-5HT	5-HT receptor agonist	Induce metamorphosis
Gramine	5-HT receptor antagonist	Inhibit metamorphosis
Mianserin	5-HT receptor antagonist	Inhibit metamorphosis
Fluoxetine	Selective serotonin re-uptake inhibitor	Induce metamorphosis

Serotonin (5-HT), 5-hydroxy-tryptophan (5-HTP), p-Chlorophenylalanine (pCPA)

Table 3.2. Two-sample t-test on the effect of gramine on metamorphosis of *Hydroides elegans*.

Concentration (µM)	t-statistic	df	p-value
10	0.691	7	Ns
20	0.159	7	Ns
40	7.31	7	0.002
60	10.27	7	< 0.001
80	16.97	7	< 0.001
100	19.95	7	<0.001

Comparisons made between the stated concentration of gramine and an ethanol control.

Figure Legends

Figure 3.1. Effects of serotonin and 5-hydroxytryptophan on metamorphosis of *Hydroides elegans.* (A.) Response to bath-applied serotonin. (B.) Response to 5-hydroxytryptophan (5HTP), mean $\pm$ 1sd. *,mean % metamorphosis different from filtered seawater (FSW) controls. (Kruskal-Wallis, χ^2 =44.16, $p < 0.0001$) for A, (Kruskal-Wallis test, χ^2 = 22.64, p =0.01) for B.

Figure 3.2. Effects of p-Chlorophenylalanine (pCPA) on metamorphosis of *H. elegans*. Larvae were pretreated for 30 min, then exposed to a microbial biofilm for 24 h. mean $\pm$ 1sd. *,mean % metamorphosis different from biofilm controls. (Kruskal-Wallis test, χ^2 = 58.13, $p <0.0001$)

Figure 3.3. Effect Fluoxetine on metamorphosis of *H. elegans* sub-optimal cues. Larvae exposed to r fluoxetine in the presence of a 24 h microbial biofilm. Larvae in the FSW controls were exposed only to 0.22 um filtered seawater. 10+ d biofilms used as positive control (Biofilm). mean $\pm$ 1sd. *,mean % metamorphosis different from controls (ANOVA, $F_{(6,46)}$= 46.12, $p<0.0001$).

Figure 3.4. Effect of serotonin-receptor agonist α-m-serotonin on metamorphosis of larvae of *H. elegans.* Larvae were exposed to compound for 24 hrs. mean $\pm$ 1sd. *,mean % metamorphosis different from seawater controls. (Kruskal-Wallis test, χ^2 = 56.33, $p <0.0001$)

Figure 3.5. Effects of serotonin-receptor antagonists on metamorphosis of *Hydroides elegans.* (A). Effect of mianserin metamorphosis of *H. elegans.* (Kruskal-Wallis test, χ^2 = 38.96, $p <0.0001$). (B.) Effect of the antagonist gramine on the response of larvae of *H. elegans* to microbial films. See Table 2 for statistics. mean $\pm$ 1sd. *,mean % metamorphosis different from biofilm controls

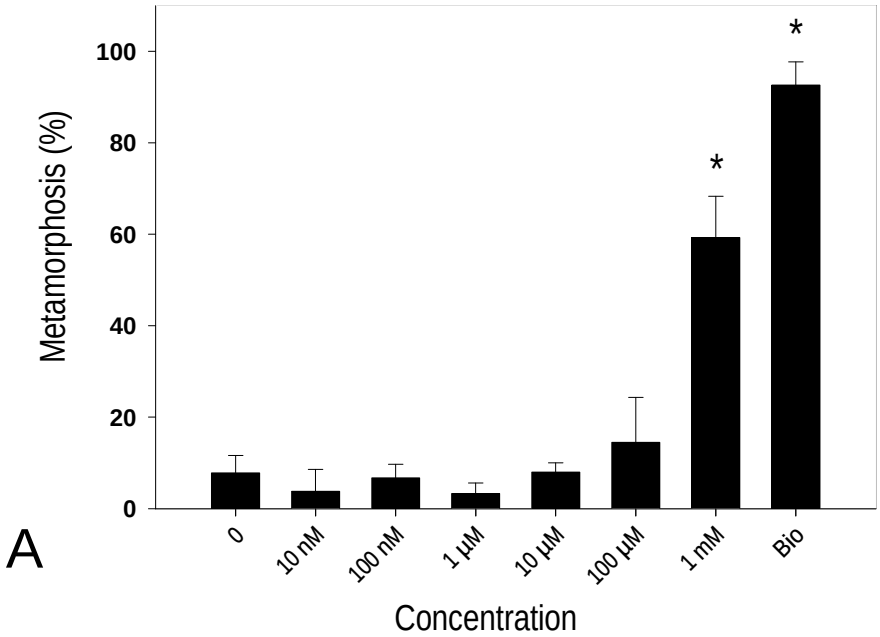
A
Metamorphosis (%)
100
80
60
40
20
0
*
*
0
10 nM
100 nM
1 µM
10 µM
100 µM
1 mM
Bio
Concentration

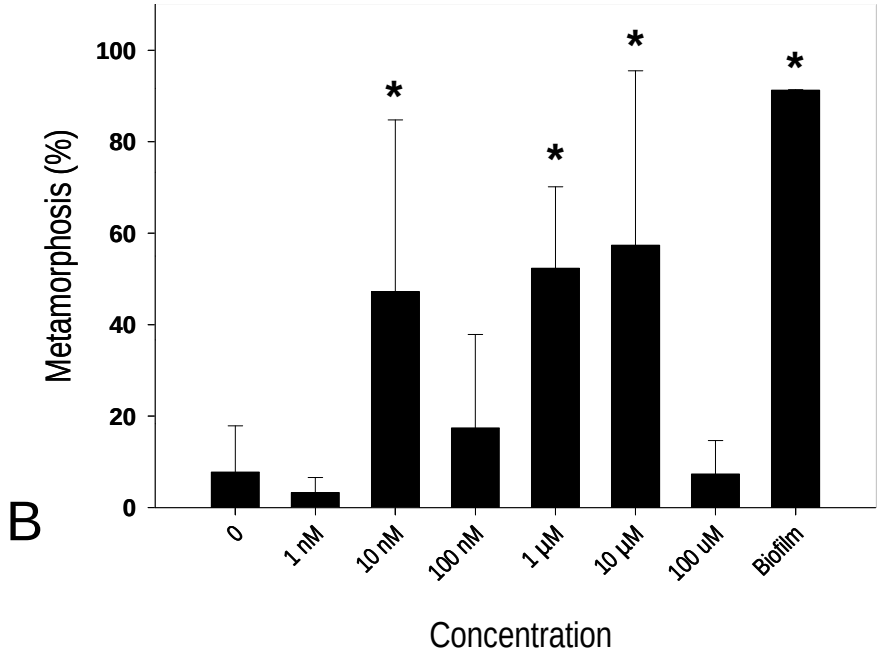
B
Metamorphosis (%)
100
80
60
40
20
0
*
*
*
*
0
1 nM
10 nM
100 nM
1 µM
10 µM
100 uM
Biofilm
Concentration

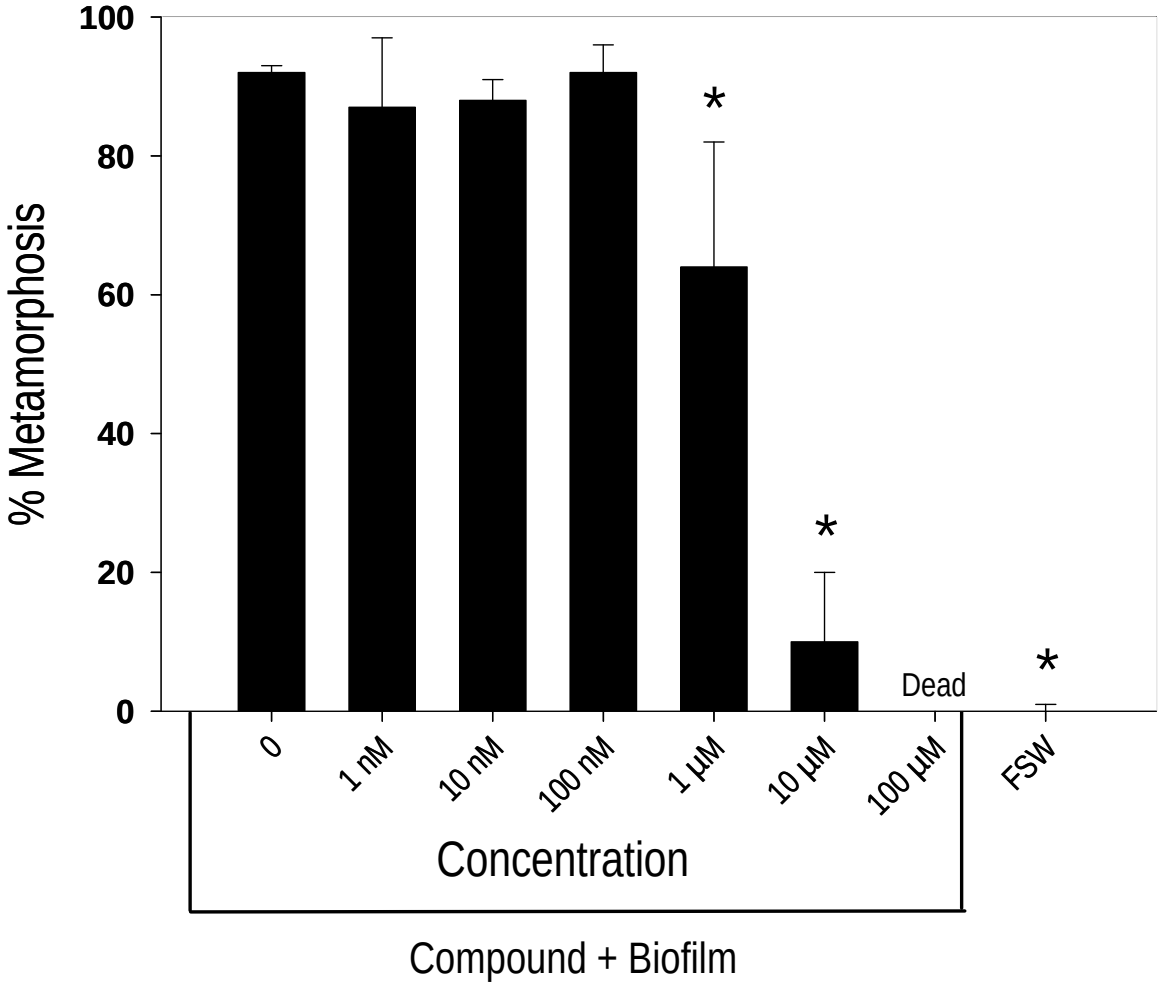
100
80
60
40
20
0
% Metamorphosis
*
*
*
Dead
0
1 nM
10 nM
100 nM
1 µM
10 µM
100 µM
FSW
Concentration
Compound + Biofilm

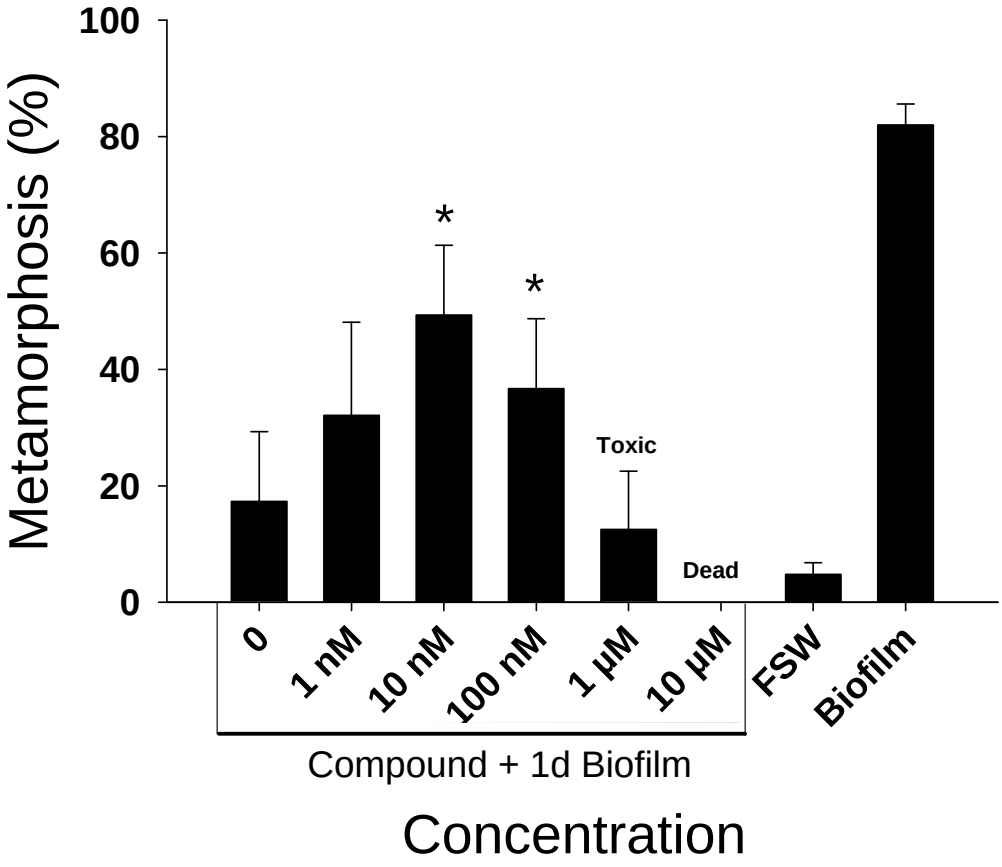
Metamorphosis (%)
100
80
60
40
20
0
*
*
Toxic
Dead
0
1 nM
10 nM
100 nM
1 µM
10 µM
FSW
Biofilm
Compound + 1d Biofilm
Concentration

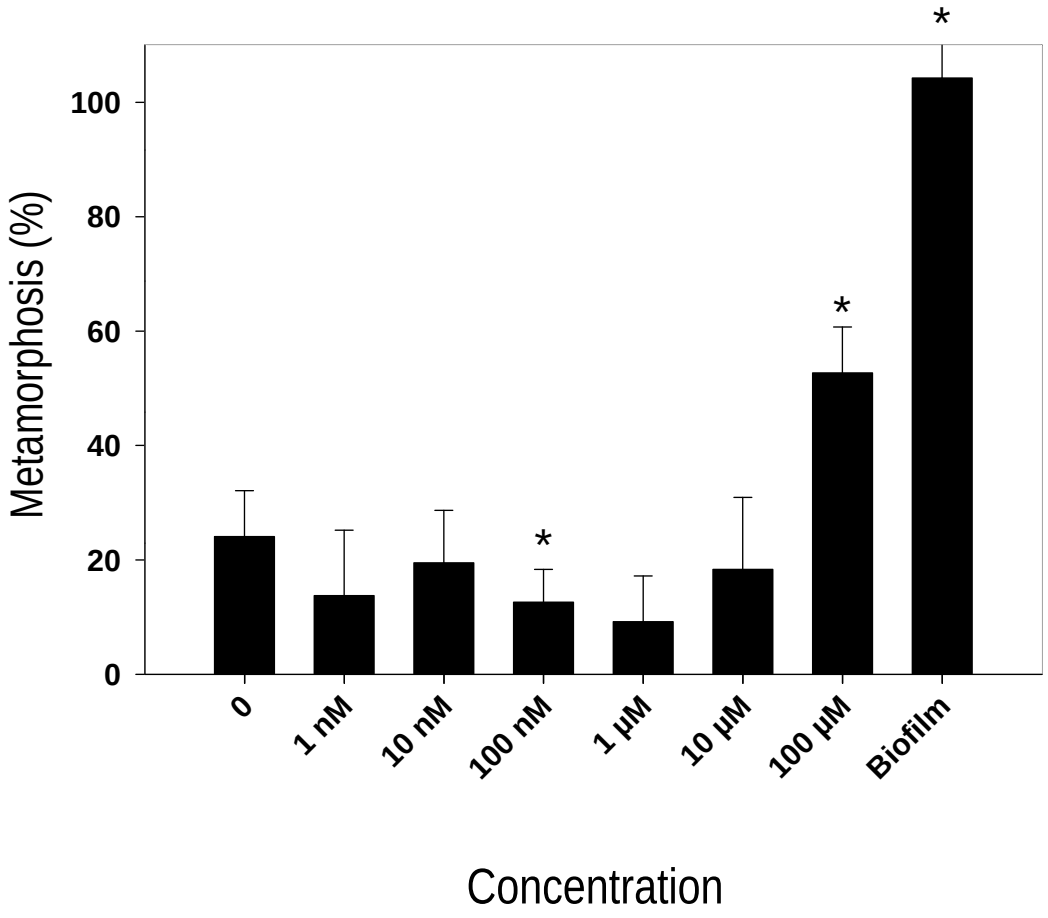
Metamorphosis (%)
0
20
40
60
80
100
*
*
*
0
1 nM
10 nM
100 nM
1 µM
10 µM
100 µM
Biofilm
Concentration

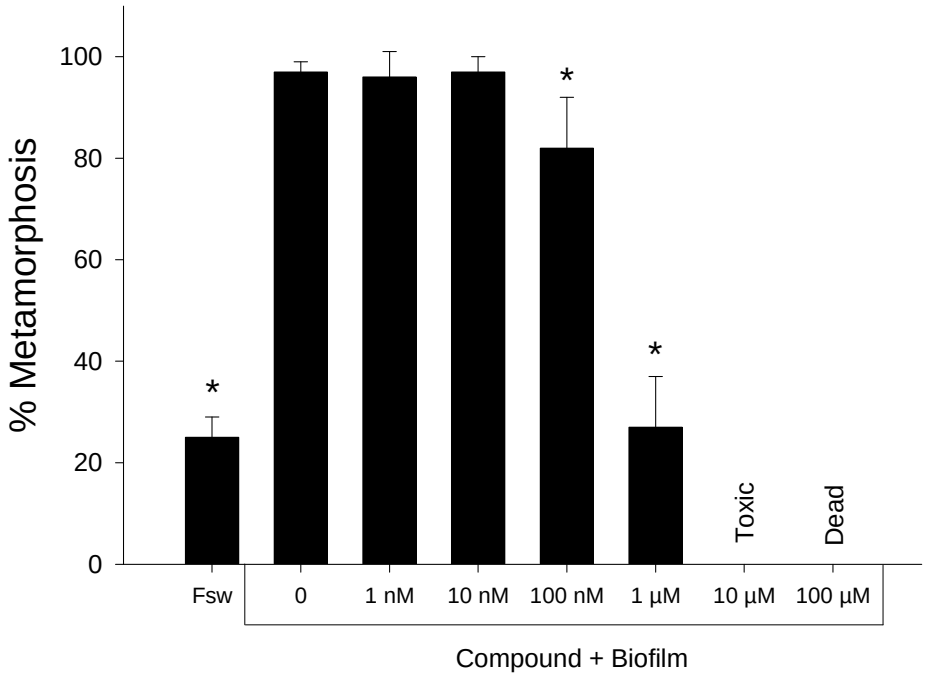
% Metamorphosis
100
80
60
40
20
0
*
*
*
Toxic
Dead
Fsw
0
1 nM
10 nM
100 nM
1 µM
10 µM
100 µM
Compound + Biofilm
Concentration

A.

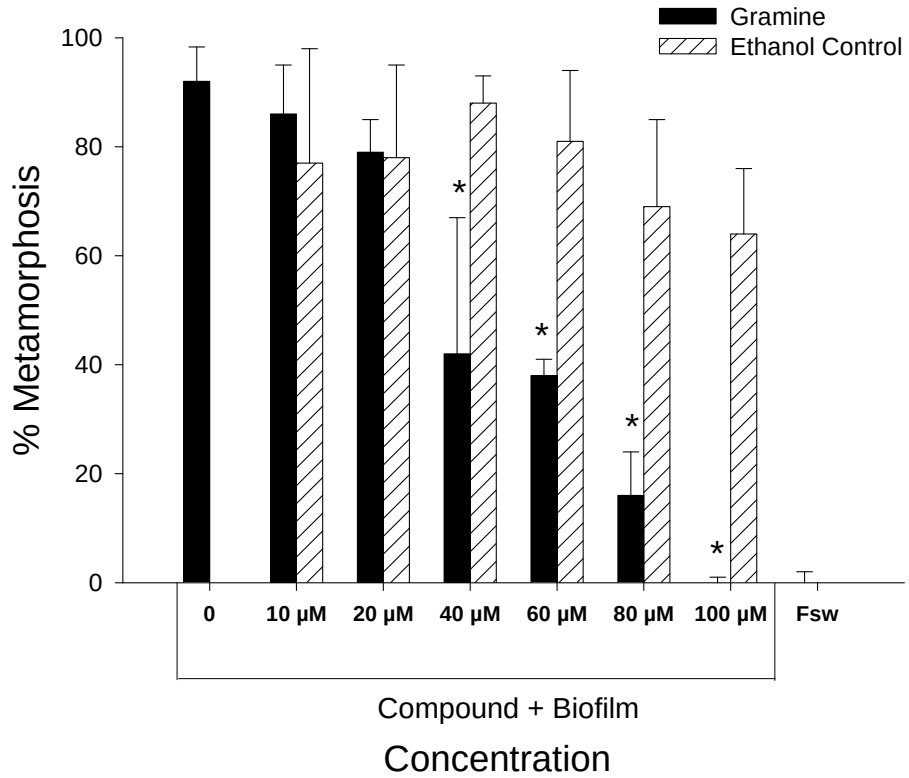
Gramine
Ethanol Control
% Metamorphosis
100
80
60
40
20
0
*
*
*
*
0
10 µM
20 µM
40 µM
60 µM
80 µM
100 µM
Fsw
Compound + Biofilm
Concentration

B.

CHAPTER 4.

TRACKING THE DEVELOPMENT AND FATE OF MUSCLES DURING LARVAL DEVELOPMENT AND METAMORPHOSIS OF THE SERPULID POLYCHAETE *HYDROIDES ELEGANS*

Introduction

The traditionally held hypothesis of the ancestral body plan of the Annelids was that of a burrowing worm that moved through the sediments using peristaltic movements (Clark, 1981). Accordingly, the ground pattern of the architecture of the body wall musculature was thought to consist of an outer layer of circular muscle that surrounded an inner layer of longitudinal muscle (Anderson, 1966; Anderson, 1973; Gardiner, 1992; Ruppert and Barnes, 1994; Tzetlin and Filippova, 2005). This anatomical pattern most closely resembled the clitellate pattern of muscle development, and, as the sister group to the polychaetes, the clitellates were thought to have ancestral traits for muscle development, including an anterior-to-posterior pattern of muscle differentiation from muscle precursors that were derived from teloblasts located in a posterior growth zone (Anderson, 1966).

However, recent investigations of polychaete muscular systems have demonstrated that the ancestral pattern for body wall musculature was less common than originally described (Tzetlin et al., 2002; Filippova et al., 2005; Tzetlin and Filippova, 2005; McDougall et al., 2006; Purschke and Muller, 2006; Rüchel and Müller, 2007; Brinkmann and Wanninger, 2010b; Filippova et al., 2010), and that there was great complexity of the architecture of the body wall musculature within the polychaetes, including the presence of complete circular muscles (Hill and Boyer, 2001; Tzetlin and Filippova, 2005; Purschke and Muller, 2006; Meyer et al., 2010), inversion of the circular and longitudinal muscles in the body wall (Filippova et al., 2005), circular muscles restricted to the spaces between parapodia (Filippova et al., 2006; Wanninger, 2009), and in as many as fourteen families of polychaetes a complete lack of circular muscles within the body wall entirely (Rüchel and Müller, 2007). Additionally, several recent

phylogenies of the annelids (McHugh, 2005; Struck et al., 2007; Dunn et al., 2008; Zrzavy et al., 2009; Dordel et al., 2010) have suggested that the clitellates were not sister taxa to the polychaetes but were a derived group within the polychaete lineage, and therefore, an earthworm-like pattern of muscle development may not be the ancestral state (Bergter et al., 2008). Additionally, the complexity of muscle patterns within adult polychaetes may hamper comparisons between groups and Bergter et al. (2008) suggested that comparative studies of muscle development in oligochaete embryos and polychaete larvae may help to improve the determination of the ancestral state of muscle arrangement and annelid evolution.

The serpulid polychaete *Hydroides elegans* is a common member of the fouling community in tropical and sub-tropical waters, and due to ease of culture, rapid larval development, and the availability of previous studies on its pattern of segmentation during larval development (Seaver et al., 2005; Seaver and Kaneshige, 2006), was a suitable species to use to follow myogenesis during larval development and to determine the fate of larval muscles through metamorphosis.

Larval development of *H. elegans* has been divided into six stages (Chapter 2). Briefly, the staging system begins with fertilization at Stage 0, passes through hatching (Stage 1), development of a trochophore larva (Stages 2 and 3), development of a segmented metatrochophore (Stages 4 and 5), and culminates with the nectochaete stage (Stage 6) that has attained metamorphic competence (Fig. 4.1). After achieving competence, larvae of *H. elegans* rapidly metamorphose after induction by bacterial cues (Hadfield et al., 1994; Carpizo-Ituarte and Hadfield, 1998). The metamorphic progression of *H. elegans* has also been previously described (Wisely, 1958 *(as H. norvegica*); Carpizo-Ituarte and Hadfield, 1998).

The current study had two aims, first, to examine myogenesis in larvae of the serpulid polychaete *Hydroides elegans,* and then to track the fate of these muscle groups through metamorphosis. A fluorescent analog of the mushroom toxin phalloidin and confocal scanning laser microscopy were employed. Phalloidin binds to filamentous actin within myocytes and has been used to label muscles in numerous annelid species (Hill and Boyer, 2001; Tzetlin et al., 2002; Filippova et al., 2005; Tzetlin and Filippova, 2005; Tzetlin and Purschke, 2005; Wanniger et al., 2005; Filippova et al., 2006; Tzetlin

and Purschke, 2006; Wanninger, 2008; Vortsepneva et al., 2009a; Vortsepneva et al., 2009b; Wanninger, 2009; Brinkmann and Wanninger, 2010b; a; Filippova et al., 2010; Meyer et al., 2010)

Materials and Methods

Larval Culture

Adults of *Hydroides elegans* were collected from Pearl Harbor, Hawaii and kept in running seawater tables at the Kewalo Marine Laboratory. When embryos were needed, several adults were placed in small dishes containing 0.22 μm filtered seawater (FSW), and removed from their tubes to induce spawning of both male and female worms. Fertilization occurred rapidly and embryos were separated from adult worms and debris by passage through a 325 μm nylon mesh (Nitex, Small Parts Inc., Miami Lakes, FL). Larvae were cultured through competence as described in Chapter 1. When needed for labeling, larvae were concentrated by sieving cultures through a 41 μm Nitex sieve and then relaxed in 3.7% $MgCl_2$ in FSW for 2-5 minutes at room temperature. Larvae were then fixed for 1 h in 3.7% formaldehyde in 0.22 μm filtered seawater (4°C).

Collection of metamorphosing larvae

22 X 22 mm glass coverslips (Fisher Scientific, Pittsburgh, PA) were placed in sea tables with constantly flowing seawater for a minimum of 10 days to obtain a biofilm. Previous studies have shown that microbial biofilms form on these surfaces and high percentages of larvae quickly metamorphose on them (Hadfield et al., 1994; Holm et al., 1998; Unabia and Hadfield, 1999). The biofilmed coverslips were placed in 35 x 10 mm polystyrene Petri dishes (Fisher Scientific) containing FSW, and 50-100 competent larvae of *H. elegans* were added to each dish and allowed to metamorphose. After 15 minutes, larvae had begun to metamorphose and attached themselves to the surface of the coverslips by secreting a primary tube. Coverslips and metamorphosing larvae (metamorphs) were removed from the dishes containing larvae and transferred to new dishes containing FSW. At described intervals (Fig. 3), the metamorphs attached to the coverslips were relaxed in 3.7% $MgCl_2$ (5-10 min.) and fixed (5 min) in 3.7% formaldehyde in FSW. After this brief fixation, early-stage metamorphs were removed from their primary tubes using insect pins (#00, Fisher Scientific) and placed back into fixative for 1 h (4° C). After a brief fixation (5 min), the secondary tubes of later stage

metamorphs were decalcified by placing coverslips with metamorphs into 100 mM EDTA for 5 minutes. After decalcification, metamorphs were rinsed several times in FSW, removed from their tubes using insect pins, and placed back into fixative for 1 h (4° C).

Phalloidin labeling

After fixation, larvae and metamorphs were washed (3 X 5 minutes) in phosphate buffered saline (PBS; 50 mM Na_2PO_4, 140 mM NaCl pH 7.4) and were then washed (3 X 30 minutes) in PBT (PBS + 0.01% Triton X100). Larvae and metamorphs were incubated overnight in Alexa Fluor® 594 conjugated Phalloidin (1:500 dilution, Molecular probes) in PBT (4°C). After incubation in phalloidin, preparations were washed several times in PBS, immersed overnight in 3:1 glycerol: PBS, and mounted on glass microscope slides in the PBS: glycerol solution that included the anti-fading agent 2% n-propyl-gallate (Giloh and Sedat 1982).

Controls

As negative controls, larvae and metamorphs were processed without incubation in phalloidin and did not exhibit detectable fluorescence.

Photography

A minimum of 10-15 whole mount specimens was examined at each stage using a Zeiss LSM 510 scanning confocal microscope (Zeiss, Germany) equipped with the appropriate laser and filter combinations. Maximum intensity projections of z-stack optical sections of the preparations were produced using the Zen 2009 Light Edition (Zeiss, Germany). Plates of these images were constructed using Adobe Photoshop CS3 (Adobe Systems, San Jose, CA), and the brightness and contrast of each figure was adjusted to provide consistency within the plate.

Results

Myogenesis in larvae of H. elegans

The larval gut of *H. elegans* is divided into three parts; the description of the gut in *H. elegans* used in this study, follows the conventions described by Boyle and Seaver (2008) for *Capitella* sp. I. The gut of *H. elegans* includes a foregut composed of a larval pharynx and stomach, a midgut, and short hindgut that was separated from the midgut by a sphincter. The earliest phalloidin labeling was apparent in a set of muscle fibers in the larval gut and in a ring underneath the prototroch (PM). The reactive fibers wrapped

around with the pharynx of the foregut, and were present in a highly-reactive u-shaped gutter within the larval midgut (Fig 4.2A) in early Stage 2 larvae. While contraction of the midgut could easily be seen in live preparations, it was difficult to tell if the immunoreactive gutter within the midgut could contract independently.

Slightly later in larval development, an additional muscle ring had formed around the opening of the larval mouth. Additionally, there were increased numbers of fibers in the pharynx, and a single muscle fiber in the sphincter that separated the larval midgut and hindgut (arrowhead, Fig 4.2B). The rudiments of the paired longitudinal ventral muscles (LVM) developed as a horseshoe shaped mass fibers positioned posterior to the larval apical sensory organ (Fig. 2B). Finally, three rings of muscle fibers were present underneath the prototroch, metatroch, and third fiber located between these ciliary bands in the food groove of a Stage 2 trochophore (Fig. 4.2B).

In Stage 3 larvae, the three muscles associated with the ciliary bands had expanded, showed greater reactivity to phalloidin (Fig 4.2C), and could be contracted in living preparations at this stage. The out pocketing of the midgut was still reactive to phalloidin as was the sphincter separating the midgut from the hindgut. In addition to these persisting muscles, several new groups of muscles had also developed. A single pair of longitudinal fibers (LVM) that originated as an arch beneath the apical organ developed posteriorly in ventral portions of the larval episphere and hyposphere, but had not reached the pygidium of the larva (arrowheads, Fig. 4.2C). Additionally, two oblique muscles had developed on top of the larval esophagus (Fig 4.2C). A pretrochal muscle (PTM) developed and was composed of two muscle fibers that originated on an anterior portion of the pharynx and formed a loop on top of the anterior region of the larval stomach. The anterior arches of the LVM were positioned inside the loop of the PTM. A second muscle composed of two fibers looped obliquely across the larval stomach from the just in front of the apical muscle fibers and encircled a more posterior portion of the larval stomach (arrow, Fig 4.2C)

At Stage 4, larvae had developed segments and, the pair longitudinal ventral muscles (LVM) developed posteriorly and terminated in the pygidium of larvae, and an additional dorsally positioned pair of longitudinal muscles (LDM) had developed (Fig 2D). The muscles underlying the prototroch, food groove, and metatroch persisted in

Stage 4 larvae, although the reactivity of the food groove fiber had diminished. Three pairs of chaetae had developed between the longitudinal muscles in the hyposphere in the thoracic segments and several small muscles associated with the chaetal sac began to develop (green arrowheads, Fig. 4.2D).

The complexity of the musculature had greatly increased in Stage 6 larvae of *H. elegans* and was composed of both larval muscles and nascent adult musculature (Fig. 4.2E). There were four prominent muscle rings in the episphere. The anterior most muscle ring was the pretrochal muscle (PTM); it remained anterior to of the anterior portion of the larval pharynx and encircled a portion of both the ventral and dorsal longitudinal muscles (Fig. 4.2E). Posterior of this muscle was the prototroch muscle (PM). It ran beneath the prototroch and consisted of several thick phalloidin reactive fibers (Fig. 2E). Immediately posterior of the prototroch muscle was the food groove muscle (FGM), and the most posterior muscle ring in the episphere was the metatroch muscle (MM, Fig. 4.2E). Several muscle filaments of the ventral longitudinal muscle had spread out and the plexus inserted against the both the larval epidermis (black arrowheads) and the larval pharynx (white arrowheads, Fig. 4.2F).

In the larval hyposphere, the posterior portions of both the ventral and dorsal longitudinal muscles had expanded and the addition of new fibers caused; the ventral longitudinal muscle to be much thicker than the dorsal muscles throughout its length (Fig. 4.2E). Several filaments of the dorsal longitudinal muscles extended into the pygidium. One set of muscle fibers inserted against the posterior epidermis of the pygidium (Fig. 2G). A second pair of muscle fibers extended medially and diagonally and inserted on the sphincter that separated the mid- and hindgut of the larvae (arrowheads, Fig. 4.2G). These two fibers and portions of the sphincter formed an X-shaped muscle complex within the pygidium of Stage 6 larvae of *H. elegans*.

Finally, the chaetal musculature had developed and expanded in the hyposphere of Stage 6 larvae of *H. elegans*. This musculature was complex and sandwiched between the dorsal and ventral longitudinal muscles. In each thoracic segment, four bundles of capillary chaetae had developed in each of the thoracic segment of Stage 6 larvae (Seaver and Kaneshige, 2006). In each hemisegment, an anterior chaetal bundle (bun1) was positioned closer to the ventral midline than the more posterior bundle (bun2, Fig 4.2H).

The proximal ends of each bundle of chaetae were located in a ventromedial position with the larval hyposphere, and the distal ends of the chaetae had erupted from the body wall. The individual chaetae were strongly autofluorescent and the proximal ends of each chaeta appeared as bright dots within the hyposphere of the Stage 6 larvae (Fig. 4.2H). The proximal portions of both chaetal sacs were covered with numerous phalloidin reactive fibers and several muscle fibers had developed that connected the chaetae to both the larval epidermis and a newly developed longitudinal median muscle (LMM, Fig. 2H). The first pair of these myofibers was an anterior lateral diagonal muscle (ALDM) that was positioned between the lateral epidermis and the anterior edge of distal end of chaetal bundle two (bun2), and a short posterior lateral muscle ran between the posterior edge of distal end of the chaetal bundle (bun2) and the body wall (Fig. 2H). A second pair of fibers ran obliquely from the body wall to the proximal ends of the medial chaetal bundle (bun1). An anterior medial oblique muscle (AMOM) originated at the proximal end of chaetal bundle 1 and inserted against the body wall directly adjacent to the end of the anterior lateral diagonal muscle (Fig. 2H). A posterior medial oblique muscle (PMOM) was located between the posterior portion of the proximal end of chaetal bundle 1 and the body wall (Fig. 4.2H). Finally, two pairs of muscles connected the chaetal bundles to the longitudinal medial muscle (LMM, Fig. 2H). The anterior diagonal muscle (ADM) originated at the LMM and inserted against the proximal end of the chaetal sac of bun1 (Fig. 4.2H). The last muscle was the posterior diagonal muscle (PDM) and it was positioned between the LMM and the distal end of the bun2. The coordination of these muscles allowed Stage 6 larvae to move their chaetae in both the anterior-posterior and dorsal-ventral axes of the larva.

Morphogenesis associated with metamorphosis.

Competent larvae of *H. elegans* initiated metamorphosis almost immediately after contacting inductive, biofilmed surfaces and began the process by secreting a sticky thread from their posterior ends that served to tether the larvae to the substratum. Almost immediately, larvae laid flat on the surface and began secreting a primary tube from most or all of the hyposphere (Fig. 4.3A). Larvae then shaped the newly secreted tube by rotating within it as they erected their chaetae to push the primary tube away from their

bodies. The secretion of the primary tube, which can be completed in as little as 10 minutes after contact with a surface, was an irreversible process that permanently attached a larva to the substratum. As the primary tube was secreted, the collar was everted, the area immediately anterior and posterior of the collar constricted, the larval body elongated, and the metatroch cilia were lost (Fig. 4.3A). Simultaneously, the pair of lobes that are the precursors to the branchial radioles became apparent on the anterolateral margins of the episphere of the juvenile (Fig. 4.3B).

Secretion of the calcified secondary tube began at the anterior margin of the primary tube approximately 2 hrs after the commencement of metamorphosis, after which new material was added to the secondary tube continuously. About 4 hrs after the induction of metamorphosis, the prototroch cilia had resorbed and three branchial radioles began to differentiate from the anterior lobes in the episphere (Fig. 4.3B). Eight hours after the induction of metamorphosis, the branchial rudiments had divided into three lobes (Fig. 4.3C), and the position of the mouth began to shift from a ventral position to the anterior one (Fig. 4.3C). Metamorphosis was complete and juvenile development had commenced by 11-12 hrs post-settlement (Fig. 4.3D).

Fate of musculature during metamorphosis of H. elegans

Shortly after contact with a bacterial biofilm, the rings of muscle underneath the trochal bands and food grove contracted and caused constriction around the collar (Fig. 4.4A). The pretrochal muscle ring also contracted and reduced the diameter of the larval episphere (Figs. 4.4A and B). The remaining musculature remained unchanged early in the metamorphic process.

An hour after the induction of metamorphosis in *H. elegans,* the prototroch and metatroch muscles remained in tetanic contraction, and the food grove muscle had disappeared (Fig 4.4C). Later in the metamorphic progression, the only loss of musculature occurred about 4 hours after the induction of metamorphosis. At this stage, the metatroch muscle was no longer reactive to phalloidin and may have deteriorated (Fig. 4.4D). The prototroch muscle remained tightly contracted and the diameter of the pretrochal muscle had greatly diminished. This contraction also diminished the width of the larval episphere (Fig. 4.4D). Additionally, a number of thin, newly-formed myofibers

were reactive to phalloidin in the developing branchial rudiments (Fig. 4.4D). Finally, the muscles surrounding the chaetae had thickened (compare Figs 4.4A and D).

Eight hours after the induction of metamorphosis, two muscle fibers had developed in each of the lobes of the tentacle rudiments, and the pretrochal muscle had disappeared (arrows, Fig. 5.5A). The prototrochal muscle was still present, but the number and thickness of fibers within it had decreased (Figs. 4.5A and D). In the hyposphere, the longitudinal ventral muscle (LVM) had thickened and was strongly reactive to phalloidin throughout its length. A new pair of muscles had developed from the anterior portion of the LVM and had extended and arborized into the ventrolateral portions of the collar (Fig 4.5A). These muscles were the earliest sign of the collar muscles that are present in juvenile and adult *H. elegans*.

In the final stage examined, (12 hrs after post-induction), the only major changes in the overall muscle patterning occurred around the mouth and pharynx. The mouth had shifted from a ventral position to a more anterior one (Figs 4.5B and E) and rings of muscle that encircled the mouth had broken down as the mouth moved anteriorly (asterisks, Fig. 4.5E). The remaining muscles had further developed and thickened in the intervening time period, and numerous additional fibers had developed in the chaetal musculature (Fig 5C).

Discussion

Even though there is a great diversity in the patterns of body wall musculature in adult annelids (reviewed by Tzetlin and Filippova, 2005), recent studies of myogenesis during embryonic and larval development suggest that there may be two conserved patterns of muscle development (Bergter et al., 2007; Bergter et al., 2008; Wanninger, 2009; Brinkmann and Wanninger, 2010b). Brinkmann and Wanninger (2010b) suggest that the patterns of myogenesis may also correlate with the mode of larval development in annelids.

In the first conserved mode, which is utilized by direct developing oligochaetes and lecithotrophic polychaete larvae, the body wall musculature develops before muscles develop within the gut (McDougall et al., 2006; Brinkmann and Wanninger, 2010b). In this developmental mode, the earliest muscles that develop are around the stomadeum and longitudinal muscle bands differentiate shortly after in the body wall (Hill and Boyer,

2001; Bergter et al., 2008; Meyer et al., 2010). Usually, rings of circular muscles develop after the appearance of the longitudinal muscles. In the lecithotrophic larvae of *Ophryotrocha diadema*, the circular muscles are largely absent in the body wall (Bergter et al., 2008).

A second pattern of myodevelopment occurs in planktotrophic polychaete larvae. Unlike the previous model, the earliest muscles to develop in these larvae are the muscles that surround feeding structures, and the development of body wall muscles gets delayed until later in larval development (Lacalli, 1984; McDougall et al., 2006; Brinkmann and Wanninger, 2010b). In all planktotrophic polychaete larvae studies thus far, 2 pairs of longitudinal muscles develop in the post-trochal regions of the larvae (McDougall et al., 2006; Brinkmann and Wanninger, 2010b). Myogenesis in larvae of *H. elegans* follows this pattern and most closely resembles myodevelopment in larvae of *Pomatoceros lamarckii* (McDougall et al., 2006).

A limitation of both of these models is the small number of developmental patterns that were used to compile them. This shortcoming is illustrated when the finer details of both of these models are explored. For example, the only the current study and one performed on larvae of *Sabellaria alveolata* examined enough developmental stages to determine that there were slight differences in the timing of the development of the ventral and dorsal longitudinal muscles in feeding polychaete larvae. Brinkmann and Wanninger (2010) showed that the dorsal longitudinal muscles developed first Brinkmann and Wanninger (2010b) showed that the pair of dorsal longitudinal fibers develops early in *Sabellaria alveolata*, while the opposite developmental sequence occurs late in Stage 3 larvae of *H. elegans*. In *H. elegans*, the ventral longitudinal muscles develop before the dorsal pair and extended more than half way down the hyposphere before the dorsal pair first appeared (Fig. 4.2C). However, this asymmetric pattern does not persist for long, as two pairs of longitudinal muscles are present throughout the hyposphere by the time morphological segmentation was observed in Stage 4 larvae of *H. elegans* (Fig 2D). The lack of detailed descriptions of myogenesis during segmentation in other planktotrophic larvae make it difficult to make compare *H.* elegans with other larvae and to determine if the pattern observed in *H. elegans* represents a conserved mode of longitudinal muscle development in feeding larvae.

The complex musculature that controls movement of the chaetae in Stage 4 larvae of *H. elegans* develops simultaneously in all three thoracic segments (Fig. 4.2D), a pattern of simultaneous development that is similar to that in segmented larvae of *Pomatoceros lamarckii* (McDougall et al., 2006). However, this pattern may not be conserved within the Serpulidae. The chaetal musculature of larvae of the *Filograna implexa* develops sequentially within the post-trochal region of segmented larvae; with the most developed chaetal muscles appearing in the first thoracic segment (Wanninger, 2009). However, the pattern observed in *F. implexa* may be a consequence of lecithotrophic development in larvae of *F. implexa*. Examination of the development of the chaetal musculature in other non-feeding serpulid larvae (i.e., *Spirobis* cf *spirobis*) might help determine if the sequential development of muscle in thoracic segments is unique to *F. implexa*. Taken together, the patterns of muscle development suggest that myogenesis is a complex process and an area of particular interest.

Fate of the musculature during metamorphosis of H. elegans

By the time larvae of *Hydroides elegans* reach metamorphic competence, both larval and adult muscles have developed. Larval muscles are defined as the pretrochal muscle and those muscles that ring the prototroch, metatroch, food groove and mouth (Figs 4.2A-C) because these muscles develop early in larval development. The adult muscles are defined as the muscles surrounding the chaetae, plus the two pairs of longitudinal muscle bands in the larval hyposphere (Figs 4.2D-F). The muscles surrounding the gut (pharyngeal muscles, muscles of the midgut, and sphincter) are difficult to categorize as either strictly larval or adult muscles because they first appear early in larval development (Figs. 4.2A and B) and persist with minor rearrangement through metamorphosis (Figs 4.4 and 4.5).

After the induction of metamorphosis, the larval musculature is sequentially lost. The first larval muscle to be resorbed is the food groove muscle, followed by the metatroch muscle, the muscles surrounding the mouth, and finally the pretrochal and prototroch muscles. Curiously, the timing of the loss of cilia from the trochal cells is separated from the resorption of the muscles associated with these ciliary bands. For example, the cilia of metatroch are lost as soon as 15 minutes after the induction of metamorphosis by bacterial biofilms (pers. obs.), but the metatrochal muscle does not

disappear until approximately four hours later (Fig. 4.4D). Similarly, the prototrochal cilia are lost approximately four hours after the induction of metamorphosis, but the prototroch muscle remains for a minimum four additional hours (Fig. 4.5A and D). This delay may suggest that the trochal muscles function during metamorphosis. The tetanic contraction of these muscles (Figs 4.4 and 4.5A) may be required to retain the constricted shape around the collar without utilization of other cellular processes (Hadfield et al., 2001; Carpizo-Ituarte and Hadfield, 2003) until the time that new gene transcription and translation begins late in the metamorphic cascade (Carpizo-Ituarte and Hadfield, 2003).

The precocious development of adult muscles during larval development may be an evolutionary advantage that allows for the rapid metamorphosis after brief contact with a metamorphic cue. Hadfield et al. (2001) hypothesized that "preformed" adult structures in larvae of *Hydroides elegans* allow them to rapidly metamorphose and minimize the vulnerable period when the larva is between body plans. Both the timing of the development of the adult musculature prior to metamorphosis and the relatively small overall changes in musculature during metamorphosis may allow larvae of *H. elegans* for this rapid transition.

References

Anderson DT. 1966. The comparative embryology of the polychaeta. Acta Zool 47:1-42.

Anderson DT. 1973. Embryology and phylogeny of annelids and arthropods. New York: Pergamon Press.

Bergter A, Brubacher J, Paululat A. 2008. Muscle formation during embryogenesis of the polychaete Ophryotrocha diadema (Dorvilleidae) - new insights into annelid muscle patterns. Frontiers in Zoology 5(1):1.

Boyle MJ, Seaver EC. 2008. Developmental expression of foxA and gata genes during gut formation in the polychaete annelid, Capitella sp I. Evolution & Development 10(1):89-105.

Brinkmann N, Wanninger A. 2010a. Capitellid connections: contributions from neuromuscular development of the maldanid polychaete *Axiothella rubrocincta* (Annelida). BMC Evol Biol 10(1):168.

Brinkmann N, Wanninger A. 2010b. Integrative analysis of polychaete ontogeny: cell proliferation patterns and myogenesis in trochophore larvae of *Sabellaria alveolata*. Evolution & Development 12(1):5-15.

Carpizo-Ituarte E, Hadfield MG. 1998. Stimulation of Metamorphosis in the Polychaete *Hydroides elegans* Haswell (Serpulidae). Biol Bull 194:14-24.

Clark RB. 1981. Locomotion and phylogeny of the Metazoa. Boll Zool 48:11-28.

Dordel J, Fisse F, Purschke G, Struck TH. 2010. Phylogenetic position of Sipuncula derived from multi-gene and phylogenomic data and its implication for the evolution of segmentation. Journal of Zoological Systematics and Evolutionary Research 48(3):197-207.

Dunn CW, Hejnol A, Matus DQ, Pang K, Browne WE, Smith SA, Seaver E, Rouse GW, Obst M, Edgecombe GD, Sorensen MV, Haddock SHD, Schmidt-Rhaesa A, Okusu A, Kristensen RM, Wheeler WC, Martindale MQ, Giribet G. 2008. Broad phylogenomic sampling improves resolution of the animal tree of life. Nature 452(7188):745-749.

Filippova A, Purschke G, Tzetlin AB, Müller MCM. 2005. Reconstruction of the musculature of *Magelona cf. mirabilis* (Magelonidae) and *Prionospio cirrifera* (Spionidae) (Polychaeta, Annelida) by phalloidin labeling and cLSM. Zoomorphologie 124(1):1-8.

Filippova A, Purschke G, Tzetlin AB, Müller MCM. 2006. Three-dimensional reconstruction of the F-actin musculature of *Dorvillea kastjani* (Dorvilleidae, Polychaeta) by means of phalloidin-labelling and cLSM. Scientia Marina 70(S3):293-300.

Filippova A, Purschke G, Tzetlin AB, Müller MCM. 2010. Musculature in polychaetes: comparison of *Myrianida prolifera* (Syllidae) and *Sphaerodoropsis* sp. (Sphaerodoridae). Invert Biol 129(2):184-198.

Gardiner S. 1992. General organization, integument, musculature, coelom and vascular system. In: Harrison FW, editor. Microscopic Anatomy of Invertebrates. New York: Wiley-Liss. p 19–52.

Hadfield MG, Unabia CC, Smith CM, Michael TM. 1994. Settlement preferences of the ubiquitious fouler *Hydroides elegans*. In: Thompson MF, Nagabhushanam R, Sarojini R, Fingerman M, editors. Recent Developments in Biofouling Control. New Delhi: Oxford and IBH Pub. Co. p 450.

Hill SD, Boyer BC. 2001. Phalloidin labeling of developing muscle in embryos of the polychaete *Capitella* sp. I. Biol Bull 201(2):257-258.

Holm ER, Nedved BT, Carpizo-Ituarte E, Hadfield MG. 1998. Metamorphic-signal transduction in *Hydroides elegans* (Polychaeta: Serpulidae) is not mediated by a G-Protein. Biol Bull 195:21-29.

McDougall C, Chen WC, Shimeld SM, Ferrier DE. 2006. The development of the larval nervous system, musculature and ciliary bands of *Pomatoceros lamarckii* (Annelida): heterochrony in polychaetes. Front Zool 3:16.

McHugh D. 2005. Molecular systematics of polychaetes (Annelida). Hydrobiologia 535/536:309-318.

Meyer N, Boyle M, Martindale M, Seaver E. 2010. A comprehensive fate map by intracellular injection of identified blastomeres in the marine polychaete *Capitella teleta*. EvoDevo 1(1):8.

Purschke G, Muller MCM. 2006. Evolution of body wall musculature. Integrative and Comparative Biology 46(4):497-507.

Rüchel J, Müller MCM. 2007. F-actin framework in *Spirorbis* cf. *spirorbis* (Annelida: Serpulidae): phalloidin staining investigated and reconstructed by cLSM. Invert Biol 126(2):173-182.

Ruppert EE, Barnes RD. 1994. Invertebrate Zoology. Orlando, Florida: Saunders College Publishing, Harcourt Brace and Company.

Seaver EC, Kaneshige LM. 2006. Expression of 'segmentation' genes during larval and juvenile development in the polychaetes *Capitella sp. I* and *H. elegans*. Dev Biol 289(1):179-194.

Seaver EC, Thamm K, Hill SD. 2005. Growth patterns during segmentation in the two polychaete annelids, *Capitella sp*. I and *Hydroides elegans*: comparisons at distinct life history stages. Evol Dev 7(4):312-326.

Struck TH, Schult N, Kusen T, Hickman E, Bleidorn C, McHugh D, Halanych KM. 2007. Annelid phylogeny and the status of Sipuncula and Echiura. BMC Evol Biol 7:57.

Tzetlin A, Filippova A. 2005. Muscular system in polychaetes (Annelida). Hydrobiologia 535-536(1):113-126.

Tzetlin A, Purschke G. 2005. Pharynx and intestine. Hydrobiologia 535/536(1-3):199-225.

Tzetlin A, Purschke G. 2006. Fine structure of the pharyngeal apparatus of the pelagosphera larva in Phascolosoma agassizii (Sipuncula) and its phylogenetic significance. Zoomorphologie 125(3):109-117.

Tzetlin AB, Zhadan A, Ivanov I, Muller MCM, Purschke G. 2002. On the absence of circular muscle elements in the body wall of *Dysponetus pygmaeu*s (Chrysopetalidae, 'Polychaeta', Annelida). Acta Zool 83(1):81-85.

Unabia CRC, Hadfield MG. 1999. Role of bacteria in larval settlement and metamorphosis of the polychaete *Hydroides elegans*. Mar Biol 133:55-64.

Vortsepneva E, Tzetlin A, Tsitrin E. 2009a. Anterior muscular system of the dwarf ectoparasitic male *Scolelepis laonicola* (Tzetlin, 1985) (Polychaeta, Spionidae). Zoosymposia 2:429-435.

Vortsepneva E, Tzetlin AB, Tsitrin E. 2009b. Nervous system of the dwarf ectoparasitic male of *Scolelepis laonicola* (Polychaeta, Spionidae). Zoosymposia 2:437-445.

Wanniger A, Koop D, Bromham L, Noonan E, Degnan BM. 2005. Nervous and muscle system development in *Phascolion strombus* (Sipuncula). Dev Genes Evol 215:509-518.

Wanninger A. 2008. Comparative lophotrochozoan neurogenesis and larval neuroanatomy: Recent advances from previously neglected taxa. Acta Biol Hung 59(Supplement 2):127-136.

Wanninger A. 2009. Shaping the Things to Come: Ontogeny of Lophotrochozoan Neuromuscular Systems and the Tetraneuralia Concept. Biol Bull 216(3):293-306.

Wisely B. 1958. The Development of a Serpulid Worm, *Hydroides norvegica*, Gunnerus (Polychaeta). Aust J Mar Freshwater Res 9:351-361.

Zrzavy J, Riha P, Pialek L, Janouskovec J. 2009. Phylogeny of Annelida (Lophotrochozoa): total-evidence analysis of morphology and six genes. BMC Evol Biol 9(1):189.

Figure Legends

Figure 4.1 Schematic of larval development in *Hydroides elegans*. Hpf represents hours post fertilization at 25° C. After Seaver et al. (2005)

Figure 4.2 Myogenesis in larvae of *Hydroides elegans*. A. Right lateral view of an early Stage 2 larva. Muscles have developed in larval gut and as a ring in the prototroch. Scale B. Right lateral view of late Stage 2 larva. Larva is tilted slightly to the left. New myofibers had developed beneath the food groove, metatroch and in sphincter separating the larval midgut and hindgut. Rudiments of the longitudinal ventral muscles had developed directly posterior of the apical sensory organ (arrowheads). C. Right lateral view of Stage 3 trochophore. Two new rings of muscle had developed in the larval episphere. The pretrochal muscle was the more anterior ring and it encircled the longitudinal ventral muscle (LVM). The LVM continued to develop posteriorly into the larval hyposphere had not yet reached the future site of the pygidium (arrowheads) a second ring of muscle developed in the episphere and was positioned on top of the dorsal portion of the larval stomach (arrow). D. Muscles in a Stage 4 larva of *H. elegans*. Left lateral view. Larva is tilted to the right. Two pairs of longitudinal muscles had developed in the larval hyposphere. Both pairs of muscles originated below the apical sensory organ and terminated in the pygidium of the larva. Only the left longitudinal ventral (LVM) and left longitudinal dorsal muscles (DVM) are shown. Chaetae and rudiments of the chaetal muscles had developed in the each of the three thoracic segments in the hyposphere of the larva (black arrowheads). E. Ventral view of muscle development in Stage 6 larva. No muscles had disappeared from the previous stage. Both the longitudinal ventral and dorsal muscles had expanded and thickened in the hyposphere of the larva. An additional unpaired longitudinal muscle developed in the ventromedial portion of the hyposphere (LMM) and served a point of connection for the muscles associated with the chaetae. F. Magnified region of the right longitudinal ventral muscle at the prototroch of a Stage 6 larva. Portions of this muscle filament terminated against both the larval epidermis (black arrowheads) and posterior portion of the larval stomach (white arrowheads). G. Muscles in the pygidium of Stage 6 larva. Several muscle filaments projected from the dorsal longitudinal muscle. The more lateral

fibers (arrows) terminated against the larval epidermis in posterior portions of the pygidium. An additional pair of medially directed myofibers (arrowheads) interacted with the sphincter at the midgut and together formed an X-shaped septum in the pygidium. H. Ventral view of the chaetal musculature in Stage 6 larva. Labels were added to the chaetal muscles of the second thoracic segment. The medial (bun1) and lateral (bun2) chaetal sacs are labeled on the right side of the larvae. The 3 pairs of diagonal and oblique fibers were labeled on the left side of the second segment. Shows anterior diagonal muscle (ADM), posterior diagonal muscle (PDM), anterior medial oblique muscle (AMOM), posterior medial oblique muscle (PMOM), anterior lateral diagonal muscle (ALDM), posterior lateral diagonal muscle (PLDM) and the chaetal muscles that overlay the chaetal sac. Also shown in figure are stomach (Stom), pharynx (Phar), prototroch muscle (PM), midgut muscle (mid), food groove muscle (FGM), metatroch muscle (MM), sphincter between midgut and hindgut. Scale in all parts of plate 50 μm except for E. Scale in E 100 μm. Anterior is up in all photos. All photos are maximum intensity projections of confocal z-stacks.

Figure 4.3 Metamorphic progression of larvae of *Hydroides elegans* after exposure to a bacterial biofilm. A. Dorsal view of a newly settled larva of *H. elegans.* (15 min post-exposure to biofilm) Larva had secreted a primary tube, everted the collar, and lost the cilia of the metatroch. B. Ventral view of metamorphosed larvae of *H. elegans* (4 h post-exposure). The metamorphosing worm had lost pretrochal cilia and began to secrete the calcified secondary tube. The branchial rudiments had begun to differentiate in the episphere of the larva. C. Ventral view of juvenile of *H. elegans* (8 h post-induction of metamorphosis). The branchial rudiments had differentiated into three lobes (1, 2, and 3) on each side of the episphere. D. Ventral view of a juvenile *H. elegans* (12 h post-induction of metamorphosis). The juvenile had completed metamorphosis. The animal had doubled in size and the mouth migrated from a ventral (larval) position to an anterior (adult) position. The juvenile worm had the ability developed the ability to trap food particles by the branchial rudiments and ingest them in the newly positioned mouth. Asterisks indicate position of mouth. Scale in A and B 50 μm and 100 μm in C and D. Shows collar (col), branchial rudiments (BR), and calcified secondary tube (ST). After Carpizo-Ituarte et al. 1998

Figure 4.4. Fate of larval muscles during early metamorphosis of *H. elegans*. A. Dorsal view of phalloidin labeled larvae 15 minutes after induction of metamorphosis. The most conspicuous change in the morphology of the muscles was the contraction of the pretrochal, prototroch, food groove, and metatroch muscles. Contraction of these muscles caused the constriction of the collar region of the larva. B. Magnified photo of the episphere of the larva in (A). C. Ventral view of the episphere of a metamorphosing larva (1 h post-induction of metamorphosis). The pretrochal, prototroch and metatroch muscles remained tetanic contraction. The food groove muscle is no longer visible. D. Dorsal view of a juvenile worm (4h post-induction of metamorphosis). The majority of the muscles that had developed during the larval stages of *H. elegans* remained reactive to phalloidin. The muscle fiber in the metatroch had degenerated but both the pretrochal and prototroch muscles remained tight contracted in the anterior of the metamorphosing worm. The lobes branchial rudiments had begun to differentiate and a pair of horseshoe shaped muscles (arrowheads) had begun to develop in the lumen of the branchial rudiments. The reactive myofilaments in the paired longitudinal muscles, the muscle in the midgut, and the sphincter between the mid- and hindgut remained. Further, the chaetal muscles had continued to develop and were highly reactive to the fluorescently labeled phalloidin. Shows longitudinal dorsal muscle (LDM), longitudinal ventral muscle (LVM), prototroch muscle (PM), food groove muscle (FGM), metatroch muscle (MM), pretrochal muscle (PTM), muscle in the midgut (Mid) and sphincter (SP). Anterior is up in all photos. Scale is 100 μm in A and D and 50 μm in B and C. All images are maximum intensity projections of confocal z-stacks.

Figure 4.5. Fate of muscles during late metamorphosis of *Hydroides elegans*. A. Ventral view of metamorphosing larva of *H. elegans* (8 h post-induction). The longitudinal ventral muscles (LVM), longitudinal medial muscle (LMM), sphincter (SP) and muscle within the midgut of the larva remain. The pretrochal muscle has disappeared and only the prototroch muscle remains. The lumen of the branchial rudiments has expanded and there are now two muscle fibers within them (arrowheads). The mouth was still ventrally positioned (asterisk), and the rudiments

of the collar muscles had developed and arborized with the collar (arrows). B. Ventral view of a juvenile worm of *H. elegans* (12 h post-induction). The larval mouth has shifted anteriorly and was positioned between the tentacle rudiments (asterisk) and the pharynx had expanded and shifted anteriorly (arrowheads). The prototroch muscle has disappeared. The longitudinal ventral and medial muscles have further developed and thickened, and the rudiments of the collar muscles had expanded within the collar (arrowheads). C. Dorsal view of the same juvenile as in (B). The musculature of the chaetae had further developed and increased in complexity and the longitudinal dorsal muscle (LDM) remained much smaller than the LVM. D. Magnification of mouth in (A). The prototroch muscle (PM) remained in this stage, but the muscle degenerates as the mouth shifts anteriorly. E. Magnification of the mouth in (B). Anterior is up in all photos. Images are maximum intensity projections of confocal z-stacks. Scale in A and B 100 μm, 200 μm in C and 50 μm in D and E.

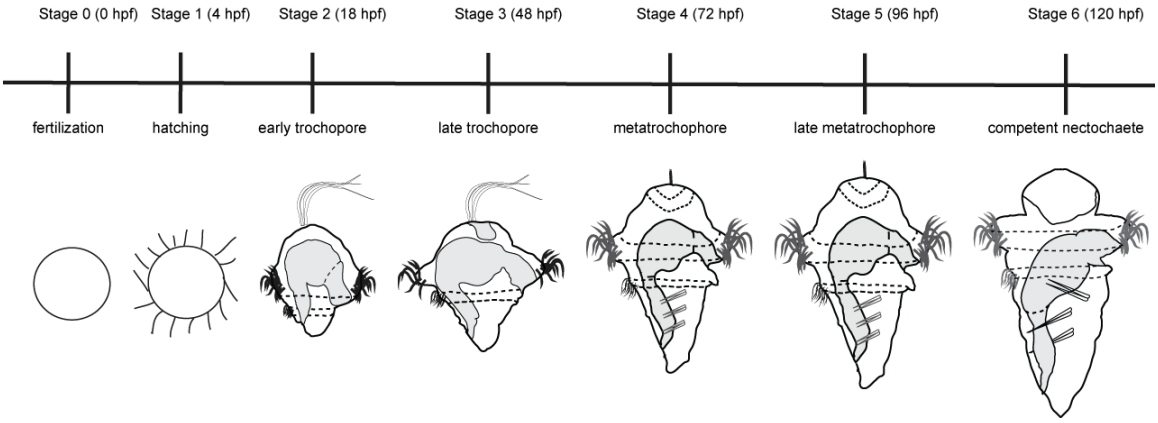
Stage 0 (0 hpf)
Stage 1 (4 hpf)
Stage 2 (18 hpf)
Stage 3 (48 hpf)
Stage 4 (72 hpf)
Stage 5 (96 hpf)
Stage 6 (120 hpf)
fertilization
hatching
early trochopore
late trochopore
metatrochophore
late metatrochophore
competent nectochaete

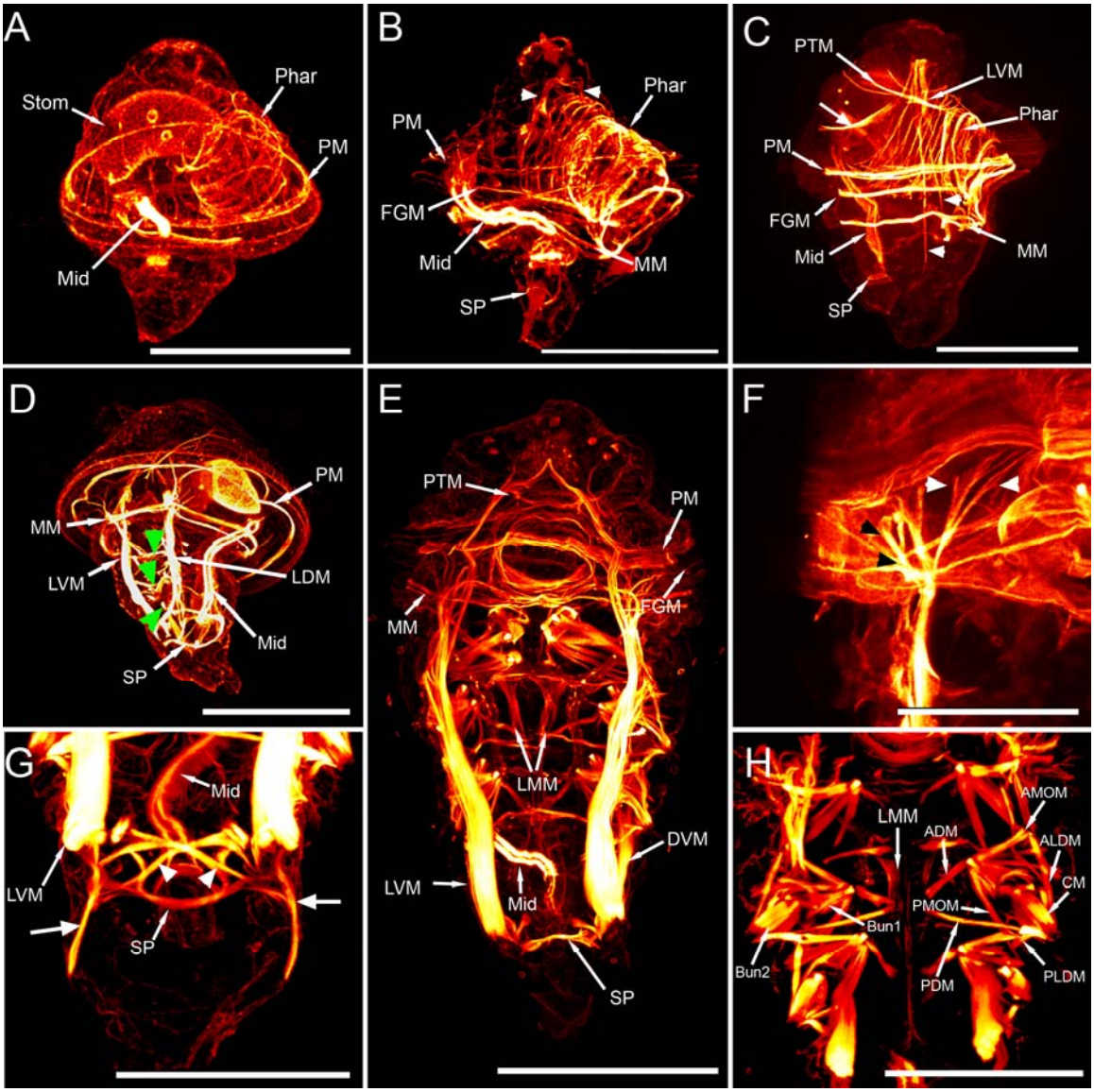
A
Stom
Phar
PM
Mid
B
Phar
PM
FGM
Mid
MM
SP
C
PTM
LVM
Phar
PM
FGM
Mid
MM
SP
D
PM
MM
LVM
LDM
Mid
SP
E
PTM
PM
FGM
MM
LMM
DVM
LVM
Mid
SP
F
G
Mid
LVM
SP
H
LMM
AMOM
ADM
ALDM
CM
PMOM
Bun1
Bun2
PDM
PLDM

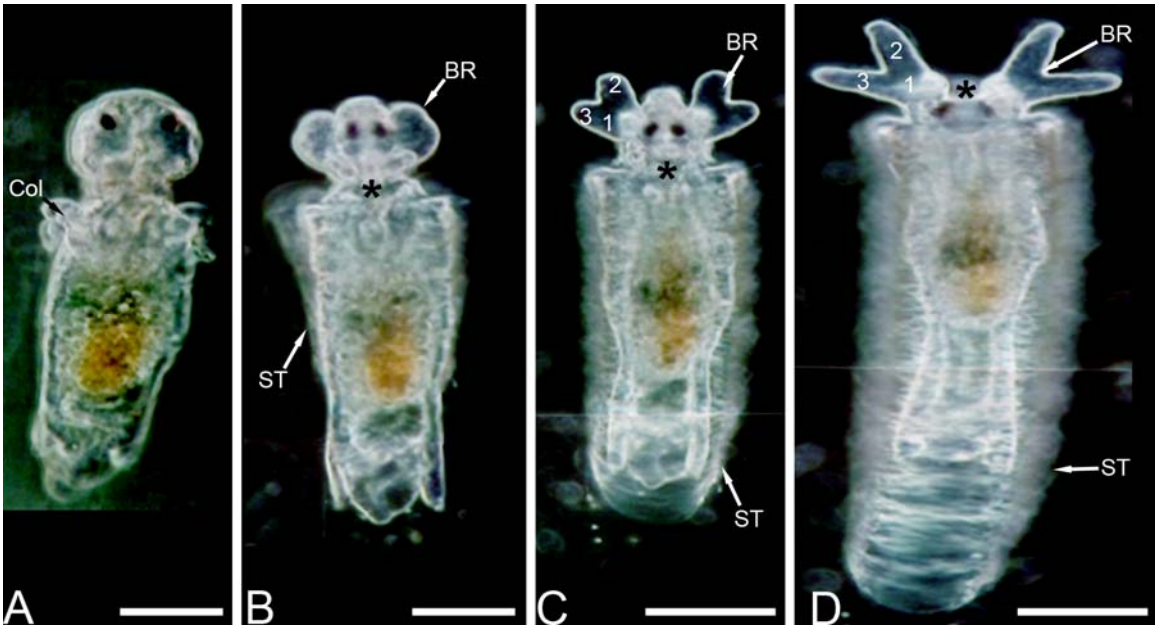
Col
A
BR
ST
B
BR
2
3
1
ST
C
2
3
1
BR
ST
D

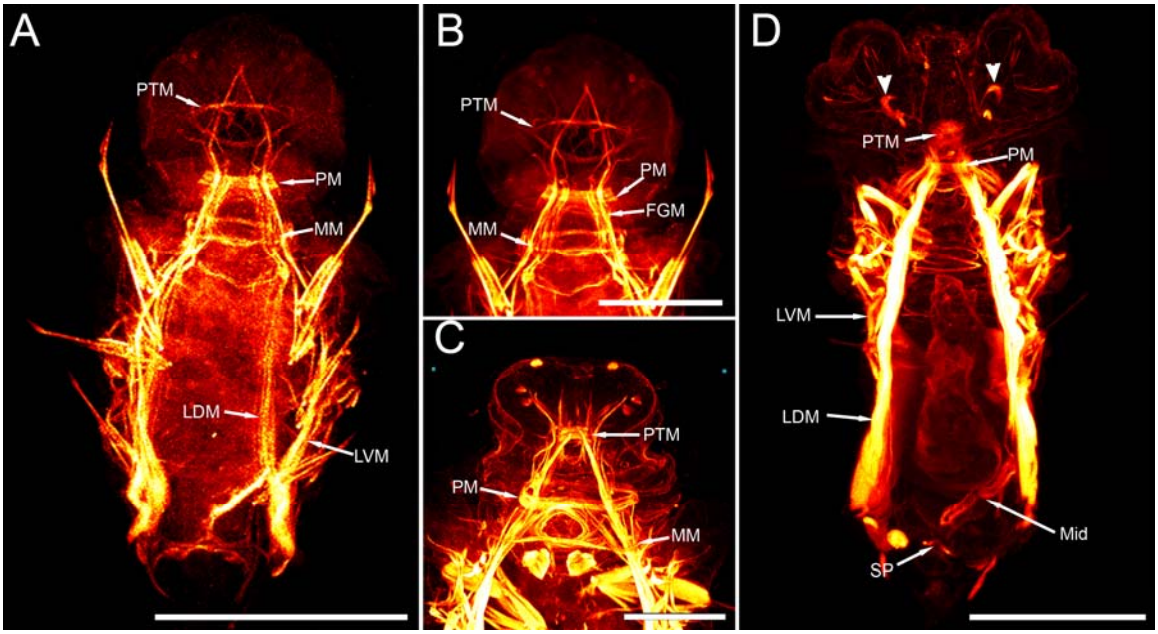
A
PTM
PM
MM
LDM
LVM
B
PTM
PM
FGM
MM
C
PTM
PM
MM
D
PTM
PM
LVM
LDM
Mid
SP

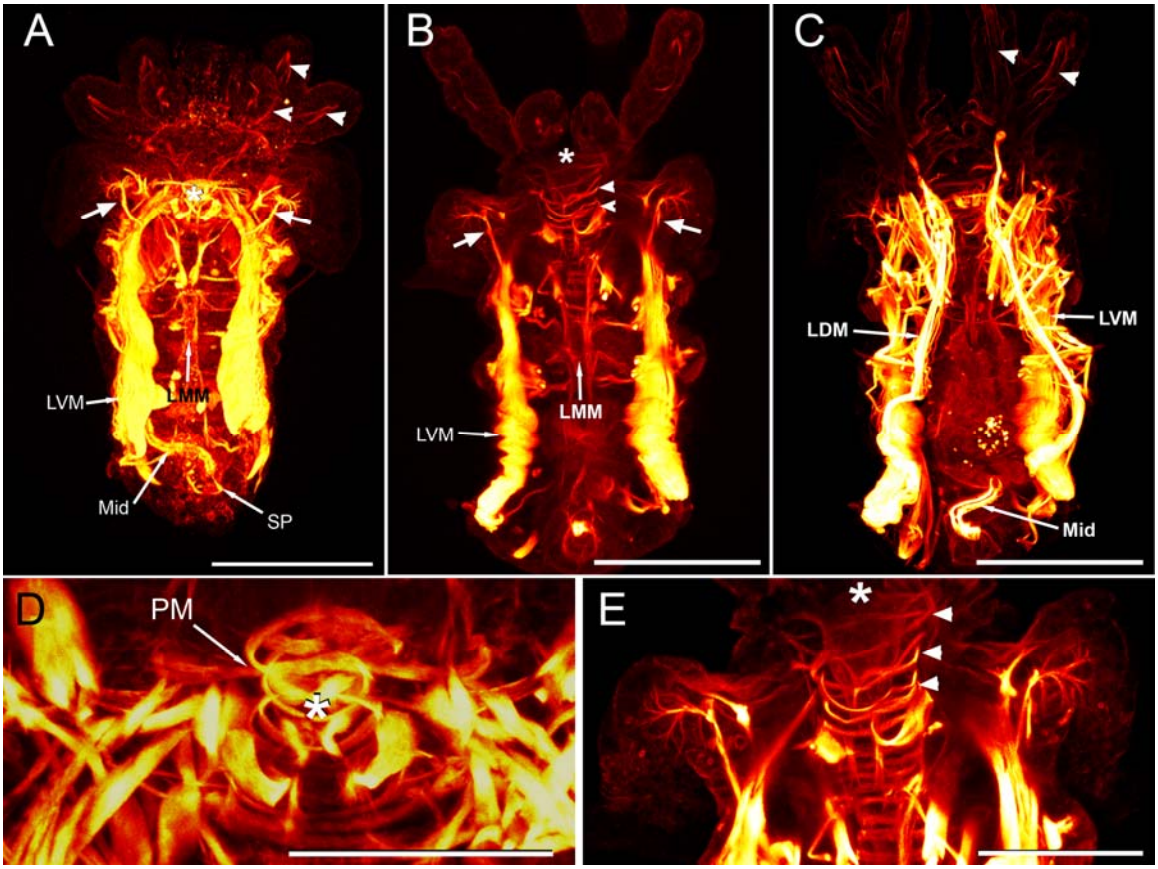
A
LVM
LMM
Mid
SP
B
LMM
LVM
C
LDM
LVM
Mid
D
PM
E